

**Fluorescence Spectroscopic Studies of  
Pressure and Temperature Effects on  
Na<sup>+</sup>,K<sup>+</sup>-ATPase Reconstituted into  
Phospholipid Bilayers and Model Raft  
Mixture**

DISSERTATION

Zur Erlangung des akademischen Grades

Doktor der Naturwissenschaften

(Dr. rer. nat.)

vergelegt von

**Ewa Powalska**

(Master of Science in Chemistry)

Geboren am 24.12.1979

In Elblag Polen

eingereicht beim

Fachbereich Chemie

der Universität Dortmund

Dortmund 2006

Erstgutachter:

Prof. Dr. R. Winter

Zweitgutachter:

PD Dr. Claus Czeslik

Tag der mündlichen Prüfung:

17.08.2006

## Acknowledgments

Foremost I would like to thank my supervisor Prof. Dr. R. Winter for giving me the opportunity to work in his research group in University of Dortmund, for his guidance, patience and support throughout my PhD work.

Very special thanks to Dr. Dahabada Lopes for her friendship, advises and support in completing my work. Being a “daughter” was a very nice thing.

I wish to thank to Prof. J.Mignaco, Prof. F. Fontes from Rio de Janeiro University and Dr. Sascha Janosh for the Na<sup>+</sup>,K<sup>+</sup>-ATPase isolation.

I thank to PD Dr. Claus Czeslik and Dr. Jens Müller for being my examination committee.

I thank PD Dr. Claus Czeslik and Stefan Grudzielanek for their help with fluorescence measurements.

I also would like to thank Dr. Karsten Vogt, who allowed me to maintain my (in)sanity during my stay in Germany, and for writing Zusammenfassung.

The large diversity of nationalities in the working group was a great opportunity to meet a very different people and get to know new traditions, therefore I would like to thank especially, Nadeem Javid, Dr. Guido Jackler, Lally Mitra, Vytautas Smirnovas, Shuang Zhao, Nagarajan Periasamy, Gurpreet Singh, Michael Sulc, Chiara Nicolini.

Special thanks to Dr. Sascha Janosch, Andrea Kreusel, Dr. W.Horstmann and Nicolai Smolin for their help after my arrival to Germany, and Berti Schuppan for continually help and a very nice working companion.

Specjalne podziękowania należą się przede wszystkim mojemu tacie oraz całej mojej najbliższej rodzinie, która jak nikt inny dopingowała mnie w trakcie mojej pracy doktoranckiej. A także najbliższym przyjaciółom: Adze oraz jej mamie Magdzie, Fani, Krysi, Macce i Gosi Xeroxom, alchemowi, gosicy, verce oraz kiziorowi.

## Table of Contents

<b>1 Introduction</b> .....	1
<b>2 Biological Membranes</b> .....	4
2.1 Organization of the Membrane.....	4
<b>2.1.1 Lipids</b>	
2.1.1.1 The Structures of Mesophases Lipids.....	10
2.1.1.2 Lipid Phase Transition.....	13
2.1.1.3 The Lateral Pressure Profile.....	14
2.1.1.4 Membrane Fluidity.....	15
<b>2.1.2 Lipid Rafts</b> .....	17
<b>2.1.3 Membrane Proteins</b> .....	19
2.1.3.1 Hydrophobic Matching.....	20
<b>2.1.4 Na<sup>+</sup>,K<sup>+</sup>-ATPase</b> .....	22
<b>2.1.5 Detergents</b> .....	26
2.1.5.1 Protein Solubilization.....	29
2.1.5.2 Protein Reconstitution.....	29
<b>3 Fluorescence Spectroscopy</b> .....	32
3.1 Basic Fluorescence Theory.....	32
<b>3.1.1 Steady-State Measurements</b> .....	35
<b>3.1.2 Fluorescence Lifetime and Quantum Yield</b> .....	35
<b>3.1.3 Fluorophores</b> .....	36
<b>3.1.4 Generalized Polarization</b> .....	41
3.2 Fluorescence Spectrometer.....	42
<b>3.2.1 High Pressure Cell</b> .....	44
3.3 Absorption Spectroscopy.....	46
<b>4 Samples Preparation</b> .....	48
4.1 Isolation and Purification of Na <sup>+</sup> , K <sup>+</sup> -ATPase.....	48
<b>4.1.1 Isolation of Na<sup>+</sup>, K<sup>+</sup>-ATPase from Pig Kidney</b> .....	50
4.2 Chemical Reagents.....	52
4.3 Lipid - Sample Preparation for Fluorescence Spectroscopy.....	53
4.4 Protein Solubilization.....	53
4.5 Protein-Lipid Reconstitution.....	53
4.6 Measurement of the Enzyme Activity.....	54
<b>5 Results and Discussion</b> .....	55
5.1 Naturally Derived Na <sup>+</sup> ,K <sup>+</sup> -ATPase.....	55
5.2 Protein Solubilization.....	58

5.3 Protein-Lipid Reconstitution.....	60
<b>5.3.1 Enzyme Activity in Various Reconstituted Lipid Systems</b>	
<b>at 37 °C.....</b>	<b>62</b>
5.3.1.1 DMPC and DOPC.....	63
5.3.1.2 DMPC with Addition of 15 and 30 mol% of Cholesterol.....	64
5.3.1.3 DOPC with Addition of 15 mol% Cholesterol.....	65
5.3.1.4 DMPC with Addition of 10 mol% DMPS.....	66
5.3.1.5 DOPC/DOPE in Molar Ratio 3:2.....	67
5.3.1.6 POCP/Chol/SM as a Model Raft-Mixture.....	68
<b>5.3.2 Pressure Dependence of the Enzyme Activity at 37 °C.....</b>	<b>69</b>
<b>5.3.3 Pressure/Temperature Dependence of GP Values of the Various</b>	
<b>Lipid Bilayer and Reconstituted Lipid-Enzyme Systems.....</b>	<b>77</b>
<b>6 Summary.....</b>	<b>92</b>
<b>7 Zusammenfassung.....</b>	<b>96</b>
<b>8 References.....</b>	<b>101</b>

# 1 Introduction

The cell is highly organized with many functional units or organelles. Most of these units are surrounded by one or more membranes. The biological membrane is the essential capsule of life. To perform the physiological function of the organelle, the membrane is specialized and contains specific proteins and lipid components that enable them to perform their unique roles. The organization of lipids surrounding membrane proteins can influence their properties. Lipids constitute the fundamental matrix of natural membranes and represent the environment in which many proteins and enzymes display their activity [Parasassi 1990]. In order to understand how proteins and enzymes function in membranes, e.g., in relation to transport, biochemical signaling, energy transduction, receptor-ligand interactions, and nerve activity, it is necessary to determine the ways in which proteins interact with the lipid bilayer, specifically how the proteins influence the local structure and composition of the bilayer, on the one hand, and how changes in the lipid-bilayer properties modulate the functional state of the proteins on the other hand [Mouristen 2005].

In the last decade, many efforts have been devoted to the investigation of the properties of natural membrane components. Among the different spectroscopic techniques employed for the study of phase coexistence and dynamics, fluorescence spectroscopy offers several advantages. In fluorescence, absorption of light of a given wavelength by a fluorescent molecule is followed by the emission of light at longer wavelengths. Fluorescent detection has three major advantages over other light-based investigation methods: high sensitivity, high speed, and safety. Sensitivity is an important issue because the fluorescent signal is proportional to the concentration of the substance being investigated. Relatively small changes in ion concentration in living cells can have significant physiological effects. Fluorescence techniques can accurately measure concentration in the pico- and even femtomolar range. Quantities less than an atomole ( $<10^{-18}$  mol) may be detected.

Temperature and high hydrostatic pressure are well known parameters, often used in studies of bimolecular systems. Mostly, temperature has been used to study the thermodynamic, structural and dynamic properties of membranes. A change in temperature of a system leads to changes of the thermal energy and density at the same time, whereas pressure-dependent studies at constant temperature introduce only changes in density and change intermolecular separations of the system, hence

providing additional information about the energetic and phase behavior of the system without disturbing thermally activated processes [Periasamy 2006]. In physico-chemical and biophysical studies, the interest in pressure as a variable to study also protein un- and refolding has been growing over the last years [Heremans 1998]. Very little is known about pressure effects on membrane proteins, however. Generally, pressure affects chemical equilibria and reaction rates. For example, the activation volume,  $\Delta V^\ddagger$ , of a reaction is given by the pressure dependence of the rate of the reaction,  $k$ ;  $\Delta V^\ddagger = -RT \partial(\ln k / \partial p)_T$ . High hydrostatic pressure has also been exploited in diverse areas of biotechnology, including the ability to modify the catalytic behaviour of enzymes. Reasons for high hydrostatic pressure-induced changes in the rate of enzyme-catalysed reactions may be classified into three main groups: 1) changes in the structure of the enzyme, 2) changes in the reaction mechanism, and 3) the effect of a particular rate-determining step on the overall rate [Parkson 1985]. The effect of pressure on the function of membrane proteins might be due to an increase in lipid packing density or change in phase state, which might lead to a change of the conformation and dynamics of the embedded protein. Furthermore, a direct influence on the structure and conformational dynamics of the enzyme or a change in the substrate binding reaction dynamics could play a role.

Reconstitution of membrane proteins into lipid bilayers is a powerful tool to analyze functional as well as structural areas of membrane protein research. In this study, using fluorescence spectroscopic techniques, the effect of various phospholipid bilayer systems and model raft mixtures on the activity of the enzyme  $\text{Na}^+, \text{K}^+$ -ATPase was investigated.

The  $\text{Na}^+, \text{K}^+$ -ATPase is a member of the P-type ion-transport ATPase that is present in animal plasma membranes and required for cellular homeostasis [Cornelius 2003]. Although investigations on the enzyme have been continuing for more than 40 years, important aspects of this ion-pump are still largely unknown. This includes for example, the modulation of the catalytic activity of the  $\text{Na}^+, \text{K}^+$ -ATPase by plasma membrane lipids into which it is suspended [Cornelius 2001].

First, the activity of  $\text{Na}^+, \text{K}^+$ -ATPase from rabbit kidney – enriched in its partially natural plasma membrane environment - was measured as a function of high hydrostatic pressure, using a kinetic assay which couples ATP hydrolysis to NADH oxidation. In the next step the isolation of a higher amount of the enzyme

from pig kidney was carried out and the enzyme was reconstituted in different kinds of lipid bilayer systems. The lipid bilayer systems were chosen so as to be able to explore various membrane physical properties on the enzyme activity, such as hydrophobic matching, curvature elastic stress, fluidity, and heterogeneity (DMPC, DMPC/15, 30 mol% cholesterol, DOPC, DOPC/DOPE 3:2, DOPC/15, 30 mol% cholesterol, POPC/SM/cholesterol), and the enzyme activity was measured over a wide pressure range. The main goal was to study the effects of hydrostatic pressure and to correlate the structure and conformational properties of the lipid matrix to the function of the enzyme. To this end, enzyme activity studies were also performed over a wide pressure range, varying from ambient pressure up to about 2 kbar. Moreover, the conformation and phase state of the lipid and reconstituted lipid-protein systems have been measured by the Laurdan fluorescence technique. To reveal, if the decrease in enzyme activity upon pressurization is related to pressure-induced lipid phase transitions, the temperature and pressure depended Laurdan generalized polarization (*GP*) values of the various lipid and reconstituted proteolipid systems were measured as a function of temperature and pressure as well. In fact, the lipid matrix turned out to have a drastic effect on the function of the protein also upon pressurization. Interestingly, a biphasic effect of pressure on the activity of the enzyme was found.



## **2 Biological Membranes**

Cell membranes constitute one of the fundamental structural and functional elements of living organisms. The plasma membrane that encloses every cell defines the cell's extent and maintains the essential differences between its contents and the environment [Alberts 1983]. But biological membranes are more than just an inner barrier or covering: they play an active part in the life of the cell. They are highly selective filters, which control the movement of substances into and out of the cells, and regulating the composition of the fluid within individual cells [Brown 1996]. Many important biological processes in the cell either take place at membranes or are mediated by membranes, such as transport, growth, neural function, immunological response, signaling, and enzymatic activity [Mourtsen 2005].

Membranes are also asymmetric; the spaces inside and outside the closed compartments formed by cellular membranes usually have very different composition. That is, each type of integral protein has a single, specific orientation with respect to the cytosolic and exoplasmic faces of a cellular membrane. This absolute asymmetry in protein orientation confers different properties of the two membrane faces [Lodish 2005].

### **2.1 Organization of the Membrane**

Biological membranes are made of three major components: lipids, proteins and carbohydrates [Yeagle 1993]. All, including the plasma membrane and the internal membranes of eukaryotic cells, have a common general structure [Alberts 1983] (Fig. 2.1) According to the Fluid Mosaic Model, a biological membrane is a two-dimensional fluid of oriented proteins and lipids. The lipid bilayer is the basic structure of all cell and organelle membranes. [Singer 1972]. It is now evident that in the plasma membrane of almost all mammalian cells exist also unique lipid domains known as lipid rafts, made up in particular of sphingomyelin, which contain long saturated acyl chains, cholesterol and unsaturated phosphatidylcholines [Eidin 2003, Ahmed 1997]. They have been implicated in processes as diverse as signal transduction, endocytosis and cholesterol trafficking [Pike 2004]. The lipid bilayer is extremely thin in comparison to the cell it encapsulates and its molecular composition depends on the type of cell. Carbohydrates are a minor component with less than 10%

of the dry mass. Lipids and proteins are held together mainly by non-covalent interactions. Weight ratio of proteins and lipids can vary from 1:5 to 5:1 [Mourtsen 2005].

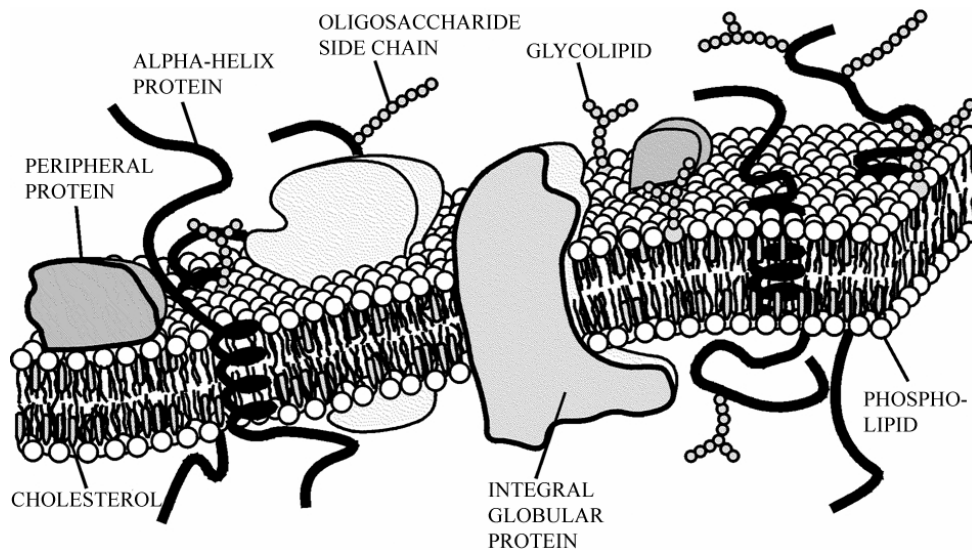


**Figure 2.1:** Scheme of a Biological Membrane composed of a lipid bilayer and proteins.

### 2.1.1 Lipids

The general definition of a lipid is a biological material soluble in organic solvents, such as ether or chloroform. There are approximately  $5 \times 10^6$  lipid molecules in a  $1 \mu\text{m} \times 1 \mu\text{m}$  area of lipid bilayer, or about  $10^9$  lipid molecules in the plasma membrane of a small animal cell.

A common feature of membrane lipids is that they are amphipathic (amphiphilic), which means that they have two different natures, one is polar (hydrophilic) and is stable in aqueous solution, the other is a non polar (hydrophobic) aliphatic or aromatic hydrocarbon, which is most stable in a non-aqueous environment [Houslay 1982].

Hydrocarbon chains can contain different numbers of carbon atoms, and the bonds between the carbons atoms can be single (saturated) or double (unsaturated). A hydrocarbon chain can be turned into a *fatty acid* by attaching a  $-\text{COOH}$  group at the end. The fatty acids are the fundamental building blocks of all lipids in living matter. Plants and animals use a variety of fatty acids with chain lengths ranging from two to

thirty six. The most common chain lengths fall between fourteen and twenty two. Fatty acids are rarely found free in the cell; instead they are chemically linked to a hydrophobic group, e.g., *glycerol*. Glycerol acts as the backbone of the lipid molecule [Mourtisen 2005].

Although biological membranes contain an astonishing variety of lipids we can divide them into three general types:

- Phospholipids
- Glycolipids
- Cholesterol

### ***Phospholipids***

Phospholipids are the major types in the eukaryotic cells. They constitute the fundamental matrix of natural membranes and represent the environment in which many proteins and enzymes display their activity [Parasassi 1990]. Predominant are glycerol-based phospholipids (Fig. 2.2), including phosphatidylcholine PC, phosphatidylethanolamine PE, phosphatidylserine PS, phosphatidylinositol PI and cardiolipin [Vance 1996]. While PC and PE are neutral (zwitter-ionic), PS and PI lipids can be electrically charged. This difference has an important consequence for the capacity of the lipids, when incorporated into a lipid membrane, to bind protein and drugs [Mourtisen 2005].

Glycero-phospholipids are derivatives from *sn*-glycero-3-phosphoric acid with usually two fatty acids esterified in the *sn*-1 and -2 positions of the glycerol moiety. The hydrophobic tails, fatty acid chains, usually contain between 14 and 24 carbon atoms. Both of them or just one can be saturated or unsaturated. Unsaturated chains contain from one to four *cis*-double bonds. Each double bond puts a bend in the fatty acid chain [Brown 1996]. In natural membranes lipids usually contain two different chains and most often one of them is unsaturated.

In large fraction there are also present **sphingosine-based lipids**, including sphingomyelin (Fig. 2.2). It contains, instead of a glycerol backbone, sphingosine, an amino alcohol with a long unsaturated hydrocarbon chain. In sphingomyelin, the terminal hydroxyl group of sphingosine is esterified to phosphocholine, so its hydrophilic head is similar to that of phosphatidylcholine.

### Glycolipids

Glycolipids constitute about 5% of the lipid molecules in plasma membrane [Alberts 2002]. They differ from phospholipids in that glycolipids have a sugar, such as glucose, galactose or mannose, which is directly esterified to the glycerol (Fig. 2.2). Glycolipids in animal membranes almost always contain sphingosine, whereas those in plant membranes contain glycerol. In all cases glycolipids are found on the outer surface of the plasma membrane with their sugars exposed at the cell surface [Lodish 2005].

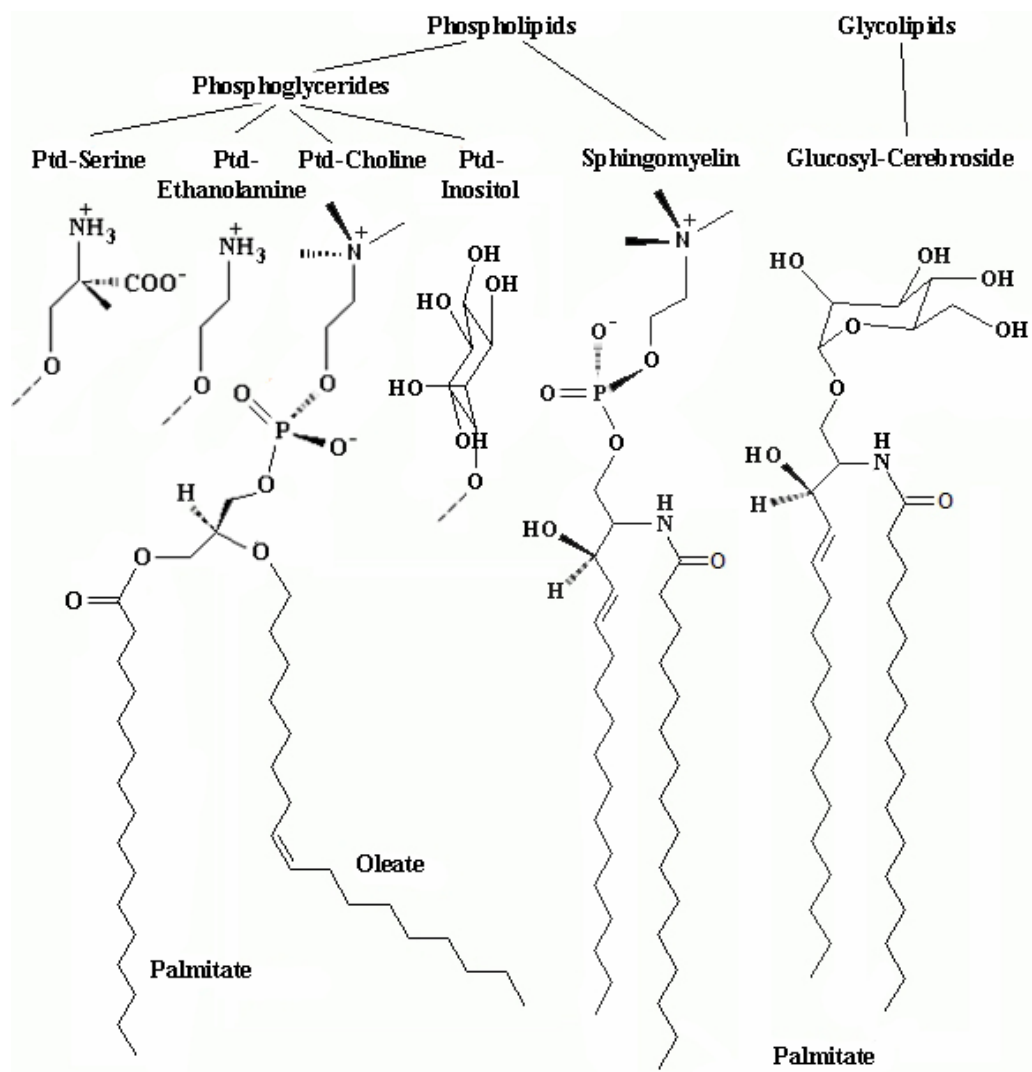


**Figure 2.2:** The major membrane lipids in the plasma membrane. Phosphoglycerides have the lipid chains attached to glycerol. Sphingomyelin contains sphingosine instead of glycerol. Ptd - phosphatidyl.

### Cholesterol

Cholesterol is a member of a further important class of membrane lipids, **the steroids**. It is an important constituent of most mammalian cell membranes and its concentration in various cellular membranes is tightly regulated. This molecule is structurally quite different from the phospholipids and glycolipids and contains a four-ring steroid structure together with a short hydrocarbon side chain and a hydroxyl group (Fig. 2.3). Eukaryotic plasma membranes contain relatively large amounts of cholesterol, in amount ranging between 15-50 % of the total lipids. In contrast, the organelle membranes contain very little: mitochondrial membranes less than 5 % and Golgi membranes about 8 %. Sterols are universally absent in the membranes of all prokaryotes [Raffy 1999].

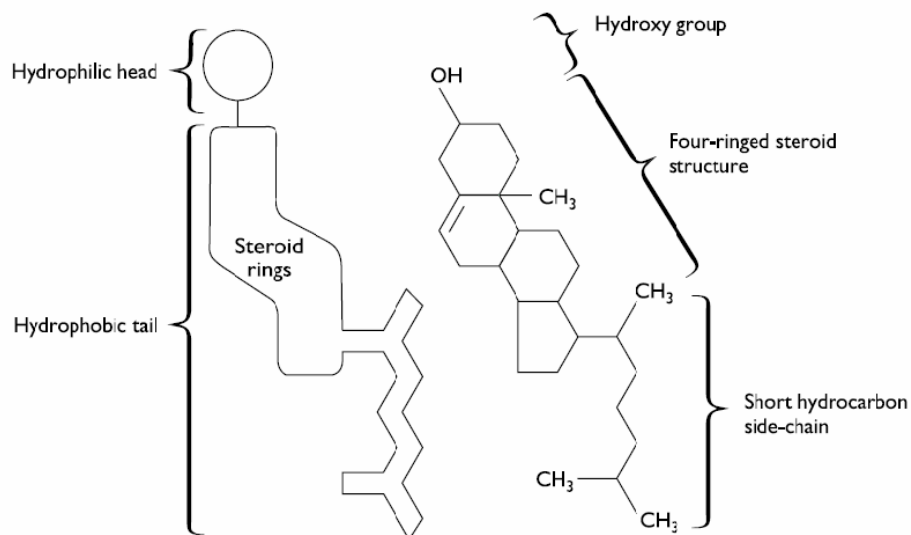


**Figure 2.3:** The structure of Cholesterol.

Cholesterol is a very important determinant of the lipid bilayer thickness, related to its strong tendency to stretch out and order the fatty-acid chains of the phospholipids.

Being an amphiphilic molecule cholesterol easily incorporates into the lipid bilayer, and fits in between the bilayer phospholipids with its hydroxyl group close to the phospholipids heads, and its hydrophobic rings and side-chain buried within the fatty acid chains of the membrane interior [Alberts 2002]. On the one side, cholesterol, due to its hydrophobically smooth and stiff steroid ring structure, has a

preference for having conformationally ordered lipid chains next to it since they provide for the tightest interactions. From this perspective, cholesterol prefers the solid-order lipid phase. On the other side, the solid-ordered phase is a crystalline phase with dense packing order among the lipid molecules. The cholesterol molecule, with its own peculiar size and shape does not fit well into this packing order, whereas there is plenty of free space into the liquid-disordered phase. From this perspective cholesterol prefers the liquid disordered phase [Mourtisen 2005, Lodish 2005]. To solve this problem in 1987 Danish biophysicists proposed a new phase the liquid-ordered phase (Fig. 2.4). This phase is in between the two normal lipid bilayer phases. This liquid-ordered phase is a genuine liquid with positional disorder and high lateral mobility of the membrane molecules. Furthermore, the lipid chains have a substantial degree of conformational order. When introduced into the liquid membrane phase, cholesterol leads to a large increase in membrane thickness.

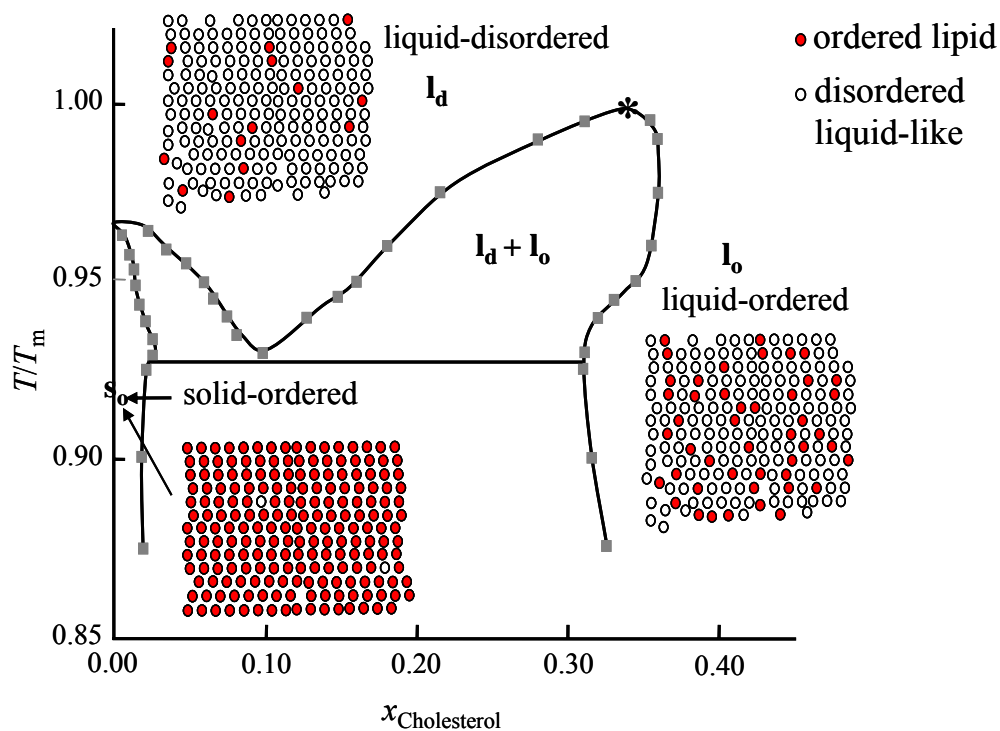


**Figure 2.4:** The proposed scheme of phases, formed by sterols.

(Ipsen et al., *BBA* **905** (1987) 162)

Consequently, cholesterol has a remarkable dual effect on membranes. The rigid steroid ring interacts with the neighboring regions of the lipid tails and stiffens them, making the membrane less fluid at growth temperatures around 37 °C. Below the temperature that causes a phase transition, cholesterol keeps the membrane in a fluid state by preventing the hydrocarbon fatty acyl chains of the membrane lipids from binding to one another, thereby offsetting the drastic reduction in fluidity that would otherwise occur at low temperature [Lodish 2005].

The molecular structure of cholesterol is very similar to that of bile salt, vitamin D, and sex hormones. Cholesterol is one of several members of the sterol family that play similar roles in different types of organisms, e.g., ergosterol in fungi and sitosterol in plants.

Cholesterol has a high priority as a research area but it also draws an even higher attention among the public. The reason for this is that cholesterol is known to be related to the number of heart disease and atherosclerosis. This is somehow paradox, since cholesterol is an important compound of all cells in our body, and metabolite and source of vitamins and hormones.

### **2.1.1.1 The Structures of Mesophases Lipid**

When lipid molecules are surrounded on all sides by an aqueous environment, they tend to aggregate so as to bury their hydrophobic tails and leave their hydrophilic heads exposed to water [Alberts 1983]. They can form spherical *micelles* (Fig 2.5b), with the tails inward or they can form bimolecular sheets, called *bilayers* (Fig 2.5a), with their hydrophobic tails sandwiched between the hydrophobic heads. Obviously open ends cannot be tolerated and the lipid bilayers have to close onto themselves and form closed objects, called *liposomes*, to eliminate the edges where the tails would be in contact with water (Fig 2.5c). Liposomes are very useful model membranes for research. Cholesterol, although amphipathic, cannot form a bilayer on its own, and only can be incorporated into phospholipid bilayers.

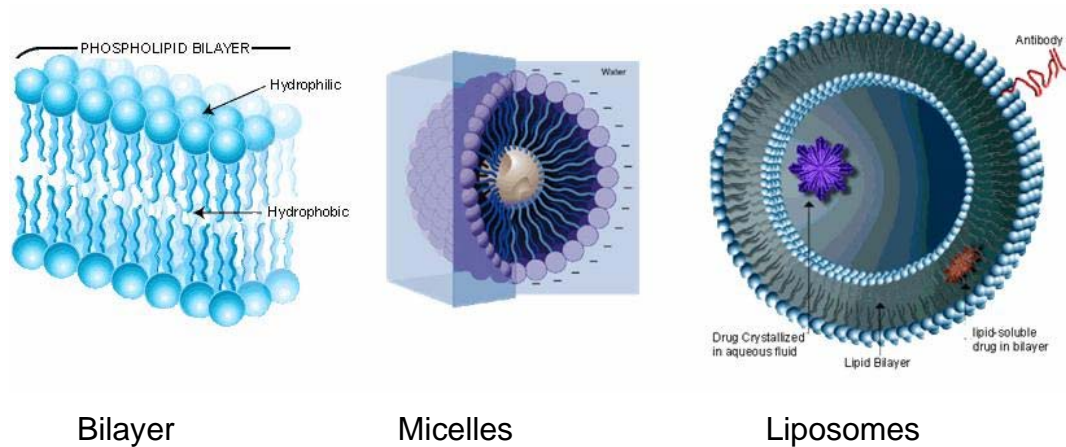


**Figure 2.5:** Self-organization of lipids in association with water

Membrane lipids are invariably polymorphic, that is, they can exist in a variety of different kinds of organized structures. Due to the large hydrophobic effect most phospholipid bilayers are able to associate with water even at extremely low concentrations (<10–12 mol/l). In addition to bilayer lamellae, polar lipids in water form a variety of structures, including tubes, rods, and three-dimensionally periodic assemblies with cubic symmetries (Fig. 2.6). The different structures have different curvature and are arranged in accordance with the value of packing parameter.

$$P = \frac{v}{a \cdot l}$$

Parameters “a”, “v” and “l” are described in Fig. 2.6. Packing parameter, describe the effective shape of a lipid molecule, as a measure of its ability to fit into a particular lipid aggregate. Since the volume of a cylinder-shaped molecule is  $a \cdot l$ , a deviation of  $P$  from unity suggests that non-lamellar aggregates can be expected.  $P > 1$  corresponds to a shift from cylindrical shape toward an inverted cone, whereas  $P < 1$  corresponds to a shift toward a normal cone. The effective shape of lipid molecules determines their ability to form a stable bilayer. The more non-cylindrical their shapes are, the less stable a bilayer will form. The monolayers display a so-called *spontaneous curvature* [Mourtisen 2005]. When a bilayer is made of monolayers with nonzero spontaneous curvature, it becomes subject to a *curvature stress field*. The stress field can be



changed enzymatically, or released locally by changes in the local molecular composition.

Phospholipids bilayers are important model systems for biological membranes, which have been intensively studied with regard to structure, phase transitions, transport and elasticity properties, as well as interaction with other macromolecules [Cevc 1993].

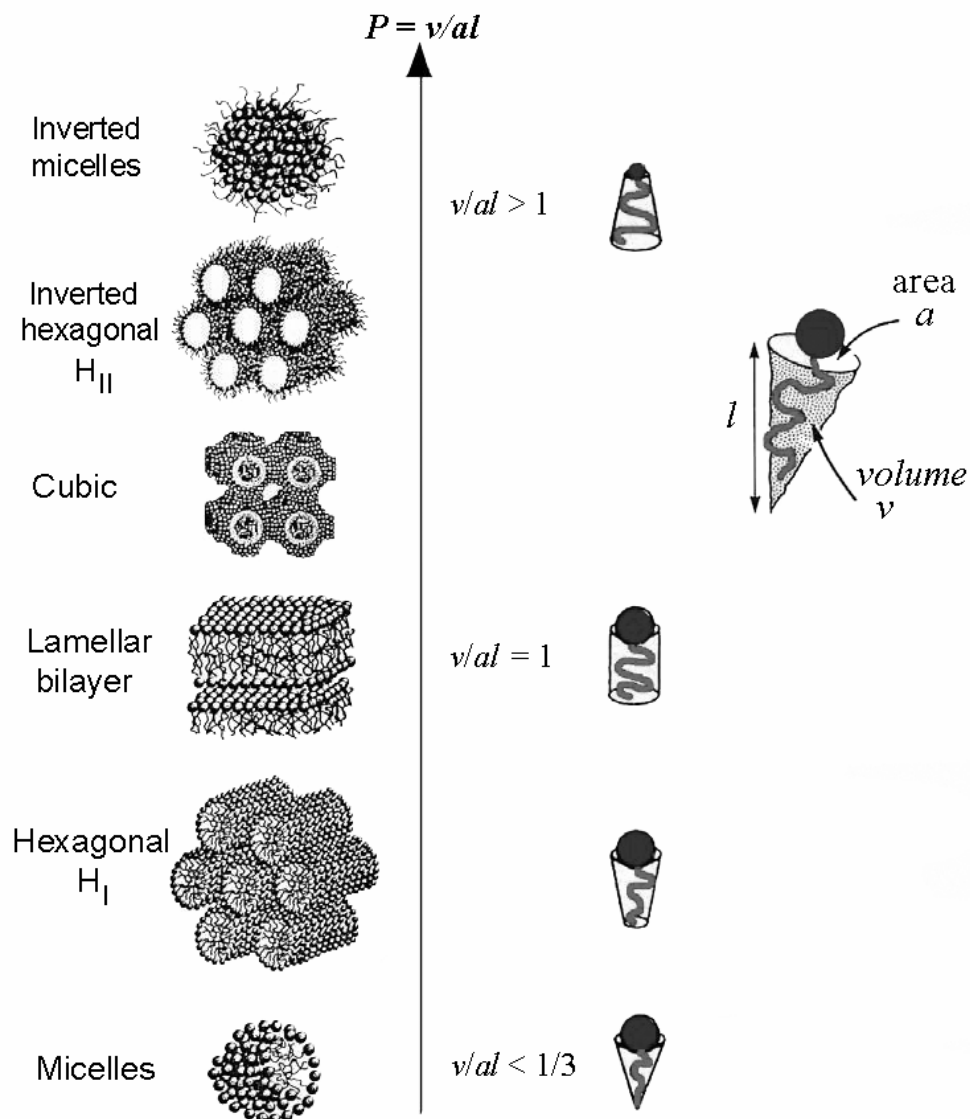


**Figure 2.6:** Different structures of lipids with different curvature, arranged in accordance with the value of the packing parameter  $P=v/al$

### 2.1.1.2 Lipid Phase Transition

A phase transition (or phase change), is the transformation of a thermodynamic system from one phase to another. The distinguishing characteristic of a phase transition is an abrupt sudden change in one or more physical properties. Saturated phospholipids often exhibit two thermotropic lamellar phase transitions, a gel to gel ( $L_{\beta'}/P_{\beta'}$ ) pre-transition and a gel to liquid-crystalline ( $P_{\beta'}/L_{\alpha}$ ) main transition at a higher temperature  $T_m$  (Fig. 2.7).

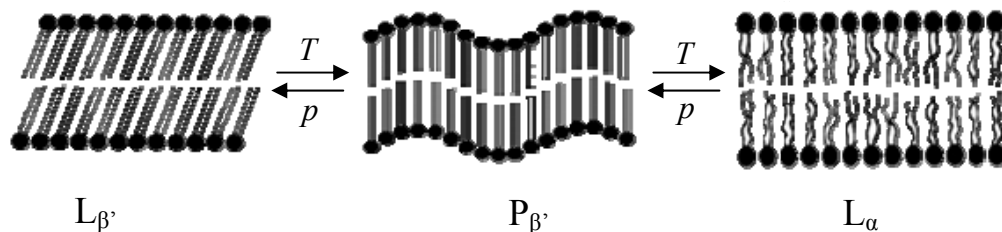


**Figure 2.7:** Phase transitions in lipid bilayers.

In the fluid-like  $L_{\alpha}$  phase the hydrocarbon chains of the lipid bilayers are conformationally disordered, whereas in the gel phases the chains are more extended and ordered. In addition to these thermo tropic phase transitions, also high hydrostatic pressure-induced phase transformations have been observed [Winter 1998]. A number of new phases, so-called *meso-phases*, in between those of solids and liquids can be found (Fig. 2.8). These phases have elements of order as well as disorder. In general, lipids with short or unsaturated fatty acyl chains undergo the phase transition at lower temperature than do lipids with long or saturated chains.

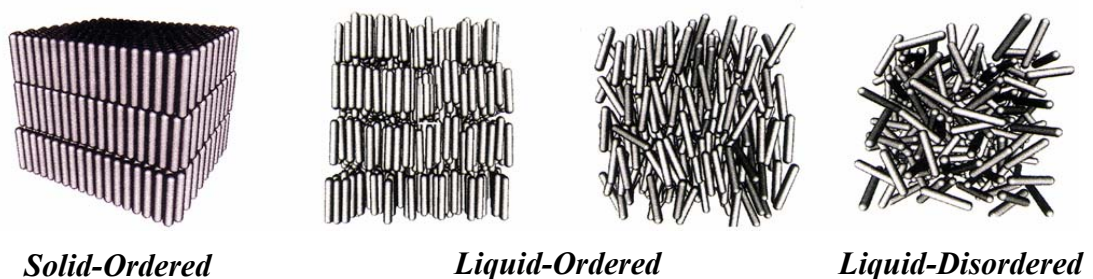


**Figure 2.8:** Different types of possible lipid phases.

### 2.1.1.3 The Lateral Pressure Profile

The lateral pressure profile is one of the fundamental physical properties of the lipid bilayer. Figure 2.9 shows a lipid bilayer indicating the forces that act to stabilize the layer. When the bilayer is in equilibrium, these forces have to sum up to zero. Since the forces, due to the finite thickness of the bilayer, operate in different planes, the pressures are distributed nonevenly across the bilayer.

The lateral pressure effect is built up from three contributions:

- A positive pressure resulting from the repulsive forces that act between head groups.
- A negative pressure (the interfacial tension) that acts in the hydrophobic-hydrophilic interface by the hydrophobic effect.
- A positive pressure arising from the entropic repulsion between the flexible fatty-acid chains.

Due to the small thickness of the bilayer, rather large interfacial tension ( $\gamma = 50$  mN/m) from the two interfaces of the bilayer has to be distributed over a very short range. This implies that the counteracting pressure from the fatty-acid chains has to have an enormous density, around several hundreds of atmospheres. The lateral pressure has to counterbalance this tension over a distance corresponding to the bilayer thickness  $d_L \sim 2.5\text{-}3$  nm. The lateral pressure density of the bilayer then becomes  $2\gamma/d_L$  which amounts on average to about 350 atm. This magnitude of pressure provides a nonspecific coupling between the lipid membrane and the function of proteins [Mourtisen 2005].

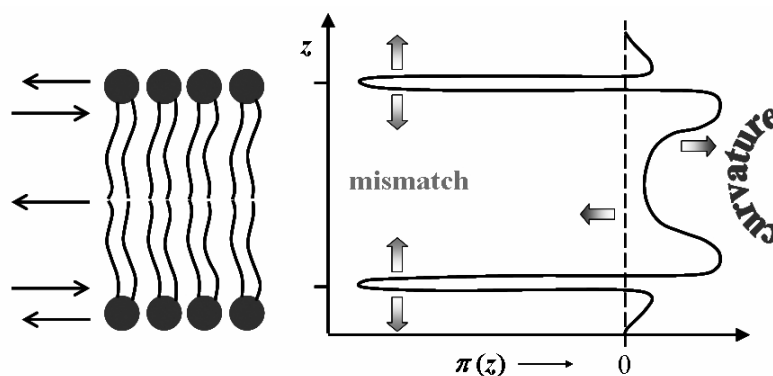


**Figure 2.9:** Lateral pressure profile of a lipid bilayer.

### 2.1.1.4 Membrane Fluidity

Cell membranes are dynamic, fluid structures, and most of their molecules are able to move in the plane of the membrane (Fig. 2.10). Fluidity is the quality of ease of movement and represents the reciprocal value of membrane viscosity [Garcia 2005]. In general the terms mean a combination of different types of mobility of membrane components. These include:

- lateral diffusion of molecules in the plane of the membrane;
- transversal diffusion of molecules from one monolayer to the other, flip-flop;
- conformational change;
- rotation
- protrusion out of the bilayer plane

These motions range over an enormous time span, from picoseconds to hours. Conformational changes and rotation are the fastest and occur in a time scale of picoseconds to nanoseconds. Due to the lateral diffusion lipids are able to explore the entire lipid bilayer or membrane. The motion of lipid molecules from one monolayer leaflet to the other, the so-called flip-flop process is extremely slow, on the scale of hours. In biological membranes, special membrane proteins facilitate and redistribute lipid molecules between two monolayer leaflets [Mourtsen 2005].

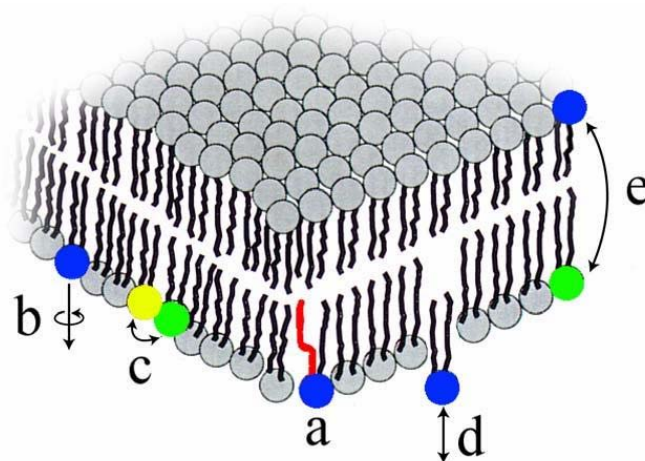


**Figure 2.10:** Types of lipid molecule motions in a lipid bilayer. a) Conformational change. b) Rotation. c) Lateral diffusion. d) Protrusion out of the bilayer plane. e) Flip-flop.

Fluid properties of biological membranes are essential for numerous cell functions including cell growth, solute transport, signal transduction and membrane – associated enzymatic activities. If the lipid membrane is taken into a solid phase, all dynamical processes slow down significantly.

The modulators of lipid fluidity can be divided into chemical and physical effectors:

- the length and degree of unsaturation of the fatty acid chains
- the nature of polar head groups, which influences the mobility of the hydrocarbon chains
- the content of cholesterol
- the level of membrane protein
- temperature
- pressure

An important determinant of membrane fluidity is cholesterol. Eukaryotic animal membranes contain approximately one cholesterol molecule for every two phospholipid molecules [Garcia 2005]. Details of the influence of cholesterol are described above.

The fluidity can also be affected by temperature and pressure. At low temperatures and high pressures, the hydrocarbon tails of lipids can pack closely to form an ordered arrangement, gel state.

### 2.1.2 Lipid Rafts

In the past few years there has been increased interest for the existence of lipid micro-domains, called lipid rafts (Fig. 2.11), in cell membranes, which may play also an important role in many biological processes. Proteins may be selectively included in or excluded from these micro-domains, which are postulated to have important roles in membrane signal transduction [Simons 1997, Simons 2000, Yuan 2002]. They can also serve as portals of entry for various pathogens, including viruses, bacteria and their toxins. There is increasing evidence that lipid rafts are involved in the conformational changes underlying the formation of amyloid plaques in Alzheimer's and prion diseases [Brown 1992].

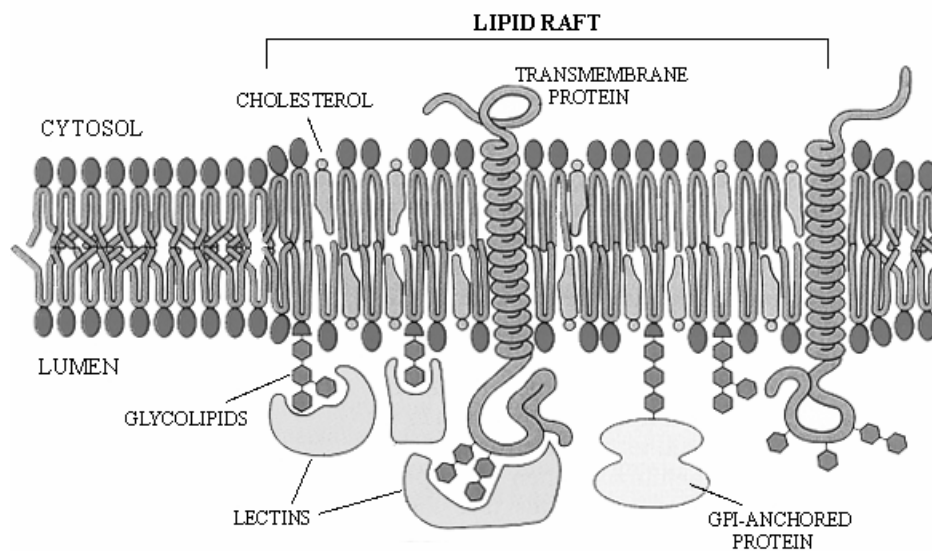


**Figure 2.11:** Proposed structure and organization of a lipid raft domain in the plasma membrane.

Rafts were first detected following extraction of chilled membranes with cold, non-ionic detergent [Brown 1992, Cerneus 1993, Gorodinsky 1995, Baird 1999, Crowe 2002]. The insoluble fraction, initially called detergent-resistant membranes (DRMs), was found to be greatly enriched in sphingolipids and cholesterol [Hanada 1995]. The presence of long and saturated acyl chains in sphingolipids allows cholesterol to become tightly intercalated with such lipids, resulting in the organization of liquid ordered ( $l_o$ ) phases. By contrast, unsaturated phospholipids are loosely packed and

form a disordered state (usually indicated as liquid crystalline or liquid-disordered  $l_d$ ) [Kahya 2003, Brown 2000]. The difference in packing ability leads to phase separation [Brown 1998, Fridriksson 1999]. More recently, along with a number of techniques employed to address questions on rafts [Heerklotz 2002, Wilson 2000, Varma 1998], important contributions have also come from optical microscopy [Kenworthy 2000, Schutz 2000]. Direct visualization of raft-like domains in model bilayer membranes has provided a tangible proof for the coexistence of liquid-ordered and liquid-disordered phases [Bagatolli 2000, Gratton 2001]. In cell membranes, individual rafts are extremely small ( $\sim 70$  nm), and are thought to diffuse freely [Varma 1998]. The rafts in cells appear to be heterogeneous both in terms of their protein and their lipid content, and can be localized to different regions of the cell. Suitable model systems for studying biophysical properties of lipid rafts are lipid vesicles composed of three-component lipid mixtures, such as POPC/SM/cholesterol, which exhibit a rich phase diagram, including raft-like liquid-ordered/liquid-disordered phase coexistence regions.

### 2.1.3 Membrane Proteins

Although the basic structure of biological membranes is provided by the lipid bilayer, membrane proteins perform most of the specific functions of membranes. Proteins in the membrane can act as pumps, channels, receptors, energy transducers and enzymes. Accordingly, the amount and types of protein vary considerably from membrane to membrane. The more active a membrane is in metabolism, the more protein it contains. The asymmetry for membrane proteins is absolute. Once proteins are assembled into a membrane, their orientation with respect to the membrane remains fixed [Reithmeier 1996].

Membrane proteins can be classified into few groups based on the nature of their interaction with the membrane (Fig. 2.12):

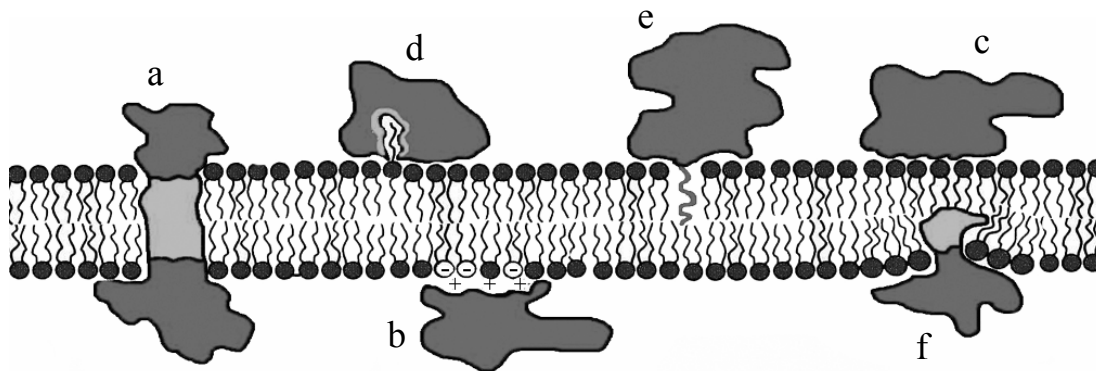


**Figure 2.12:** Different types of membrane proteins: a) Integral. b) Electrostatic binding. c) Nonspecific binding. d) Anchored. e) Anchored by a fatty-acid chain. f) Amphiphilic.

Extrinsic or peripheral proteins are not associated with the hydrophobic core of the lipid bilayer [Reithmeier 1996]. These proteins are exposed at only one side of the membrane. Some of these are anchored to the cytosolic surface by an amphipatic  $\alpha$  helix. Others are attached to the bilayer solely by a covalent attached lipid chain, either a fatty acid chain, in the cytosolic monolayer, or via an oligosaccharide linker, to phosphatidylinositol in the noncytosolic monolayer. Finally many proteins are weakly bound to one or the other surface of the membrane by non-covalent interactions with other (intrinsic) membrane proteins. All these proteins can be removed by mild treatments, for example mild non-ionic detergents such as Triton X-100 or simply by alkaline pH conditions.



Next group are intrinsic (transmembrane) membrane proteins, which extend through the lipid bilayer with part of their mass on either side. They are also amphiphatic, having hydrophobic and hydrophilic regions. Their hydrophobic regions pass through the membrane and interact with the hydrophobic tails of the lipid molecules. Their hydrophilic regions are exposed to water on either side of the membrane [Alberts 2002]. Examples of this type of proteins include channels, pore complexes, pumps, and receptors.

These proteins can be only removed by agents that disrupt hydrophobic association and destroy the bilayer.

### **2.1.3.1 Hydrophobic Matching**

Hydrophobic matching means that the hydrophobic length of the transmembrane domain is matched to the hydrophobic thickness of the lipid bilayer. This effect arises from the avoidance of water by nonpolar side-chains of amino acids such as isoleucine, leucine, valine and phenylalanine [Yeagle 1983]. It includes energetic advantages and therefore hydrophobic mismatch could be a controlling mechanism for the way proteins interact with lipids in membranes [Mourtisen 2005]. It has been recognized for some time that membrane proteins have a more hydrophobic amino acid composition than soluble proteins. For example the transmembrane portion of the photoreaction centre is enriched in hydrophobic amino acids in 44% [Yeagle 1983]. Hydrophobic interactions play a major role in stabilizing membrane structures and reconsidering the problem in terms of protein and lipid hydrophobic matching offers an attractive possibility. Any integral protein is characterized by a hydrophobic length  $d_p$  and a lipid bilayer by a hydrophobic thickness  $d_L$  directly related to the length of the acyl chains [Dumas 1999]. In lipid mixtures and as a direct consequence of the hydrophobic matching condition, a transmembrane protein is expected to be solvated by the lipid species capable of best matching its hydrophobic surface. Figure 2.13 shows an example of the hydrophobic matching principle. In panel “a” the hydrophobic thickness of a lipid bilayer is smaller than the hydrophobic length of the transmembrane protein. In order to compensate for the mismatch, the lipid molecule closest to the protein stretch out to cover the hydrophobic core of the protein. This leads to a perturbed region around the protein, which is characterized by a larger average lipid thickness and a higher conformational chain order. Panel “b” shows a

case in which the integral membrane protein is positioned in a lipid bilayer that is slightly too thick. The consequence of hydrophobic mismatch is a local thinning of the membrane around the protein.

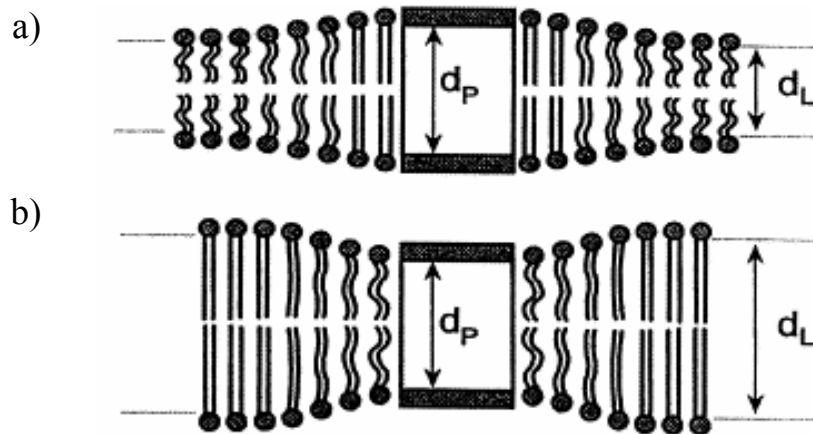


**Figure 2.13:** Schematic representation of an intrinsic membrane protein of hydrophobic length  $d_P$  embedded in a lipid bilayer in which the unperturbed hydrophobic thickness  $d_L$  is smaller (a) or larger (b) than  $d_P$ .

For the lipid bilayer with several different lipid species, the perturbed region around the mismatched protein could imply a local de-mixing of the lipid molecules such that the lipid species that provide for the better hydrophobic match are recruited at the lipid-protein interface.

If there is more than one protein, the possibility arises of two or more proteins sharing the perturbed region of lipids. This would be energetically favorable and therefore leads to an effective attraction between proteins [Mourtsen 2005].

### 2.1.4 Na<sup>+</sup>,K<sup>+</sup>-ATPase

The Na,K-ATPase is an integral membrane protein found in all superior eukaryotic cells and play a fundamental role in numerous physiological processes, e.g., nerve, kidney, and heart function. The enzyme was discovered by Skou (1957) and has been isolated in membrane-bound form from tissues rich in the protein such as mammalian kidney [Mohraz 1999].

The concentration of K<sup>+</sup> is typically 10 to 20 times higher inside cells than outside, whereas the reverse is true of Na<sup>+</sup> [Alberts 2002]. These concentration differences are maintained by a Na<sup>+</sup>, K<sup>+</sup> pump, which is responsible for the active transport of sodium and potassium ions through the plasma membrane coupled with ATP hydrolysis [Santos 2002]. This enzyme is a heterodimer consisting of three subunits: the  $\alpha$  subunit, with a molecular mass of about 110 kDa; the  $\beta$  subunit, highly glycosylated, with a molecular mass of about 50 kDa, and the  $\gamma$  subunit, with molecular mass of about 15 kDa (Fig. 2.14). The  $\alpha$  subunit is responsible for the enzymatic activity [Santos 2002]. It contains the binding and phosphorylation ATP domain, as well as essential amino acids for the binding of sodium, potassium and some inhibitors. The  $\beta$  subunit has a structural function and is important for membrane enzyme insertion [Skou 1992, Pressley 1996, Jorgensen 1998]. A small hydrophobic protein, the  $\gamma$ -subunit, has been shown to associate with the  $\alpha$ -subunit of Na<sup>+</sup>, K<sup>+</sup>-ATPase in a tissue-specific manner. The  $\gamma$ -subunit is not essential for Na<sup>+</sup>, K<sup>+</sup>-ATPase activity, but modulates the affinity of the enzyme for ATP and K<sup>+</sup> [Jorgensen 1982].

In the plasma membranes, the  $\alpha$  and  $\beta$  subunits build functional oligomers of the ( $\alpha\beta$ )<sub>2</sub> type or oligomers with superior structure ( $\alpha\beta$ )<sub>n</sub> [Brotherus 1981, Linnertz 1998, Hayashi 1997]. Na, K-ATPase is specifically inhibited by cardiac glycosides such as ouabain that bind to the extracellular domains. Another potent inhibitor of the enzyme is orthovanadate [MacGregor 1993, Kasturi 1998, Fedsova 1998].

The Na<sup>+</sup>, K<sup>+</sup>-ATPase is classified as a a member of the P-type ion-transport ATPase because the ATP hydrolysis reaction, in the presence of Na<sup>+</sup>, involves formation of an acid anhydride between phosphate and the Asp 369 amino acid residue located in the catalytic ATP site. In addition to the Na<sup>+</sup>, K<sup>+</sup> pump, the P-type transport ATPase family includes Ca<sup>2+</sup> pumps that remove Ca<sup>2+</sup> from the cytosol after

signalling events and the  $H^+$ ,  $K^+$  pumps that secrete acid from specialized epithelial cells in the lining of the stomach [Alberts 2002].

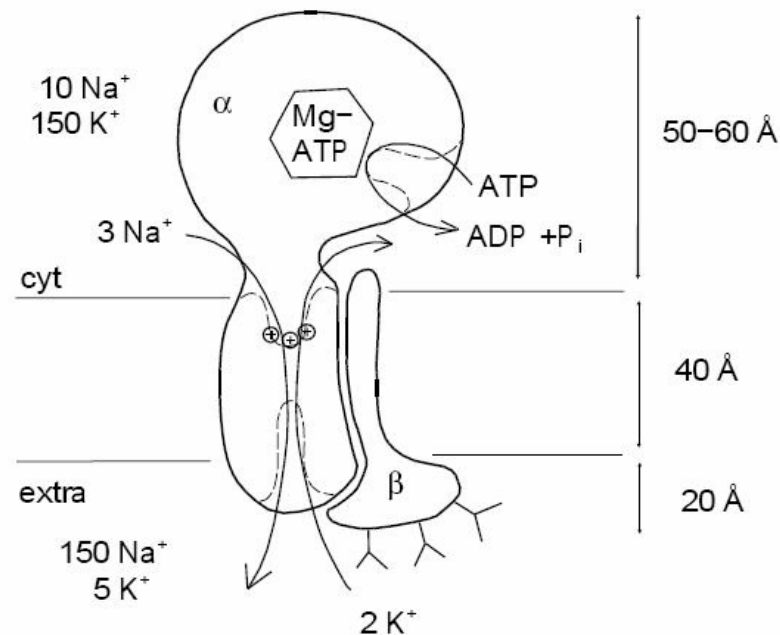


**Figure 2.14:** Scheme of subunits organization in  $Na^+,K^+$ -ATPase. (from Anne Schneeberger dissertation, Konstanz University).

The  $Na^+,K^+$ -ATPase couples the free energy of ATP hydrolysis to the establishment of the electrochemical gradients for  $Na^+$  and  $K^+$  across the plasma membrane [Cornelius 2003]. The catalytic coupling is generally described in terms of the Albers-Post model (Fig. 2.15). This simple model considers two conformations of the enzyme,  $E_1$  and  $E_2$ , which can be either in a phosphorylated or an unphosphorylated state [Humphrey 2002].

The first steps are the ATP accelerated release of two occluded  $K^+$  at the cytoplasmic face of the enzyme and subsequent binding of three cytoplasmic  $Na^+$ . This step is associated with a conformational change from the low  $Na^+$  | high  $K^+$  -affinity form ( $E_2$ ) to the high  $Na^+$  | low  $K^+$  -affinity form ( $E_1$ ). Then follows phosphorylation of the enzyme with the occlusion of  $Na^+$ . Via a conformational change from  $E_1 \sim P$  to  $E_2 \sim P$ , the three  $Na^+$  are released to the extracellular side. Finally, two extracellular  $K^+$  are bound, and dephosphorylation leads to the occlusion of the bound  $K^+$  (Fig. 2.16). Two of the reactions (1 and 3) are associated with thermally driven transitions (i.e., conformational changes) [Cornelius 2003].

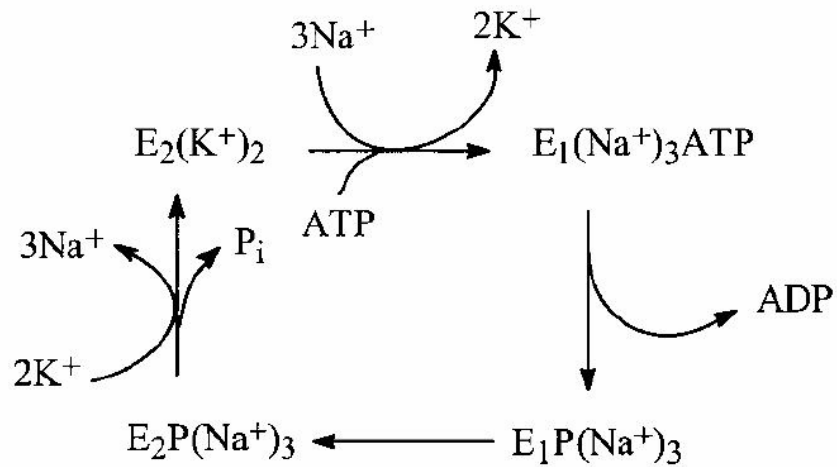


**Figure 2.15:**  $\text{Na}^+, \text{K}^+$ -ATPase cycle, described by the Albert-Post cycle.

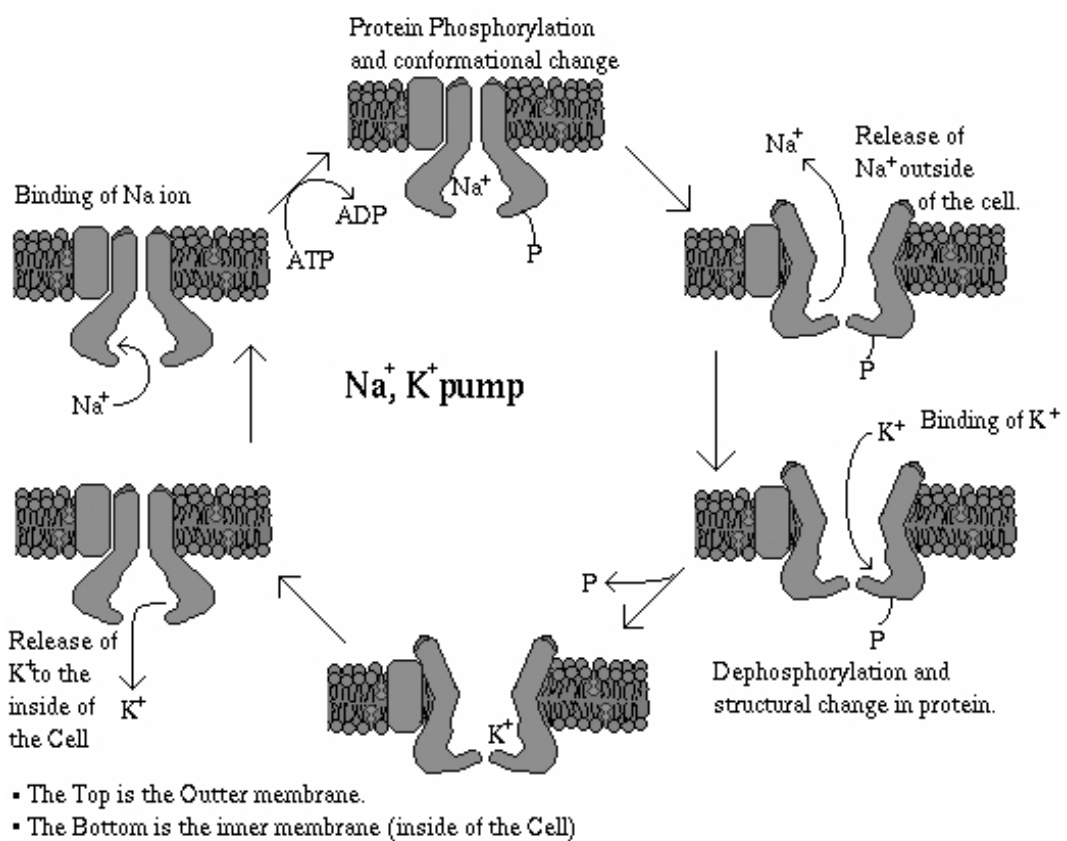


**Figure 2.16:**  $\text{Na}^+, \text{K}^+$ -ATPase cycle diagram

Temperature and high hydrostatic pressure are well known parameters, often used in bimolecular systems studies. Nowadays it is well known that proteins in solution are marginally stable under conditions of high temperature and pressure [Hermans 1998] and  $\text{Na}^+, \text{K}^+$ -ATPase is also inhibited by increased hydrostatic pressure. In principle one can postulate four general mechanisms of the enzyme inhibition [Chong 1985]:

- Increased packing and order of the lipids that would hinder conformational changes of the embedded protein
- Large volume changes of the protein that are independent of the physical state of the lipid
- Dissociation of subunits if the enzyme is oligomeric
- Decreased substrate binding

Certainly, as has been shown by many studies on phospholipid bilayer model systems, by increasing pressure of a few hundred bar, the acyl-chain conformational order drastically increases and various gel-fluid coexistence regions and gel-phases may be induced [Winter 2002, Ulmer 2002].

Later it was found that high pressures up to 2 kbar causes the dissociation of protein subunits in  $\text{Na}^+, \text{K}^+$ -ATPase in aqueous solution, and very high hydrostatic pressure, above 2.2 kbar irreversibly destroys the membrane structure, due to protein unfolding and interface separation [Kato 2002].

### 2.1.5 Detergents

Detergents are surface-active molecules that self-associate and bind to hydrophobic surfaces in a concentration-dependent manner [Gravito 2001]. The amphipatic character of detergents is evident in their structures, which consist a polar (head) group at the end of a long hydrophobic carbon chain (tail). In aqueous solution they exhibit unique properties and spontaneously form spherical structures called micelles. The interaction of detergents with membranes was actively explored 30-35 years ago, when the usefulness of detergent solubilization for isolating and characterizing integral membrane proteins was first appreciated [Brown 2000]. They serve as tools to isolate, solubilize and manipulate membrane proteins for subsequent biochemical and physical characterization. Many of the successful methods for reconstituting and crystallizing membrane proteins rely on the unique behavior of detergents (Gravito 2001). Detergents permit us to study the detailed properties of membrane proteins in protometric and self-associated states as well as their interactions with other proteins.

The most common use of detergents in biochemical research is based on their ability to solubilize membrane proteins by mimicking the lipid-bilayer environment. Micelles formed by detergents are to some extent analogous to bilayers of the biological membranes. Detergent solubilization is required as a first step for reconstitution [le Maire 2000].

The important parameter which describes one of the general properties of detergents is *critical micelle concentration* (cmc). The cmc can be defined as the minimum concentration of detergent above which monomers cluster to form micelles. The cmc varies with conditions, including pH, ionic strength, temperature as well as the presence of protein, lipid and other detergent molecules. The cmc decreases with the length of the alkyl chain of the detergent and increases with the introduction of double bonds and branch points [Bhairi 2001, Seddon 2004].

Dissolution of membranes by detergents can be divided into different stages (Fig. 2.17). At low concentration, detergents bind to the membrane by partitioning into the lipid bilayer. At higher concentrations, when the bilayers are saturated with detergents, the membranes disintegrate to form mixed micelles with the detergent molecules. In the detergent-protein mixed micelles, hydrophobic regions of the membrane proteins are surrounded by the hydrophobic chains of micelles. In the final

stages solubilization of the membranes leads to the formation of mixed micelles consisting of lipids and detergents and detergent micelles containing protein [Bhairi 2001].

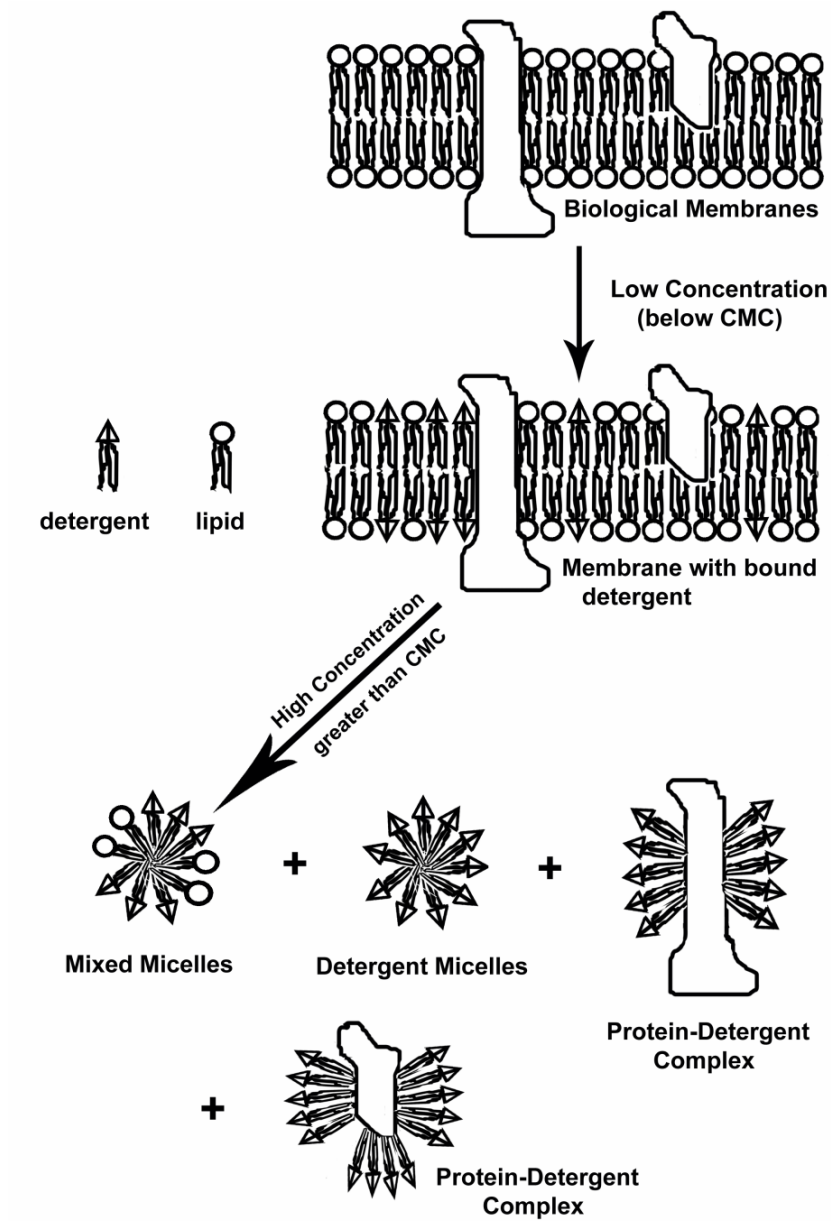


**Figure 2.17:** Scheme of the protein solubilization.



### ***Classification of detergents***

A large number of detergents with various combinations of hydrophobic and hydrophilic groups are now commercially available. The choices of detergent for solubilizing membrane proteins are influenced by the type of work to be carried out. Based on their structure detergents can be classified into four major categories:

*Ionic detergents*, which contain a head group with a net charge. They can be either negatively (anionic) or positively charged (cationic). A well known ionic detergent is sodium dodecyl sulfate, SDS, which contain the negatively charged sulfate group. These types of detergents are usually very effective in the membrane solubilization, although always denaturing to some extent.

*Nonionic detergents*, contain uncharged, hydrophilic head groups of either polyoxyethylene (Triton) or glycosidic groups (octyl glucoside) These detergents are know as “mild” and relatively non-denaturing as they suit better for breaking lipid-lipid and lipid-protein interactions rather than protein-protein interactions.

*Zwitterionic detergents*, combine the properties of both, ionic and nonionic type of detergents. In general they do not possess a net charge and they lack conductivity as nonionic detergents but are more deactivating. However, like ionic detergents they are efficient at breaking protein-protein interactions. Examples are CHAPS or Zwittergent 3-X.

*Bile Acid Salts* are ionic detergents which differ from SDS in that their backbone consist of a rigid steroidal hydrophobic group (e.g., sodium salts of cholic and deoxycholic acids). Bile acid salts have a polar and apolar face, instead of well defined polar head group. Because of this, they form small aggregates and not spherical micelles. They represent a class of relatively mild detergents.

### 2.1.5.1 Protein Solubilization

The foremost challenge in the solubilization of a membrane protein is obtaining a soluble protein in a stable form that retains its original function. A detergent that has been used with great success in  $\text{Na}^+$ ,  $\text{K}^+$ -ATPase solubilization is octaethylene glycol monododecyl ether ( $\text{C}_{12}\text{E}_8$ ). Different results showed that  $\text{Na}^+$ ,  $\text{K}^+$ -ATPase previously treated with sodium dodecyl sulphate (SDS) can be solubilized with  $\text{C}_{12}\text{E}_8$  in an active form where most of the kinetic and conformational properties of the enzyme are preserved after solubilization [Silvius 1992, Cornelius 1991]. Due to three important factors this non-ionic detergent is used for the solubilization of protein membranes: 1) its efficiency in breaking the lipid-lipid and lipid-protein interactions, 2) its inefficiency in weakening protein-protein interactions, and 3) its property of being less denaturing than the ionic detergents [Bhairi 2001, Santos 2002].

An excess of detergent is normally employed in solubilization of membrane proteins as this ensure complete dissolution of the protein. Unfortunately, this excess can disrupt and complicate further experimental work, so often must be removed.

### 2.1.5.2 Protein Reconstitution

The study of the transport process itself can only be carried out in the presence of an impermeable membrane barrier, which necessitates that the transport protein be inserted into a lipid bilayer membrane. This process is known as reconstitution and requires removal of the detergent (Fig. 2.18). Few methods are known for removal of detergents, based on detergent that we are using, the rate of detergent removal, the chosen lipids, the molecular behavior of the protein and the ionic conditions (Cornelius 2001, de Lima Santos 2005).

- *Dialysis*. It was one of the first proposed techniques for vesicle reconstitution. During this process detergent solutions are diluted below the cmc what leads to disintegration of micelles to detergent monomers. The size of monomers is smaller and they can be easily removed by dialysis. This technique is more practical with detergents with high cmc value.

- *Gel Chromatography* takes advantage of the different accessibility to the pores of a gel by mixed micelles as compared to the vesicles [Ollivon 2000].
- *Ion-exchange Chromatography*, takes advantage from the difference in charge between protein-detergent micelles and homogenous detergent vesicles. Using *nonionic* or *zwitterionic* detergents conditions can be selected so that protein-detergent micelles retain on the column and protein-free micelles pass through. The protein can then be eluted by a change in ionic strength or pH.
- *Hydrophobic Adsorption* exploits the ability of detergents to bind to insoluble hydrophobic resins or “beads”, through the interaction of their hydrophobic detergent tail with the hydrophobic surface of the bead. The resins with the bound detergent are then removed by centrifugation or filtration [Seddon 2004].

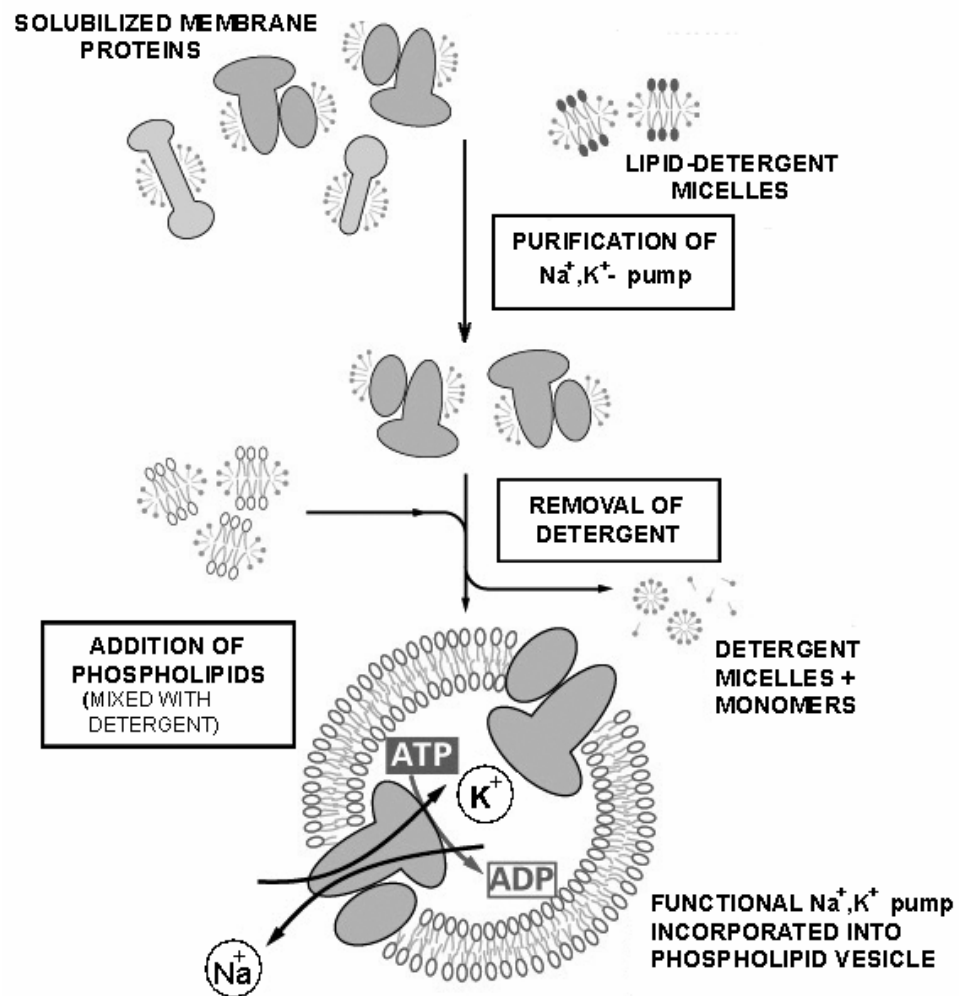


**Figure 2.18:** Scheme of the reconstitution process

A quite simple method that has proved successful, involves solubilization of the protein in a suitable detergent (in this case  $\text{C}_{12}\text{E}_8$ ) and its reconstitution with appropriate soluble lipids, in the presence of small amount of adsorbent Bio-Beads (SM2) [Cornelius 2001, Mohraz 1999].

## 3 Fluorescence Spectroscopy

Fluorescence spectroscopy is a powerful technique for studying molecular interactions in analytical chemistry, biochemistry, cell biology, photochemistry and environmental studies. Although fluorescence measurements do not provide detailed structural information, the technique has become quite popular because of its acute sensitivity to changes in the structural and dynamic properties of biomolecules and bimolecular complexes. Fluorescence spectroscopic studies can be carried out at many levels ranging from simple measurements of steady-state emission intensity to quite sophisticated time-resolved studies [Royer 1995].

### 3.1 Basic Fluorescence Theory

Luminescence is the emission of light from any substance and occurs from electronically excited states. Luminescence can be of two types: fluorescence and phosphorescence [Lakowicz 1999, Fleming 2005]. Fluorescence is a luminescence phenomenon in which electron de-excitation occurs almost spontaneously, and in which emission from a luminescent substance ceases when the exciting source is removed. In fluorescence materials, the excited state has the same spin as the ground state. If  $A^*$  denotes an excited state of a substance  $A$ , then fluorescence consists of the emission of a photon:



where  $h$  is Planck's constant and  $\nu$  is the frequency of the photon. Usually the absorbed photon is in the ultraviolet, and the emitted light (luminescence) is in the visible range.

The process of fluorescence is illustrated by the simple electronic-state diagram called "**Jablonski diagram**" (Fig. 3.1). The singlet ground, first and second electronic states are depicted by  $S_0$ ,  $S_1$ , and  $S_2$ , respectively. At each of these electronic energy levels the fluorophores can exist in a number of vibrational energy levels, denoted by 0, 1, 2 etc. Transitions between states are depicted in vertical lines to illustrate the instantaneous nature of light absorption. Following light absorption several processes usually occur. A fluorophore is excited to some higher vibrational level of either  $S_1$  or

$S_2$ . With a few rare exceptions, molecules in condensed phases are rapidly relaxed to the lowest vibrational level of  $S_1$ . This process, called internal conversion, is nonradiative and takes place in  $10^{-12}$  seconds or less. Return to the ground state occurs to a higher excited vibrational ground-state level, which then quickly reaches thermal equilibrium. An interesting consequence of emission to a higher vibrational ground state is that the emission spectrum is typically a mirror image of the absorption spectrum of the  $S_0 \rightarrow S_1$  transition. Molecules in the state  $S_1$  can also undergo a spin conversion to the first triplet state  $T_1$ . Emission from  $T_1$  is termed phosphorescence and is generally shifted to longer wavelengths relative to fluorescence [Fleming 2005]. Conversion of  $S_1$  to  $T_1$  is called intersystem crossing. Transition from  $T_1$  to the singlet state is forbidden [Lakowicz 1999].

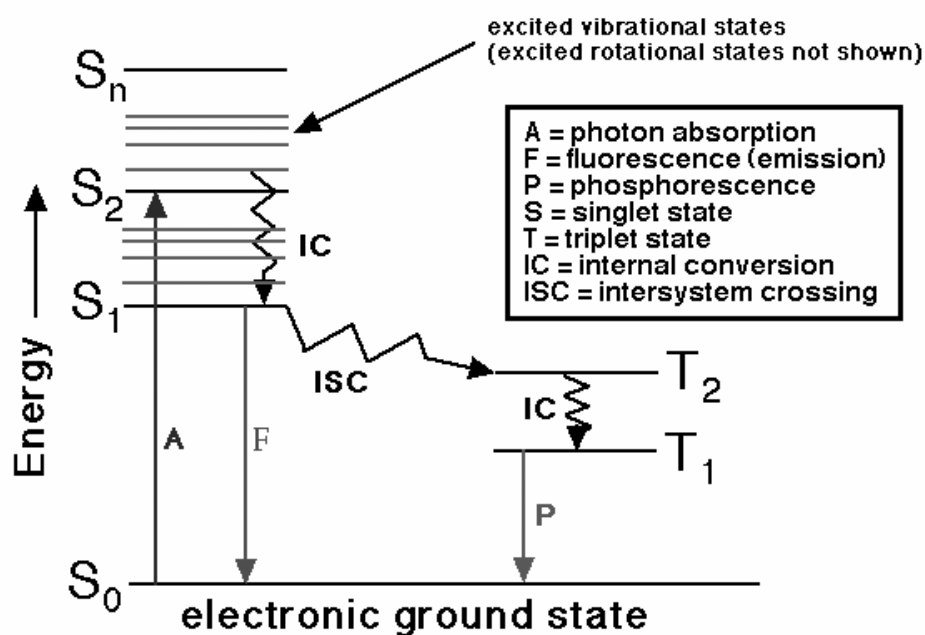


**Figure 3.1:** Jablonski diagram.

A more detailed treatment of the fluorescence technique is covered by few basic rules:

1. *The Franck Condon principle*

Classically, the Franck–Condon principle is the approximation that an electronic transition is most likely to occur without changes in the positions of the nuclei in the molecular entity and its environment. The resulting state is called a Franck–Condon state, and the transition involved a vertical transition.

2. *The Stokes shift*

The Jablonski diagram reveals that the energy of the emission is typically less than that of absorption: Stokes shift is the difference between positions of the band maxima of the absorption and fluorescence spectra of the same electronic transition. When a molecule or atom absorbs light, it enters an excited electronic state. The Stokes shift occurs because the molecule loses a small amount of the absorbed energy before re-releasing the rest of the energy as fluorescence.

3. *Kasha's rule*

Upon excitation to higher electronic and vibrational levels, the excess energy is quickly dissipated, leaving the fluorophore in the lowest vibrational level of  $S_1$ . It is from this position that a photon will be emitted. Because of this rapid relaxation, emission spectra are usually independent of the excitation wavelength.

4. *Mirror image rule*

The emission is the mirror image of the  $S_0 \rightarrow S_1$  absorption, not of the total absorption spectrum. This is a result of the same transition being involved in both absorption and emission and similarities of the vibrational levels of  $S_0$  and  $S_1$ . Although the mirror image rule often holds, many exceptions to this rule occur.

### 3.1.1 Steady-State Measurements

Fluorescence measurements can broadly be classified into two types of measurements, steady-state and time-resolved. Steady-state measurements are performed with constant illumination and observation. This is the most common type of measurements. The sample is illuminated with a continuous beam of light, and the intensity or emission spectrum is recorded. Because of the nanosecond timescale of fluorescence, most measurements are steady-state measurements. When the sample is first exposed to light, a steady-state is reached almost immediately [Lakowicz 1999]. In its simplest form the decay of the fluorescent intensity following a short excitation pulse,  $I_{(t)}$ , is a single exponential process:

$$I_{(t)} = I_0 e^{-t/\tau} \quad [1]$$

Here  $I_0$  is the fluorescence intensity at time  $t=0$ , and  $\tau$  is the fluorescence life-time. The fluorescence life-time is independent of factors such as excitation intensity, absorption effects, and fading due to photo-bleaching.

### 3.1.2 Fluorescence Lifetime and Quantum Yield

The fluorescence lifetime and quantum yield are important characteristics of a fluorophore. The quantum yield is a number of emitted photons relative to the number of absorbed photons:

$$Q = \frac{\Gamma}{\Gamma + k_{nr}} \quad [2]$$

Where  $\Gamma$  is the number of photons emitted, and  $k_{nr}$  is all forms of nonradiative decay from the excited to the ground state. The quantum yield can be close to unity if the radiationless decay rate is much smaller than the rate of radiative decay,  $k_{nr} \ll \Gamma$ .

The lifetime of the excited state is defined by the average time the molecule spends in the excited state prior to return to the ground state. Generally fluorescent lifetimes are near 10 ns.



$$\tau = \frac{1}{\Gamma + k_{nr}} \quad [3]$$

Fluorescent emission is a random process, and few molecules emit their photons at precisely  $t=\tau$ . The lifetime is an average value of the time spent in the excited state. The lifetime can be measured by an experiment in which a very short pulsed excitation is given followed by measurement of the time-dependent intensity. If we let  $n(t)$  equal the number of excited molecules at time,  $t$ , then the decay in this number is given by:

$$\frac{dn(t)}{dt} = -(\Gamma + k_{nr}) n(t) \quad [4]$$

leading to:

$$n(t) = n_0 e^{-(t/\tau)} \quad [5]$$

The actually observed quantity is intensity, which is proportional to the number of photons [equation 1]. Thus the lifetime can be calculated from the slope of a plot of  $\log I_{(t)}$  versus  $t$  [Fleming 2005].

### 3.1.3 Fluorophores

Selection of fluorescence probes is an important issue in fluorescence spectroscopy. The final analysis, the wavelength and time resolution required of the instruments are determined by the spectral properties of the fluorophores. Thousands of fluorescent probes are known. They can be broadly divided into two main classes; intrinsic and extrinsic. Intrinsic fluorophores are those which occur naturally. These include the aromatic amino acids, NADH, flavins, and derivatives of pyridoxal and chlorophyll. Extrinsic fluorophores are added to the sample to provide fluorescence when none exists or to change the spectral properties of the sample.

***NADH ( $\beta$ -nictotinamide adenine di-nucleotide)***

NADH is highly fluorescent, with absorption and emission maxima at 340 nm and 460 nm, respectively. The fluorescent group is the reduced nicotinamide ring. In solution its fluorescence is partially quenched by collisions or stacking with the adenine moiety. Upon binding to proteins, the quantum yield of the NADH generally increases fourfold. NADH is the active coenzyme form of vitamin B<sub>3</sub>. It is a naturally present in all living organisms and is necessary for the production of energy, among other functions. NADH is formed by the body and can be located in both the cytosol and the mitochondria. NADH is an important element of the electron transport chain in the mitochondria. It also acts as an intermediate in the energy conversion of glucose into ATP. NADH functions closely with NAD as well. The NADH/NAD<sup>+</sup> pair serve as donor and/or acceptor of electrons in a large number of biological redox reactions.

The reduced pyridine nucleotide NADH is the principal electron donor for the respiratory chain in mammalian cells. The oxidation of NADH by the electron transport chain is coupled to the phosphorylation of ADP by ATP synthase. The relationship between the rate of ATP production and the ratio of reduced NADH to oxidized NAD<sup>+</sup> allows the metabolic state of a cell to be measured by its NADH/NAD<sup>+</sup> ratio (Fig. 3.2 and 3.3). Fortunately, NADH is fluorescent whereas NAD<sup>+</sup> is not; hence the NADH/NAD<sup>+</sup> ratio can be measured using fluorescence techniques.

The assay is based on a reaction in which the regeneration of hydrolyzed ATP is coupled to the oxidation of NADH.

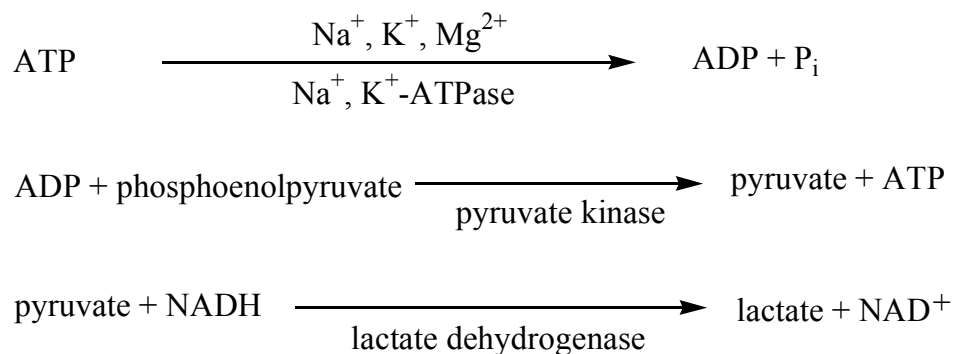


**Figure 3.2:** The principles of the Na<sup>+</sup>,K<sup>+</sup>-ATPase activity reaction.

Following each cycle of ATP hydrolysis, the regeneration system consisting of phosphoenolpyruvate (PEP) and pyruvate kinase (PK) converts one molecule of PEP to pyruvate when the ADP is converted back to the ATP. The pyruvate is subsequently converted to lactate by L-dehydrogenase (LDH) resulting in the oxidation of one NADH molecule. The assay measures the rate of NADH absorbance decrease at 340 nm, or fluorescence intensity decrease at 460 nm.

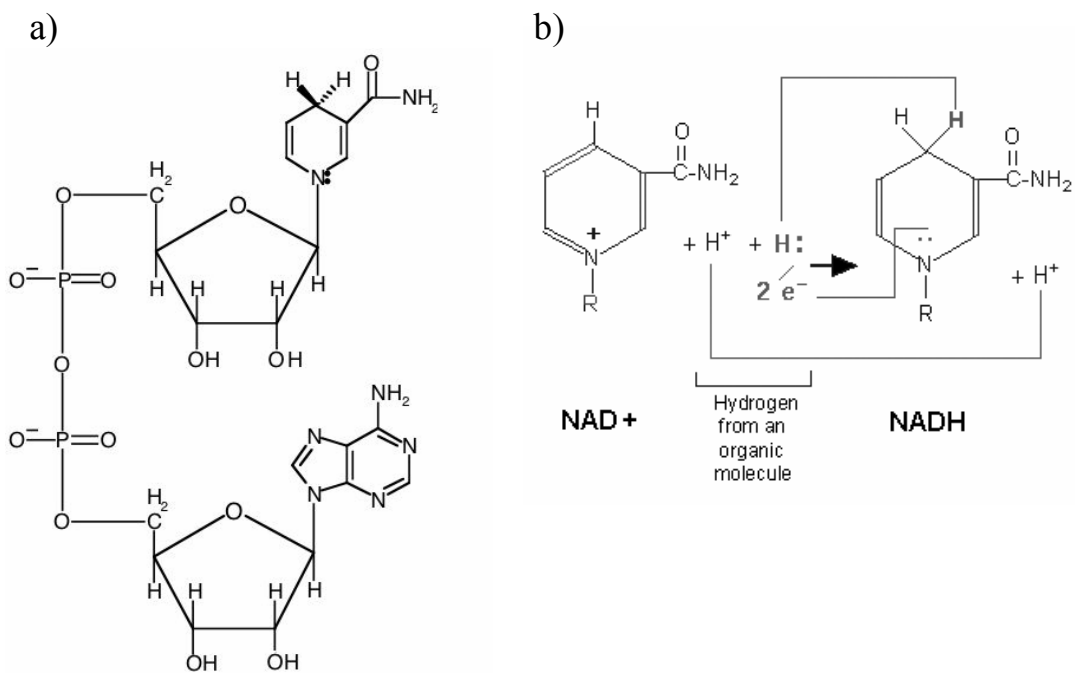


**Figure 3.3:** a) Structure of NADH. b) Redox reaction of NAD<sup>+</sup>/NADH

**Laurdan (6-dodecanoyl-2-dimethylaminonaphthalene)**

Lipids are essentially devoid of fluorescence. In this case useful fluorescence is obtained by labelling the molecule with extrinsic probes. Laurdan is a fluorescent membrane probe that has the advantage of displaying spectral sensitivity to the phospholipid phase state. The structure of Laurdan is presented on figure 3.4.

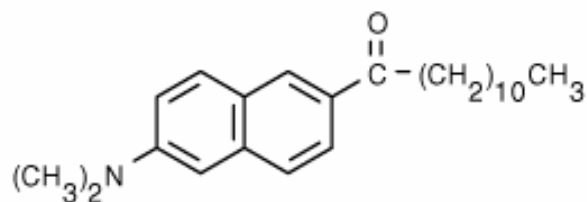


**Figure 3.4:** Chemical structure of Laurdan.

Laurdan and the other naphthalene derivative Prodan were first designed and synthesized by Gregorio Weber [Weber 1979, Parasassi 1998], to study the phenomenon of dipolar relaxation. LAURDAN possesses both an electron donor and an electron receptor, so that fluorescent excitation induces a large excited-state dipole. This strong dipole tends to locally align surrounding molecules (e.g., water), which dissipate a small fraction of the excited state energy and shift the emission spectrum toward the red. As an initial concept, a membrane with a lower interfacial tension, generally allows more water molecules to partition into the membrane, shifting LAURDAN's emission maximum further into the red. This effect can be observed only in polar solvents. The emission maxima of Laurdan and Prodan in phospholipid bilayers depend upon the phase state of the phospholipids, being blue in the gel phase (maximum emission at 440 nm) and green in the liquid crystalline phase (maximum emission at 490 nm). During the phospholipid phase transition the spectra show a continuous shift to longer wavelengths with no isosbestic point [Parasassi 1991]. The red spectral shift has been found to be independent of the polar head residues and of its charge. Instead, the shift depends only on the phase state of the bilayer [Parasassi 1998]. Thus, the origin of the dipolar relaxation observed in phospholipids has been attributed to a few water molecules present in the bilayer at the level of the glycerol backbone, where the fluorescent moiety of Laurdan and Prodan resides (Fig. 3.5). The

concentration and the molecular dynamics of these water molecules change in the two phospholipid phase states. Water reorientation along the probes excited-state dipole occurs only in the liquid-crystalline phase. In the tightly packed gel phase, a red shift of the emission can not be observed.

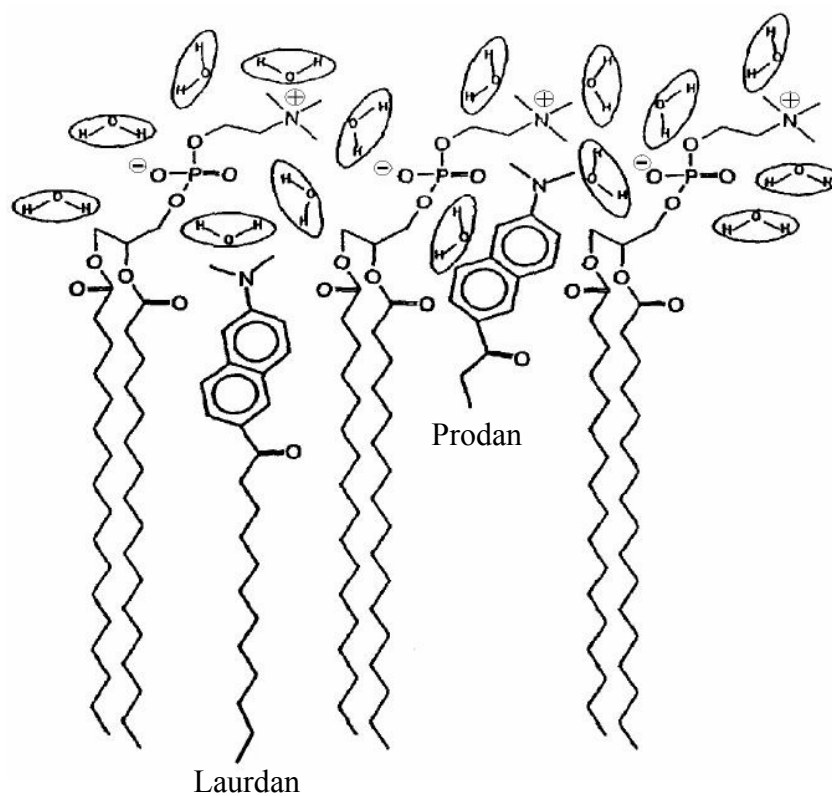


**Figure 3.5:** Scheme of Laurdan and Prodan incorporated into the lipid bilayer.

In phospholipid bilayers Laurdan is anchored in the hydrophobic core by the cooperative van der Waals interactions between the lauric acid tail and the lipid hydrocarbon chains, with its fluorescent moiety residing at the level of the phospholipid glycerol backbone. Fluorescence and infrared studies show that Laurdan is embedded in lipid bilayers deeper than Prodan and better stabilized in the lipid matrix. Prodan undergoes relocation in membranes under physical perturbations and it's also water soluble. High pressure infrared data further suggest that Laurdan causes more membrane perturbation [Zeng 1995].

### 3.1.4 Generalized Polarization (GP)

The fluorescence properties of Laurdan provide a unique possibility to study lipid domains because of the different excitation and emission spectra of a probe in the gel and in the liquid crystalline phase. The difference in excitation spectra allows photoselection of Laurdan molecules in one of the two phases. Using the difference in emission spectra it is then possible to observe interconversion between the two phases. To quantitate phase coexistence and interconversion the concept of *Generalized Polarization* has been introduced.

$$GP = \frac{I_B - I_R}{I_B + I_R}$$

$I_B$  and  $I_R$  are the steady-state intensities at the maximum emission wavelengths in the gel and in the liquid-crystalline phase appearing at about 440 and 490 nm, respectively.

One characteristic feature of  $GP$  in phospholipids is its dependence on temperature and excitation wavelengths. Once the wavelengths for excitation and emission are chosen, the  $GP$  value does not change with polar head groups or pH (in the range of 4-10) it changes only with the phase state. The “generalized polarization” values are limited to values between +1 and -1, for gel phase and liquid crystalline, respectively [Parasassi 1991].

### 3.2 Fluorescence Spectrometer

To perform fluorescence steady-state measurements the spectrometer type K2 from the company ISS (ISS Inc., Champaign, Urbana, IL) was used. The spectrometer is additionally equipped with the photon counting-mode. Figure 3.6 shows a schematic diagram of a spectrometer K2.

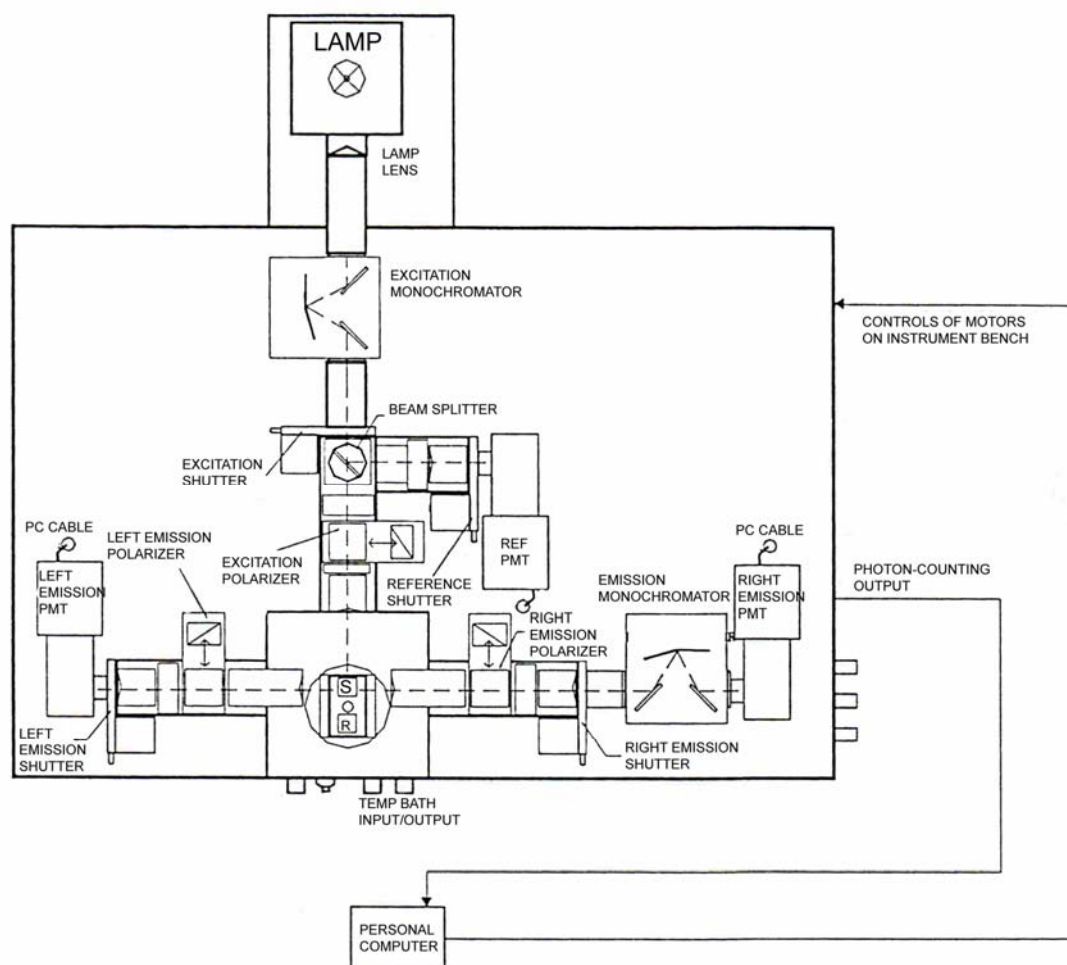


**Figure 3.6:** Schematic illustration of the K2 fluorescence spectrometer

The instrument has a xenon arc lamp as the source of excitation light. Such lamps are generally useful because of their high intensity in wavelengths range between 250 and 1100 nm. Xenon arc lamps emit a continuum of light as a result of the recombination of electrons with ionized Xe atoms. These ions are generated by collisions of Xe atoms with the electrons which flow across the arc.

The emitted light is focused with the help of lenses on the entrance slit of the excitation monochromator. A monochromator accepts incoming light and disperses it into the various colours of the spectrum. This dispersion can be accomplished using prisms or diffraction gratings. In the K2 spectrometer the spectral dispersion in the monochromator takes place in the concave, holographic gratings with 1200 grooves per millimetre, what provides very low straylight and ghost-free spectra. The spectral region is in the range of  $\lambda = 200\text{-}800$  nm with allowance of  $\Delta\lambda = 0.25$  nm. Both monochromators are equipped with a set of interchangeable slits. The slit handles are marked with the width of the slits: 2, 1, 0.5 mm. Since the linear dispersion of the monochromator is 8 nm/mm, slits have a bandwidth of 16, 8, and 4 nm.

The monochromatic light is stirred afterwards over a mirror which is fastened to the corner of a two-way polarizer, directly on a beam splitter. A beam splitter is provided in the excitation light path and reflects part of the excitation light to a reference cell, in this case Rhodamine-B, a stable reference fluorophore. Excitation spectra are distorted primarily by the wavelength dependence of the intensity of the exciting light. This intensity can be converted to a signal proportional to the number of incident photons by the use of a “quantum counter”. This concentrated solution absorbs virtually all incident light from 200-600 nm. The quantum yield and emission maximum (~630 nm) are essentially independent of excitation wavelength from 220-600 nm. Rhodamine-B remains the most generally reliable and convenient “quantum counter”.

Polarizer's are present in the both excitation and emission light paths. Generally polarizers are removable so that they can be inserted only for the measurement of fluorescence anisotropy or when it is necessary to select for particular polarized components of the emission and/or excitation.

In the sample space there are two possibilities, the temperature cell might be placed or the high-pressure autoclave.



In the right emission channel light emitted by the sample is spectrally divided by the emission monochromator in the optical path. Just like the excitation monochromator, this also contains concave holographic gratings with 1200 grooves per millimeter as a dispersive element. The emission monochromator grating is maximized for fluorescence light detection in the region  $\lambda = 350 - 800$  nm. Additionally slits for optical filter are indicated in both detection ways directly behind the polarizer. Optical filters are used to compensate for the less than ideal behavior of monochromators.

The detection of the emission can be made by the two photomultipliers, on the left and on the right side of the sample area. The emitted fluorescence radiation is bundled first by a lens. The bundled emission radiation arrived then nonpolarized to the detector. Almost all fluorimeters use photomultiplier tubes as detectors. A PMT is best regarded as accurate source, the current being proportional to the light intensity. Although a PMT responds to individual photons, these individual pulses are generally detected as an average signal.

### 3.2.1 High Pressure Cell

To accomplish high pressure measurements, a high pressure cell system for fluorescent studies was used, made by the ISS Company. The cell construction is presented in Figure 3.7 It has been specifically designed for high pressure fluorescent studies which use pressures up to 3000 bar. The cell can work up to 4 kbar, if sapphire windows are used.

Three 19 mm diameter and 8.5 mm thickness quartz windows have been placed allowing the use of the fluorescence format either with laser or with xenon lamp sources. The cell is made of a stainless steel alloy which has excellent thermal conductivity. The cell also includes a built-in circulation path for temperature control through an external liquid circulation bath. To avoid corrosion damages within the cell, as a fluid medium spectroscopically pure ethanol was used. The cell pressure was generated either through a manual pump system limited to 4 kbar (HP Technology Frankfurt), or by a computer controlling system APP limited to 3 kbar [Ithaca, NY, USA]. The accuracy of the manual pump system is indicated as 10 bar, and the accuracy for the computer controlling system as 2.1 bar.

The sample was placed inside the cell in a quartz glass bottle, covered with laboratory stretch film and closed with an o-ring made from fluorinated rubber (VI563/FPM70, Otto Gehrckens GmbH, Germany).

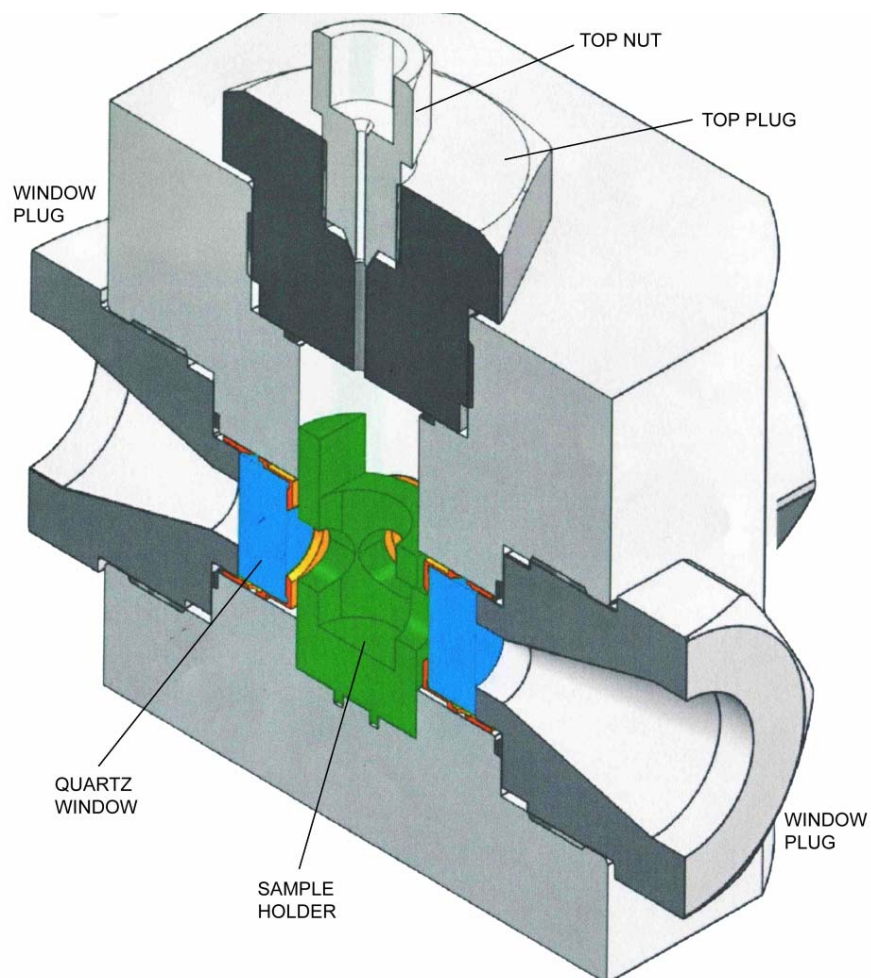


**Figure 3.7:** Scheme of the High Pressure Fluorescence Cell

### 3.3 Absorption Spectroscopy

Absorbance spectroscopy is a widely used analytical technique. This method involves comparing the light transmitted through a blank to the light transmitted through an absorbing species. If the incident light (at a specific wavelength,  $\lambda$ ) has intensity  $I_0$ , and it passes through a sample that absorbs at the wavelength  $\lambda$ , the light intensity,  $I$ , leaving the sample is attenuated. These two quantities are related by the molar extinction coefficient at the wavelength of interest  $\epsilon_\lambda$ , the concentration of the absorbing species,  $C$ , and the length of the path that the light traverses through the sample,  $l$ ;

$$-\log\left(\frac{I}{I_0}\right) = \epsilon_\lambda Cl$$

The quantity that is measured in absorption spectroscopy is the logarithmic term, which is commonly called the **absorbance**. By substituting in  $A$  for the  $-\log$  term, we get the common form of Lambert - Beer's Law.

$$A = \epsilon_\lambda Cl$$

The Lambert-Beer Law is the linear relationship between absorbance and concentration of an absorbing species.

Absorption of ultraviolet or visible radiation is restricted to certain functional groups (chromophores) that contain valence electrons of low excitation energy. When an atom or molecule absorbs energy, electrons are promoted from their ground state to an excited state. In a molecule, these atoms can rotate and vibrate with respect to each other. The energy levels that the electrons jump between extended  $\pi$  orbitals created by a series of alternating single and double bonds, often in aromatic systems. Important biological chromophores include aromatic amino acids (tyrosine, phenylalanine and tryptophan),  $\beta$ -carotene and retinal. The metal complex chromophores arise from the splitting of d-orbitals by binding of a transition metal to ligands. Examples of such chromophores can be seen in chlorophyll and hemoglobin.

NAD - Nicotinamide Adenine Dinucleotide is a nonprotein component of certain enzymes. It is called a cofactor and is involved with many types of oxidation reactions.  $\text{NAD}^+$  is the oxidized form of the NAD. One role of  $\text{NAD}^+$  is to initiate the

electron transport chain. During the oxidation reaction the nicotinamide ring takes up one hydrogen ion and two electrons. The reduced form is called NADH Figure 3.3.

The absorption spectrum of NADH and  $\text{NAD}^+$  is presented in Figure 3.8 We observe maximum of the absorption for reduced form (NADH) at 340 nm, while the oxidized form ( $\text{NAD}^+$ ) does not absorb light within this range. Because of this reactions of enzymes which need NADH as a cofactor can be easily pursued. The reduction of the NADH concentration during the reaction can be followed at 340 nm.

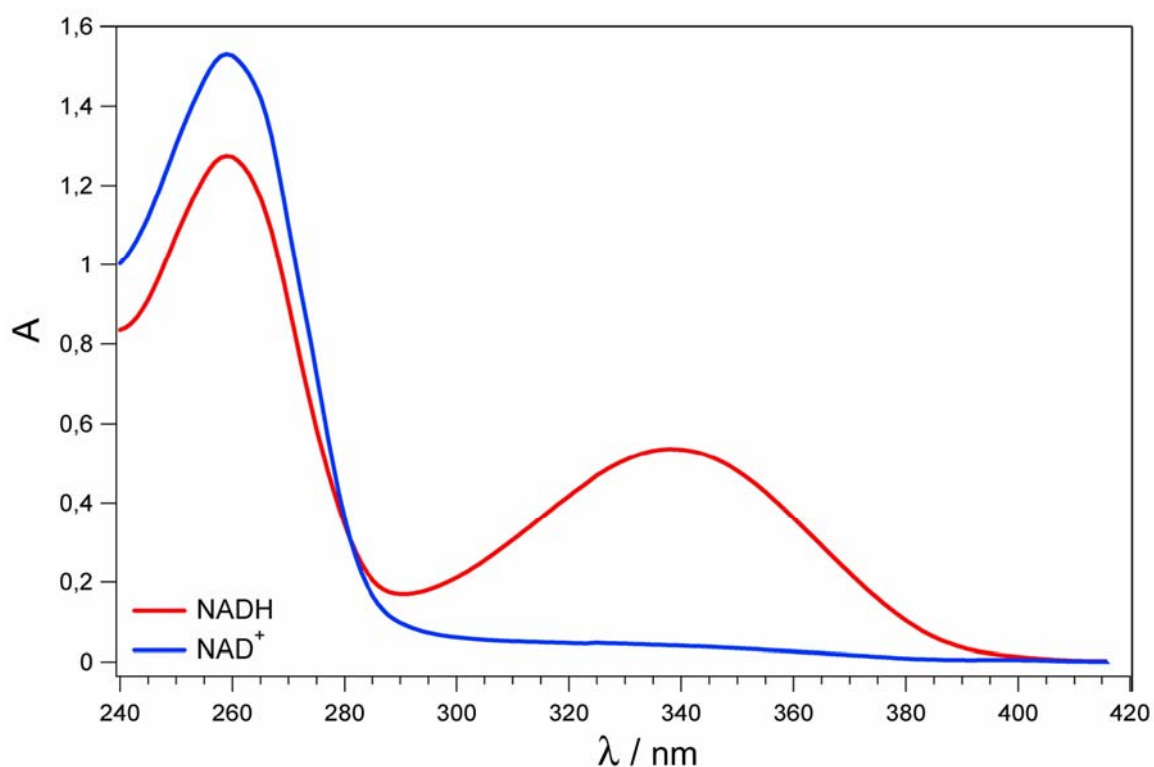


**Figure 3.8:** Absorptions spectra of NADH and  $\text{NAD}^+$

Absorption measurements were carried out on a PerkinElmer, Lambda 25 type spectrometer. The instrument covers a spectral region of 190-110 nm in 1 nm steps. Before each sample measurement, to obtain a correct absorption spectrum, the absorption of the buffer (blank) was measured. The sample was measured in Quartz glass precision cells with 10 mm light path, from the Hellma Company.

## 4 Samples Preparation

### 4.1 Isolation and Purification of $\text{Na}^+$ , $\text{K}^+$ -ATPase

$\text{Na}^+$ ,  $\text{K}^+$ -ATPase has been isolated from rabbit and pig kidneys. In the context of this work, in the first step, an enrichment of the enzyme was accomplished in the plasma membrane under the guidance of Prof. Dr. E. Kinne-Saffran (Max Planck Institute of Molecular Physiology, Dortmund). With this material in hand, first pressure-dependent activity measurements have been carried out. In a second step, with the assistance of Prof. Dr. J. Mignaco and Prof. Dr. F. Fontes (Federal University of Rio de Janeiro, Rio de Janeiro), the enzyme was isolated from pig kidney with locking SDS activation of the enzyme. The aim of this large scale preparation was to obtain enough material for a series of biophysical experiments on reconstituted vesicle preparations using different lipid bilayer systems.

#### *Enrichment of $\text{Na}^+$ , $\text{K}^+$ -ATPase in the plasma membrane.*

$\text{Na}^+$ ,  $\text{K}^+$ -ATPase was enriched in the membrane-bound form from rabbit kidney medullar tissue. To obtain renal tissue, White New Zealand rabbits (3 kg, either sex) were used. After cervical dislocation and bleeding, the kidneys were removed and placed in ice-cold ST-buffer (250 mM sucrose and 10 mM triethanolamine, pH 7.4, (adjusted with HCl). The medullar tissue was carefully excised from the cortical tissue using a stadie-riggs tissue slicer (Thomas Scientific, USA). 6 g of tissue was homogenized in 35 mL of ST-buffer in a warring blender using an adaptor suited for small volumes. Homogenization was performed in the cold (4 °C) twice for 30 s at full speed with an interval of 60 s. The resulting homogenate was poured through cheesecloth to remove any unbroken tissue. A series of centrifugation steps followed in which the cell membranes were separated from nuclei, mitochondria, and endoplasmic reticulum. The final pellet consisted of a firmly packed dark brown pellet overlaid by a loosely packed, whitish material which could be separated by swirling it off. This fraction is termed plasma membrane fraction. By this method, the  $\text{Na}^+$ ,  $\text{K}^+$ -ATPase was enriched about six-fold [Kinne 1986].

#### 4.1.1 Isolation of Na<sup>+</sup>, K<sup>+</sup>-ATPase from Pig Kidney

The isolation was carried out in two steps. 1) Fresh kidneys from pig (50-100 pieces) were taken and placed on ice. The kidneys were cut longwise and the inner medulla was removed. The pink and red tissue of the outer medulla was removed and put into beakers filled with a small amount of solution containing 30 mM histidin, 250 mM sucrose, pH 7.3 (HS solution) at 20 °C, and then placed on ice. The whole amount of HS in all beakers was equivalent to the expected amount of tissue. Per beaker, no more than 250 g pink and red tissue was used. Connective and fat tissue was avoided. The samples of the outer medulla were then cut by pressing the material through a Yeda-Press at 100 bar. It is important not to use a mixer because this will decrease the specific activity of the enzyme. The tissue was squeezed through the press equipped first with large, then with smaller holes. After this operation we obtained a thick, red tissue suspension, which was kept on ice. 2) The next day, the tissue suspension was put together with a solution containing 25 mM imidazol, 250 mM sucrose, 1 mM EDTA, pH 7.4 (20 °C) (ISE solution), into a homogenizator. The suspension was homogenized at 1500 RPM in three steps, while avoiding heating and foam formation. From the homogenized suspension, we prepared a 10 % solution adding ISE solution, thus yielding a suspension of 100 g tissue per liter. The suspension was centrifuged in an ultra refrigerated sorvall centrifuge three times for 20 min at 6000 RPM at 5 °C. The supernatant was put on ice (S1). The pellet was re-homogenized in ISE solution (as described) and centrifuged again. The supernatant (S2) was stored and the pellet was discarded. The supernatants S1 and S2 were then mixed and centrifuged for 20 min at 5 °C and 8500 RPM. The speed of centrifugation was chosen in such a way that the mitochondria became pelleted but not the microsomes. The pellet was discarded again and the supernatant was centrifuged at 20000 RPM for 40 min. At this point, the supernatant was discarded and the pellet containing the microsomes was retrieved. The pellet was resuspended in ISE solution at a ratio of 33 mL ISE / 50 g of original tissue. The microsome suspension was stored overnight at -20 °C. For a longer storage period, the microsomes should be kept at -80 °C. To determine the optimal SDS concentration for activation of the enzyme, aliquots of 3 mL were stored.

***Microsome activation by SDS***

The microsomes contain not only the enzyme but also to a large part lipids. These lipids can be largely removed by detergent, leading to an enzyme construct with tightly bound lipid molecules remaining, only. In a first step, we had to determine the optimal detergent concentration to obtain an as high as possible activity of the enzyme at a minimum concentration of the detergent.

***Determining the optimal SDS concentration***

The microsome aliquots were thawed and diluted with ISE solution to yield 4.6 g protein per mL. Fourteen aliquots of 80  $\mu$ L each of the diluted microsome solution were prepared. From a stock solution of 1 g SDS / 100 mL ISE solution, a dilution series with the following SDS concentrations in g/100 mL were prepared: 0, 0.1, 0.2, 0.3, 0.35, 0.4, 0.45, 0.5, 0.55, 0.6, 0.65, 0.7, 0.75, 0.8. 0.1 mL of the 14 samples were then incubated with the microsome suspension at room temperature for 60 min and then stored on ice. To each sample, 900  $\mu$ L ISE solution was added and the activity of the ATPase [Fiske 1925] and / or the pNPPase (p-nitrophenol-phosphomonoesterase assay) activity were measured.

***Activation of microsomes***

Activation of microsomes: Microsome suspensions diluted to 4.6 g protein / mL with ISE solution were used. The proper amount of SDS solution in ISE was added under careful stirring (1 part SDS solution to 4 parts of the microsome solution). The correct SDS concentration for this preparation was determined from the activation curve. Activated microsomes were stored overnight at room temperature. Microsomes were centrifuged 5 times at 40000 RPM for 40 min at 10 °C. The pellet was stored. After each centrifugation step, the supernatant was removed and the pellet was homogenized using a French Press in ISE solution (3 times up and down at 1500 RPM). After the last centrifugation step, the pellet was diluted in a very small amount of the ISE solution to reach a final concentration of the enzyme of 5 mg/mL (2.7 g/mL of the original tissue). One aliquot was used to determine the protein purity and the activity. The protein was stored at -20 °C until use.

Using this preparation, we obtained the enzyme with very high purity. This was confirmed by Gel SDS-PAGE electrophoresis and Western-blot analysis. A DSC thermodiagram of the SDS activated  $\text{Na}^+$ ,  $\text{K}^+$  - ATPase is shown in Fig. 4.1. The DSC scan shows, in good agreement with other results from other preparations [Grell 2001, Grinberg 2001] a DSC peak with a maximum around 58 °C. At this temperature, partial unfolding of the  $\alpha$  and  $\beta$ - subunits of  $\text{Na}^+$ ,  $\text{K}^+$ -ATPase takes place [Grinberg 2001].

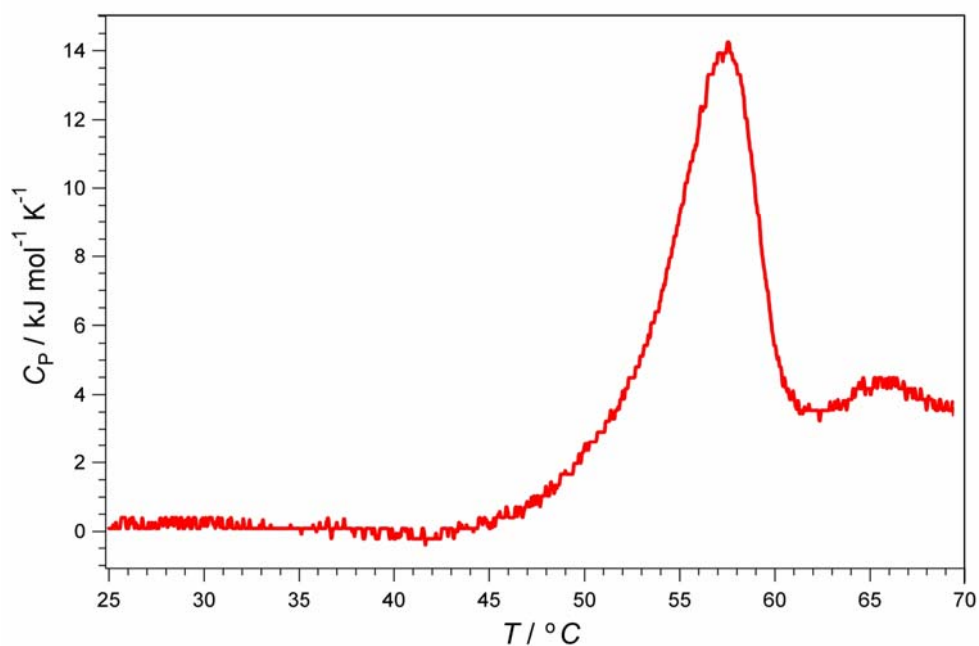


**Figure 4.1:** DSC scan of 20 mg activated  $\text{Na}^+$ ,  $\text{K}^+$ -ATPase in SDS.



## 4.2 Chemical Reagents

### **Avanti Polar Lipids:**

1,2-Dimyristoyl-*sn*-glycero-3-phosphatidylcholine (DMPC), 1,2-dioleoyl-*sn*-glycero-3-phosphatidylcholine (DOPC), 1,2-dioleoyl-*sn*-glycero-3-phosphatidylethanolamine (DOPE), 1,2-dimyristoyl-*sn*-glycero-3-phosphatidylserine (DMPS) 1-palmitoyl-2-oleoyl-*sn*-glycero-3-phosphatidylcholine (POPC), and sphingomyelin (SM) (brain, porcine)

### **Molecular Probes Inc (Eugene, OR):**

6-dodecanoyl-2-dimethylamino-naphthalene (Laurdan)

### **Bio-Rad Laboratories (München, Germany):**

Bio-beads SM-2 adsorbent

### **Roth (Carl Roth GmbH, Karlsruhe):**

Chloroform

### **Roche (Mannheim, Germany):**

purvate-kinase/L-lactate dehydrogenase (PK-L-LDH) (from rabbit muscle)

### **Fluka (Buchs, Switzerland):**

octaethylene glycol monododecyl ether (C<sub>12</sub>E<sub>8</sub>)

### **Sigma-Aldrich (München, Germany):**

adenosine 5'-triphosphate (ATP), 5-cholesten-3 $\beta$ -ol (cholesterol),  $\beta$ -nictotinamide adenine di-nucleotide (NADH), ethylenediaminetetraacetic acid (EDTA), magnesium dichloride (MgCl<sub>2</sub>), sodium chloride (NaCl), potassium chloride (KCl), imidazole, Bis-Tris, hydrochloric acid (HCl), trichloroacetic acid (TCA), phosphoenolpyruvic acid, monopotassium salt (PEP) and bovine serum albumin.

### 4.3 Lipid - Sample Preparation for Fluorescent Spectroscopy

Lipid stock solutions were prepared in chloroform. Laurdan was dissolved in chloroform at a concentration of 1 mmol/L. Vesicles containing the pure phospholipids or desired molar ratio of POPC, SM and Chol were prepared together with the Laurdan fluorophore. After co-dissolving the lipids and fluorophore, the solvent chloroform was removed by a flow of nitrogen gas. Then the samples were dried under high vacuum pumping for several hours to completely remove the remaining solvent. The remaining dry film was then resuspended in water, vortexed and sonicated for 15 min in a bath-type sonicator (Bandelin SONOREX RK100SH). Finally, several freeze-thaw-cycles were applied to achieve a better homogeneity of the vesicle preparation. The final concentration of lipid vesicles in the samples used for the fluorescence measurements was 0.3 mmol/L and that of the fluorescent probe was  $\sim 0.5 \mu\text{mol/L}$ . The final vesicle solution contained a 1:550 fluorophore to lipid mixture on a molecular basis.

### 4.4 Protein Solubilization

Solubilization was carried out at 4 °C by rapid mixing of the  $\text{Na}^+$ ,  $\text{K}^+$ -ATPase membrane fragments with octaethylene glycol monododecyl ether ( $\text{C}_{12}\text{E}_8$ ). A ratio of 1 mg enzyme / 1 mg detergent. The non-solubilized parts were removed by centrifugation at 4 °C for 1 h at 100000 g. The supernatant was taken for further experiments.

### 4.5 Protein-Lipid Reconstitution

For reconstitution, the solubilized protein at 1 mg/mL was mixed with a suspension of phospholipids (DMPC, DOPC, DMPC with 15 and 30 % of cholesterol, DMPC with 10% of DMPS, a model raft mixture and DOPC-DOPE as a stressed lipid model system, that was solubilized in the same detergent as the protein, at a predetermined protein-to-lipid ratio at temperature 20°C, however. The detergent was then removed over a period of 4-5 h by addition of proper amounts of adsorbent Bio-Beads (SM2) [Mohraz 1999], 1g per  $\sim 5\text{mL}$  solubilized protein-lipid solution.

Phospholipids were prepared according to the procedure described earlier. Prior to the reconstitution experiment lipid probes were mixed with proper amount of the detergent (0.39 molar ratio), resuspended in 500  $\mu$ l of water .and added to 4.7 mL of solubilized enzyme Reconstituted solution was determined to contain 1 mol% of protein. By the addition of Bio-Beads the concentration of C<sub>12</sub>E<sub>8</sub> is reduced below the cmc value and the lipid-protein vesicles are formed. Bio-Beads were removed by filtration.

## 4.6 Measurement of the Enzyme Activity

The Na<sup>+</sup>, K<sup>+</sup>-ATPase concentration was determined at 37 °C in an assay medium containing 20 mM HEPES buffer (pH 7.4, adjusted with Tris-base), 100 mM NaCl, 20 mM KCl, 6 mM MgCl<sub>2</sub>, 3 mM ATP, in the absence or presence of 2 mM ouabain. After 30 min of incubation, the samples were put into a boiling water bath for 2 min to stop the reaction. After centrifugation of the samples, the amount of liberated phosphate from ATP was determined in the supernatant according to Fiske and Subbarow [50]. The protein concentration was determined by the method of Lowry *et al.* after precipitation of the samples in ice-cold 10 % trichloroacetic acid, using unfractionated bovine serum albumin as standard [59].

The activity of the ATPase was measured according to the reaction scheme described earlier (see Figure 3.2). The solution for the activity measurements (total volume of 3 mL) contains 130 mM NaCl, 20 mM KCl, 0.1 mM EDTA, 4 mM MgCl<sub>2</sub>, 3 mM phosphoenolpyruvate (PEP), 0.4 mM NADH, 50 mM Tris pH 7.4, 48  $\mu$ g PK-L-LDH and 200  $\mu$ L of Na<sup>+</sup>, K<sup>+</sup>-ATPase (1 mg/mL). The reaction is started by adding 3 mM ATP.

## 5 Results and Discussion

### 5.1 Naturally derived Na<sup>+</sup>,K<sup>+</sup>-ATPase

We first measured the activity of the Na<sup>+</sup>, K<sup>+</sup>-ATPase from rabbit kidneys – enriched in its partially natural plasma membrane environment - by determining the decrease of the NADH fluorescence at 460 nm with time as a function of hydrostatic pressure. To this end, we determined the intensity decay at the excitation maximum for NADH at 340 nm and the emission maximum at 460 nm, respectively. As an example, Figure 5.1a presents representative fluorescence intensity data of NADH at 460 nm as a function of pressure at 37 °C. At ambient pressure, the enzymatic reaction is completed after about 30 min. Our data clearly show, that increasing pressure leads to a retardation of the reaction. Moreover, the measurements show that the activity of Na<sup>+</sup>, K<sup>+</sup>-ATPase is inhibited reversibly by pressures below 2 kbar, only. The enzymatic activity is completely recovered after a 15 min incubation at 1 bar after pressurization up to 2 kbar for more than one hour. On the contrary, the activity of the Na<sup>+</sup>, K<sup>+</sup>-ATPase was not recovered after incubation at higher pressures.

The activity plots  $I_F(t)$  exhibit a rather complex behaviour with a first fast increase and then a more or less slow decay of the activity upon pressurization. This indicates that the pressure-induced reaction involves two or more rate-limiting steps, which certainly is not unexpected because the ATPase reaction proceeds via several intermediate steps, which will be sensitive to pressure if significant changes in volume are involved.

Figure 5.1b presents data of the Na<sup>+</sup>, K<sup>+</sup>-ATPase activity, defined as  $k(p) = \Delta I_F / \Delta t$ , as a function of pressure at 37 °C, obtained from a linear regression method (neglecting the initial phase) of the individual measurements, such as shown in Fig. 5.1a. Clearly,  $k(p)$  decreases roughly exponentially with increasing pressure. Hence, the plot of  $\ln(k)$  vs. pressure is essentially linear at longer timescales, thus allowing for the calculating of an apparent activation volume of the pressure-induced inhibition reaction, which amounts to  $\Delta V^\ddagger = 47.1 \pm 2.3 \text{ mL} \cdot \text{mol}^{-1}$ . This surprisingly high activation volume probably cannot be accounted for by a single chemical process. For comparison, the activation volume of an organic model reaction for the hydrolysis of ATP, the hydrolysis of the acetyl phosphate dianion, is negative and  $-19 \text{ mL} \cdot \text{mol}^{-1}$  [Heremans 1978].

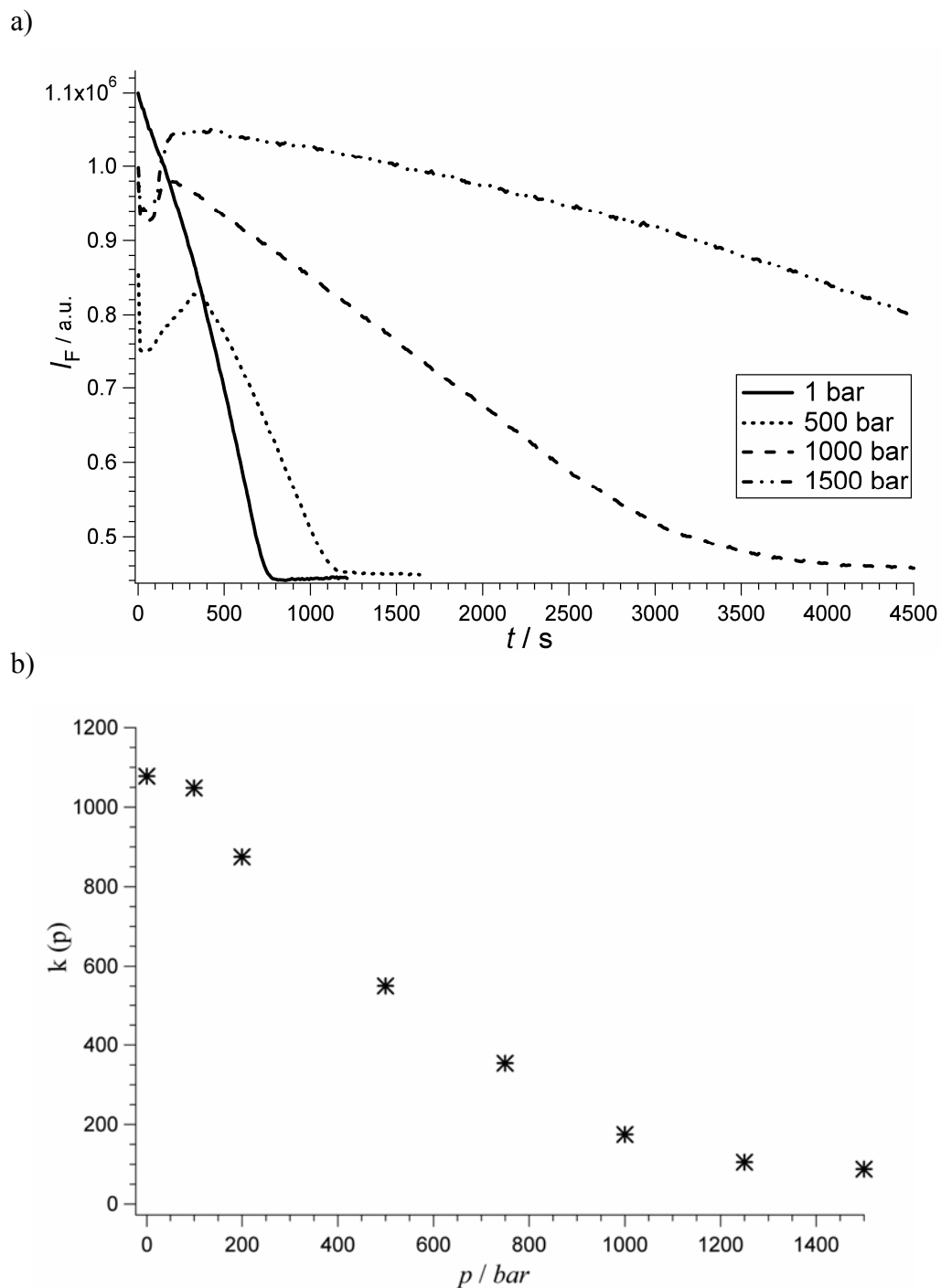


**Figure 5.1:** Activity of  $\text{Na}^+$ ,  $\text{K}^+$ -ATPase from rabbit kidney enriched in the plasma membrane. a) Decrease of the NADH fluorescence intensity ( $I_F$ , in arbitrary units) at 460 nm and selected pressures ( $T = 37^\circ\text{C}$ ). b) The rate of the NADH fluorescence intensity decay (proportional to the enzyme activity),  $k = \Delta I_F / \Delta t$ , as a function of pressure at  $37^\circ\text{C}$ .

Generally, the following mechanisms of the inhibition of the Na<sup>+</sup>, K<sup>+</sup>-ATPase activity by hydrostatic pressure could play a role: i) an increased packing and order of the lipid membrane hinders required conformational changes of the enzyme, ii) large volume changes of the enzyme during the enzymatic reaction, which may be independent of the lipid phase state, iii) subunit dissociation, and iv) a decrease of substrate binding, owing to a positive activation volume. As has been shown by many studies on phospholipid bilayer model systems, upon a pressure increase of a few hundred bar, the acyl-chain conformational order drastically increases and various fluid-gel coexistence regions and gel-phases may be induced [Winter 1998, Winter 2002, Winter 2005], which might hinder conformational transitions associated with rate-limiting steps of the Na<sup>+</sup>, K<sup>+</sup>-ATPase reaction. As the plasma membrane consists of a very complex mixture of dozens of different lipids, no clear-cut pressure-induced fluid-to-gel transition pressure region is expected. We note that in binary and ternary phospholipid mixtures including model rafts mixtures, transition pressures to an overall ordered state of about 2-3 kbar are observed at ambient temperatures [Nicolini 2006]. This would be in accord with the findings of De Smedt et al. [De Smedt 1979], who suggested that the inhibition by pressure is due to a shift in the melting temperature of the lipid aliphatic chains. They measured the activity of the Na<sup>+</sup>, K<sup>+</sup>-ATPase at different temperatures up to 600 bar and found that the breakpoint in the activity is in good agreement with the pressure shift for the melting transition in phospholipids and aliphatic chains. Because of the relatively low pressures applied, a reversible inhibition of the enzyme was observed, only.

## 5.2 Protein Solubilization

Solubilization of the protein is an important step before reconstitution of the enzyme in selected lipid systems. The bound lipid molecules are replaced by detergent molecules. For enzyme solubilization the  $C_{12}E_8$  detergent was used. In the detergent-protein mixed micelles, hydrophobic regions of the membrane proteins are surrounded by the hydrophobic chains of micelles. In the final stage, solubilization of the membranes leads to the formation of mixed micelles consisting of lipids and detergents and detergent micelles containing proteins.

Before reconstitution of the protein it was also essential to determine the proper amount of detergent to solubilize the phospholipid. This step is of a special importance because the correct quantity of the detergent has a significant influence for the further reconstitution experiment. A too low and too high detergent concentration must be avoided. If the amount of the detergent is too small it leads to a not complete destruction of the original bilayer structure and thus problems with reconstitution. If it is too high, there will be the problem to remove it completely during reconstitution. To this end, Laurdan fluorescence spectroscopic measurements at a molar ratio detergent to lipid of 0.2, 0.39 and 0.56 were carried out in addition to DMPC and DMPC/Chol 15% (Figures 5.2a and b). An indication of the proper amount of detergent is given for that  $C_{12}E_8$  concentration where the main phospholipid phase transition is abolished. Already addition of 2 mg of the detergent leads to some changes in the lipid system. The  $GP$  values decrease because of the increasing destruction of original liposomes. The  $GP$  data exhibited that for the detergent to lipid ratio of 0.39, no phase transition in case of DMPC could be detected any more, indicating that the lipid bilayer system has been dissolved, with  $GP$  values around zero, typical for fluid mixed micellar systems.

For all further experiments a molar ratio of 0.39 for the lipid/detergent mixture was used.

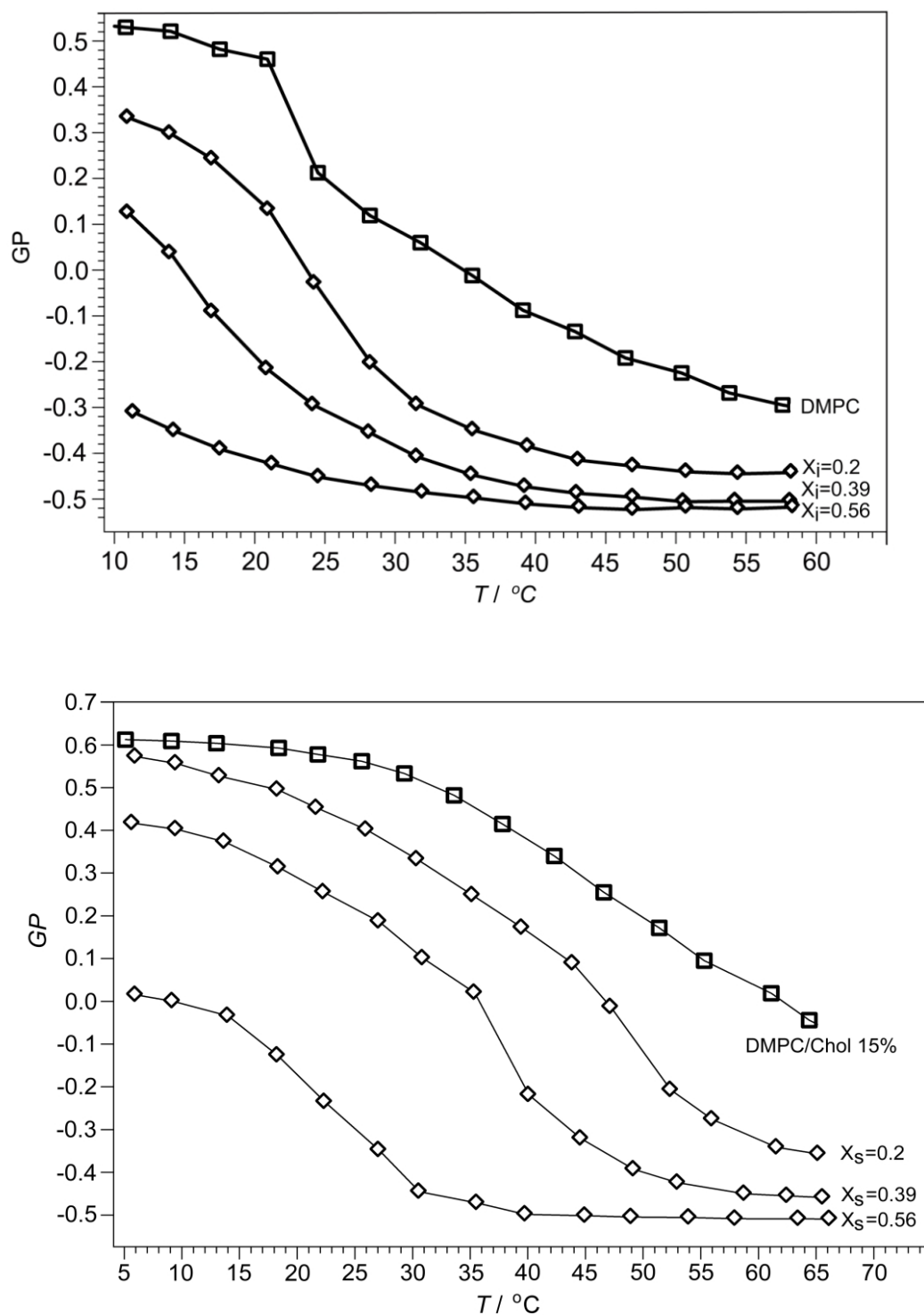


**Figure 5.2:** Generalized polarization ( $GP$ ) measurement of a) DMPC and b) DMPC/Chol 15% vesicles with different amounts of  $C_{12}E_8$  detergent as a function of temperature.

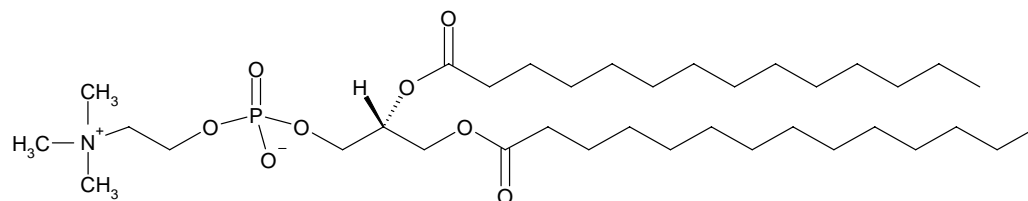


### 5.3 Protein-Lipid Reconstitution

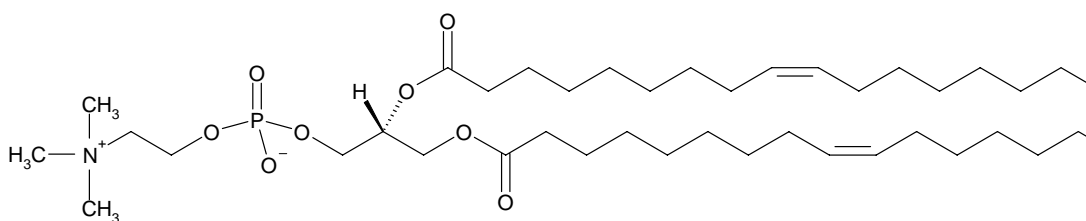
The procedure for reconstitution of the membrane transporter involves the removal of detergent from the solution containing the solubilized protein and the chosen lipids. Both lipids and protein are present in the detergent solution as mixed lipid-detergent and protein-lipid-detergent micelles, respectively. For the removal of the detergent the adsorbent Bio-Beads SM-2 with hydrophobic surface was used. The reduction of the detergent concentration, below the cmc value, leads to liposome formation which incorporated protein.

Reconstitution was carried out in different lipid bilayer systems, differing in chain length, degree of unsaturation and phase state: DMPC (1,2-dimyristoyl-*sn*-glycero-3-phosphatidylcholine; gel/fluid transition temperature at  $T_m = 23^\circ\text{C}$ ); DOPC (1,2-dioleoyl-*sn*-glycero-3-phosphatidylcholine;  $T_m = -20^\circ\text{C}$ ); DOPC / DOPE (1,2-dioleoyl-*sn*-glycero-3-phosphatidylethanolamine) in 3:2 molar ratio; DMPC with 15 and 30 molar% of cholesterol and the model raft mixture POPC/SM/Chol (1:1:1 molar ratio) (POPC: 1-palmitoyl-2-oleoyl-*sn*-glycero-3-phosphatidylcholine, Chol: cholesterol, SM: sphingomyelin). According to the phase diagram of the ternary system POPC/SM/Chol as given in Almeida et al. [De Almeida 2003], the 1:1:1 mixture has coexisting  $l_o$  and  $l_d$  domains at ambient temperature. The chemical structures of all incorporated lipids are presented below.

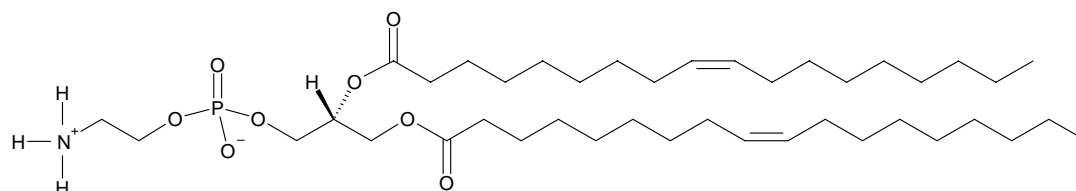
DMPC



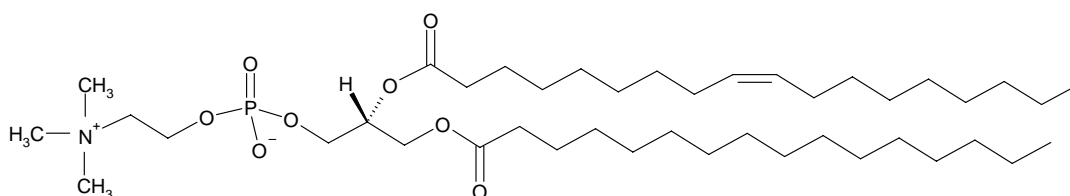
DOPC



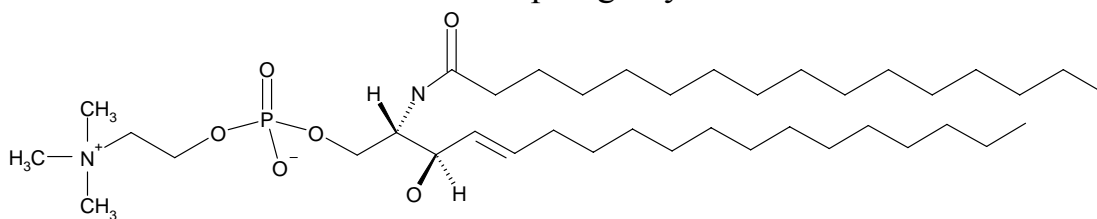
DOPE



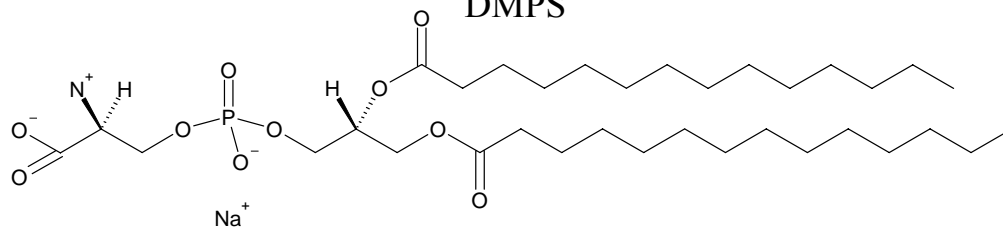
POPC



Sphingomyelin



DMPS



### 5.3.1 Enzyme Activity in Various Reconstituted Lipid Systems

The enzyme activity of all reconstituted systems was first measured by NADH fluorescence at  $T = 37\text{ }^{\circ}\text{C}$  and ambient pressure. The data shown are normalized to the maximum intensity values given at  $t = 0$ . As can be clearly seen in Fig. 5.4, the activities for all the reconstituted systems are lower than the activity of the enzyme enriched in the plasma membrane. In the case of the reconstituted systems, depending on the lipid bilayer systems, a retardation of the reaction by a factor 4-7 is observed, which is partially also due to the enzyme not being inside-out oriented, but rather non-oriented in the membrane. The slowest reaction occurs in the double-*cis*-unsaturated DOPC bilayers and in DMPC with 30 mol% of cholesterol.

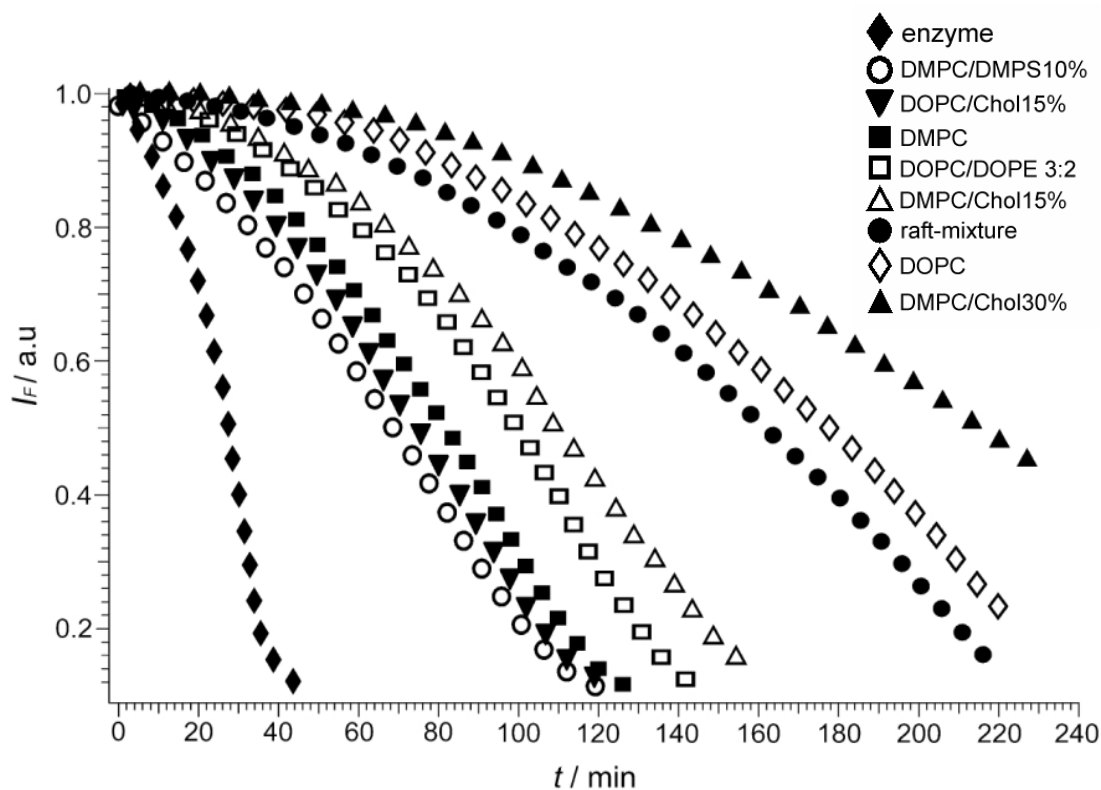


**Figure 5.3:** Comparison of the activity of plasma membrane-enriched  $\text{Na}^+$ ,  $\text{K}^+$ -ATPase and  $\text{Na}^+$ ,  $\text{K}^+$ -ATPase reconstituted into different lipid systems as determined by the NADH fluorescence intensity decay at 460 nm (at 1 bar and  $T = 37\text{ }^{\circ}\text{C}$ ).

The enzyme activity was also checked by UV-Vis spectrometry at  $37\text{ }^{\circ}\text{C}$  for selected lipid systems. The results are presented on Figure 5.4. The differences in time are a consequence of the different amount of NADH used in the case of the absorbance

spectroscopy measurements, which allowed to obtain higher absorbance values and clearly seen the differences between the different reconstituted systems.

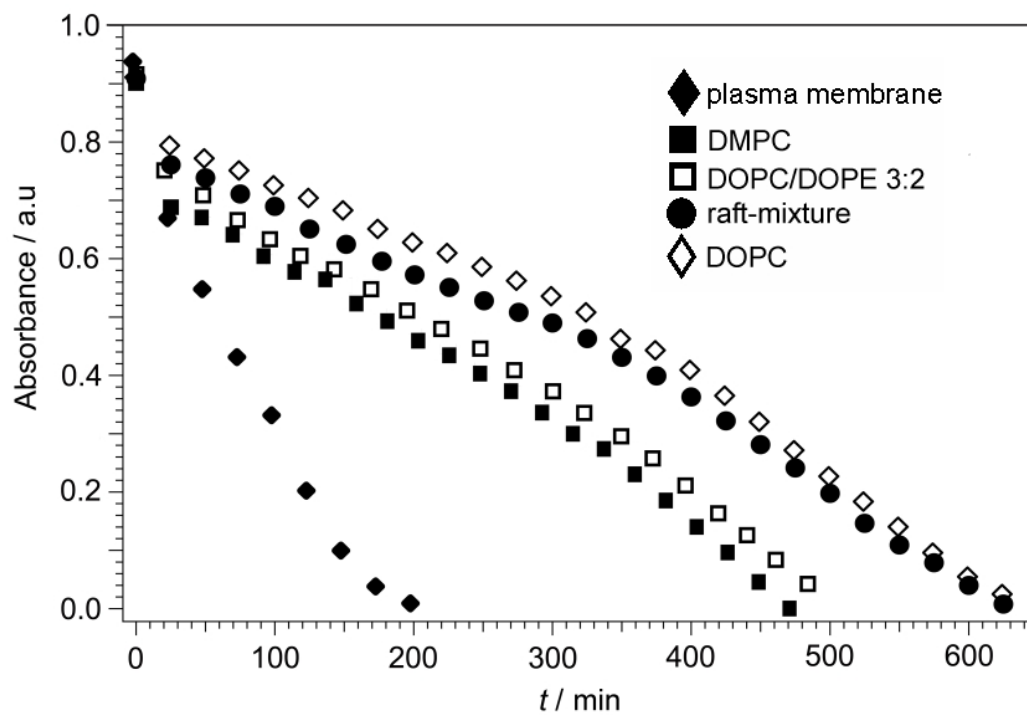


**Figure 5.4:** Comparison of the activity of plasma membrane-enriched  $\text{Na}^+$ ,  $\text{K}^+$ -ATPase and  $\text{Na}^+$ ,  $\text{K}^+$ -ATPase reconstituted into different lipid systems as determined by the NADH Absorbance Spectrometry at 340 nm (at 1 bar and  $T = 37^\circ\text{C}$ ).

The fluorescence and absorbance data clearly show that the ATP hydrolysis activity of the reconstituted enzyme is dependent on the type of lipid bilayer system used. There can be several reasons for this observation.

### 5.3.1.1 DMPC and DOPC

Generally, natural membranes are composed of many different lipids as well as sterols, which might have been optimised for the function of the membrane protein, for example with respect to hydrophobic matching between lipid and protein, and the curvature elastic stress field. Although, the main determinant of the phospholipids phase behavior is the type of hydrocarbon chains. Increasing chain length causes all

transition temperatures at which the interfacial packing density decreases to become higher. Chain unsaturation effectively decouples the parts of the hydrocarbon chain on either side of the double bond or the side chain. Corresponding chain modifications thus reduce the length of parallel, strongly interacting chain segments and thus mimic the consequences of chain shortening. When a chain contains a *cis* unsaturated bond, transition temperatures decrease drastically, however, increasing the number of double bonds per chain causes only a small further decrease of  $T_m$ .

DMPC contains 14 fully saturated carbons in the acyl-chains (di-C<sub>14</sub>). Mohraz reconstituted the enzyme in different types of lipids and suggested that one reason could be connected to the chain lengths of the lipids. He found that lipids with chain-lengths of less than 14 carbons lead to an incomplete recovery of the activity after reconstitution [Mohraz 1999]. Other works [de Lima Santos 2005] showed that an increase in acyl-chain length to 18 carbon atoms (such as in DSPC) causes the enzyme reconstitution less effective, leading to a reduced enzyme incorporation. Best results were obtained for a chain-length of 16 C-atoms. It has been surmised that the increase in length of saturated acyl-chains in the phospholipid bilayer system diminishes the fluidity of the membrane, thus causing a loss of activity of the reconstituted enzyme.

DOPC contains 18 carbons in the acyl-chains, with one *cis*-unsaturated bond (di-C<sub>18:1</sub>). The recovery of the enzyme activity for DOPC reconstitution system was one of the lowest obtained during the experiment. Acyl-chains of fluid DOPC are very highly disordered and this might be unfavorable for the enzyme activity.

### 5.3.1.2 DMPC with Addition of 15 and 30 mol% of Cholesterol

Cholesterol is the major sterol component in most mammalian membranes. Being an amphiphilic molecule, cholesterol easily incorporates into lipid bilayers with its hydrophilic –OH head group at the bilayer-water interface and the steroid skeleton inside the hydrophobic core. Cholesterol has a concentration-dependent effect on membrane organization. When present in large amounts, it acts as a permeability barrier for the membrane by introducing conformational ordering of the lipid chain [Raffy 1999].

Because pure cholesterol cannot form bilayers there must be an upper limit on the cholesterol concentration that can be accommodated within any phospholipid bilayer. In excess cholesterol will tend to precipitate from the membrane as crystals of pure cholesterol monohydrate [Huang 1999]. There are many different solubility limits in the literature which depends on acyl chain length, degree of unsaturation and temperature in lipid-cholesterol mixtures.

Most animal plasma membranes contain 30-40 mol% cholesterol. The addition of cholesterol into fluid phase phospholipids is known to increase the acyl-chain order parameter, leading to an increase in lipid packing and acyl-chain length [Cevc 1993]. Cholesterol > 25 mol% promotes formation of the liquid-ordered phase, which is fluid from the point of view of lateral disorder and diffusivity, but at the same time the acyl-chains are highly ordered. As is also seen in Fig. 5.3, the addition of cholesterol at levels of 15 and 30 mol% at 37 °C has an increasingly retarding effect on the enzyme activity. For fully saturated lipids, addition of cholesterol usually inhibits activity of the enzyme, whereas for unsaturated lipids one has observed an acceleration of activity [Mohraz 1999]. Also the amount of cholesterol in isolated material is different, dependent on which animal and which tissue the enzyme has been isolated from. For example, according to Wu et al. [Wu 2001], Na<sup>+</sup>, K<sup>+</sup>-ATPase isolated from rat kidney contains around 15% and from toad kidney around 24 % cholesterol. Some earlier cholesterol studies showed the best activity at the native membrane's cholesterol content [Yeagle 1988]. The amount of cholesterol in pig kidney was experimentally established to be around 16 % [Sotomayor 2000]. In our experiments, the enzyme reconstituted in the DMPC/30 mol% cholesterol mixture exhibits the lowest activity. As the addition of cholesterol to DMPC at temperatures as high as 37 °C does not drastically change the fluid-like character of the bilayer [69] system, the observed decrease in enzyme activity in the DMPC/cholesterol mixtures is probably due to an increasingly hydrophobic mismatch between the lipid bilayer and membrane protein's hydrophobic core.

### **5.3.1.3 DOPC with Addition of 15 mol% cholesterol**

Furthermore the enzyme was reconstituted in DOPC with addition of 15% cholesterol. In comparison to the result for DMPC/15% Chol, where inhibition of the activity was observed, for unsaturated lipids addition of cholesterol seems to be favorable. At 37

°C we observe a large difference in lipid order for DMPC and DOPC (Fig 5.8 and 5.9), for DOPC being much more disordered. From this perspective, cholesterol prefers the liquid-disordered phase.

The thickness of a lipid bilayer membrane depends on the length and degree of saturation of the fatty-acid chains. The longer the chains and the more saturated they are, the thicker the bilayer will be. The thickness also depends on the degree of hydration. The less hydrated the thicker the bilayer will be. Cholesterol is a very important determinant of lipid bilayer thickness. When introduced into the liquid membrane phase, cholesterol leads to a large increase in membrane thickness. This proves that hydrophobic thickness must be of importance for the activity of an integral enzyme as same as membrane fluidity.

#### **5.3.1.4 DMPC with Addition of 10 mol% DMPS**

The physical state of bilayer membranes is also affected by electrostatic effects at the membrane surface. All phospholipids carry atomic, local excess charges on their surface polar residues. Most of the lipids (PC, PE) carry one negative and one positive charge and are thus zwitterionic. Some lipids (PS, PG) may possess a net, normally negative, charge on the phosphate or carboxylic groups [Cevc 1993]. This difference has an important consequence for the capacity of the lipids, when incorporated into a lipid membrane, to bind proteins and drugs [Mouritsen 2005]. They are also signaling lipids since their regulated formation can constitute an important signal for downstream responses [Stace, Ktistakis 2006]. The amount of charge lipids is about 10 % of total lipids in plasma membranes. Incorporation of these lipids into a lipid bilayer results in a negative charge density for the membrane. The charged layer can interact electrostatically with ions and other charged molecules near the membrane.

At pH 7 or higher, phosphatidylserine possesses two negative groups per molecule. The difference in charges may have important implications on the physiological function of this phospholipid.

Incorporation of 10 mol% phosphatidylserine into the reconstituted lipid bilayer system leads to a small but noticeable acceleration of the enzyme activity. We can conclude that there is some favorable electrostatic interaction between charged lipids and the enzyme. Due to the electrostatic interactions between anionic groups and positively charged amino acid residues, these lipids might play an important role in

the membrane-proteins interactions. It was also proved that for transmembrane proteins, increasing fraction of charged lipids, give rise to a higher number of peptides bound to the bilayer [Taheri-Araghi 2006]. The stimulatory effect of negatively charged lipid incorporation into phosphatidylcholine (PC) proteoliposomes was also found in  $\text{Ca}^{2+}$ -ATPase research. The enzyme was reconstituted in PC and than in mixture of PC/PS and PC/PI. Enrichment of PC proteoliposomes by PS caused a high degree of stimulation of  $\text{Ca}^{2+}$ -ATPase activity [Szymanska 1991]. According to Ktistakis []  $\text{Na}^+, \text{K}^+$  - ATPase is one of the protein, that binding to PS-rich membranes is crucial for their function.

### 5.3.1.5 DOPC/DOPE in Molar Ratio 3:2

The effective shape of the lipid molecules determines their ability to form a stable bilayer. Bilayer-forming lipids have a curvature of zero; non-bilayer ones may have either positive or negative values [Dan 1998]. When a bilayer is made of monolayers with nonzero spontaneous curvature it becomes subject to built-in frustration termed a *curvature stress field*.

Most phospholipids are approximately cylindrical in shape, so they form bilayers. However, some phospholipids, such as unsaturated phosphatidylethanolamine (PE), tend to form hexagonal phases ( $\text{H}_{\text{II}}$ ), since they have relatively small head groups compared to the excluded volume of their hydrocarbon chain region [Cevc 1993]. A substantial part of non-bilayer lipids has been found in natural membranes. This instability must have some advantages for function. One could imagine the instability to be locally released in connection with protein binding, protein insertion, membrane fusion, and conformational changes in the cycle of protein functions [Jensen 2004].

The stress field can be changed enzymatically by specific enzymes that change the  $\text{H}_{\text{II}}$  propensity of the lipids while they reside in the bilayer, e.g., by enzymatically cleaving off the polar head or removing one of the fatty acid chains. The resulting stress may be also released locally, e.g., by changes in the local molecular composition, by binding a protein [Mouristen 2005].

To also study the effect of an increase of the curvature elastic stress of the lipid membrane on the  $\text{Na}^+, \text{K}^+$ -ATPase activity, reconstitution into a DOPC/DOPE 3:2 mixture was carried out (Fig. 5.3). Phosphatidylcholine (PC) and phosphatidylethanolamine (PE) are both zwitterionic lipids with similar chemical



structures. However, PE lacks the three methyl groups on its head group moiety and as a consequence it has a much greater propensity of forming inverted (type II) phases. Adding DOPE to DOPC vesicles increases the desire for curvature toward the water and hence increases the local lateral stress [Mourtisen 2005, de Pont 1978]. For the type II lipid amphiphile DOPE, the total stored curvature elastic stress for each DOPE molecule in a flat monolayer has been determined to be about  $1 k_B T$  [de Pont 1978]. The activity curve at 37 °C and ambient pressure is displayed in Fig. 5 as well. Compared to the pure DOPC bilayer, the activity drastically increases, and a rate similar to that in DMPC fluid bilayers is reached. This indicates that an increase of curvature elastic stress may be favourable for  $\text{Na}^+$ ,  $\text{K}^+$ -ATPase activity.

It was suggested that because cells homeostatically adjust their curvature, some protein must be sensitive to that curvature. Recent investigations suggest that there is indeed a correlation between the spontaneous curvature of the membrane and the performance of embedded proteins. Similarly, there have been reports that at least some cell proteins cannot function except in the presence of specific non-bilayer forming lipids [Dan 1998].

#### **5.3.1.6 POCP/Chol/SM as a Model Raft-Mixture**

The activity of the enzyme in the model raft mixture POPC/SM/cholesterol 1:1:1 displaying  $l_d$  and  $l_o$  domain coexistence regions at that temperature is observed to be only slightly higher than in DOPC bilayers. From the results we can conclude that the presence of longer-chain liquid-ordered domains is unfavourable with respect to enzymatic activity.

### 5.3.2 Pressure Dependence of the Enzyme Activity at 37 °C

Non-covalent interactions constitute the main target for the modulation of biomolecular characteristics through pressure, mainly because they stabilize nearly all the biochemical compounds. On the other hand, the two parameters, pressure and temperature must be considered in close relationship since their effects on equilibrium or kinetics - where the weak interactions are predominant - are antagonistic in molecular terms [Balny 2004]. In principle, an increase in pressure at constant temperature leads to an ordering of molecules or a decrease in the entropy of the system.

The activity of the enzyme reconstituted into DMPC, DOPC, the model raft and DOPC/DOPE mixture has also been measured in the pressure range from ambient pressure up to ~2 kbar at 37 °C. All intensity data were then normalized to their maximum values. Two examples of measurements carried out are shown in Fig. 5.5 a and b. For both systems, DMPC and the model raft mixture, we can clearly see the inhibition of activity upon pressurization. Figures 5.6 a-d shows the activities in terms of  $\Delta I_F/\Delta t$  as a function of pressure for all reconstituted lipid systems studied. Similar to the enzyme enriched in the plasma membrane, for all the reconstituted systems, a significant decrease of activity is observed at high pressure. At pressures of about 2.0 - 2.2 kbar, the enzyme activity decreases to zero within the time range of the experiment (~6 h). The rate of the pressure-induced decrease of the enzyme activity depends on the specific properties of the lipid bilayer system, however.

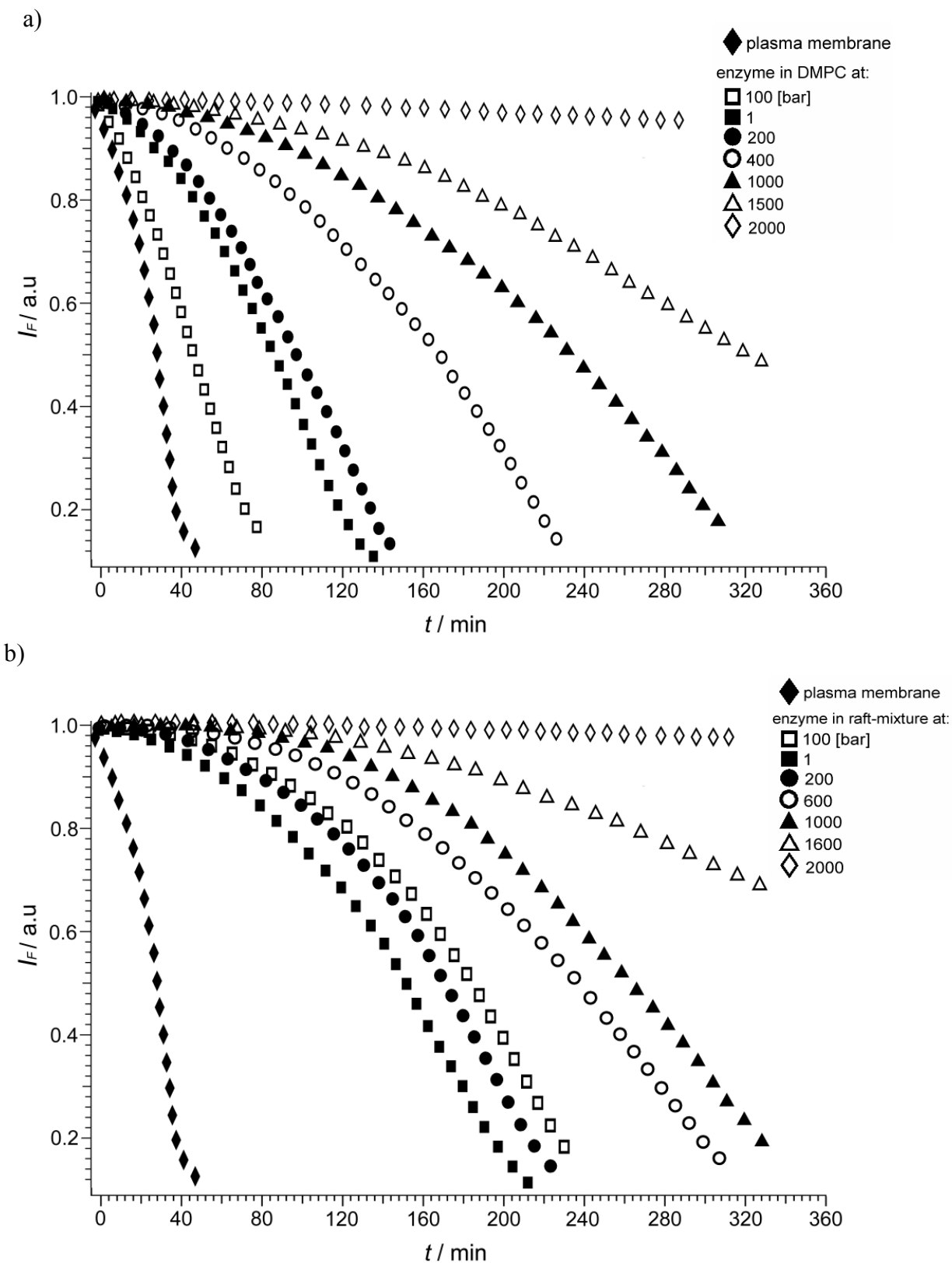
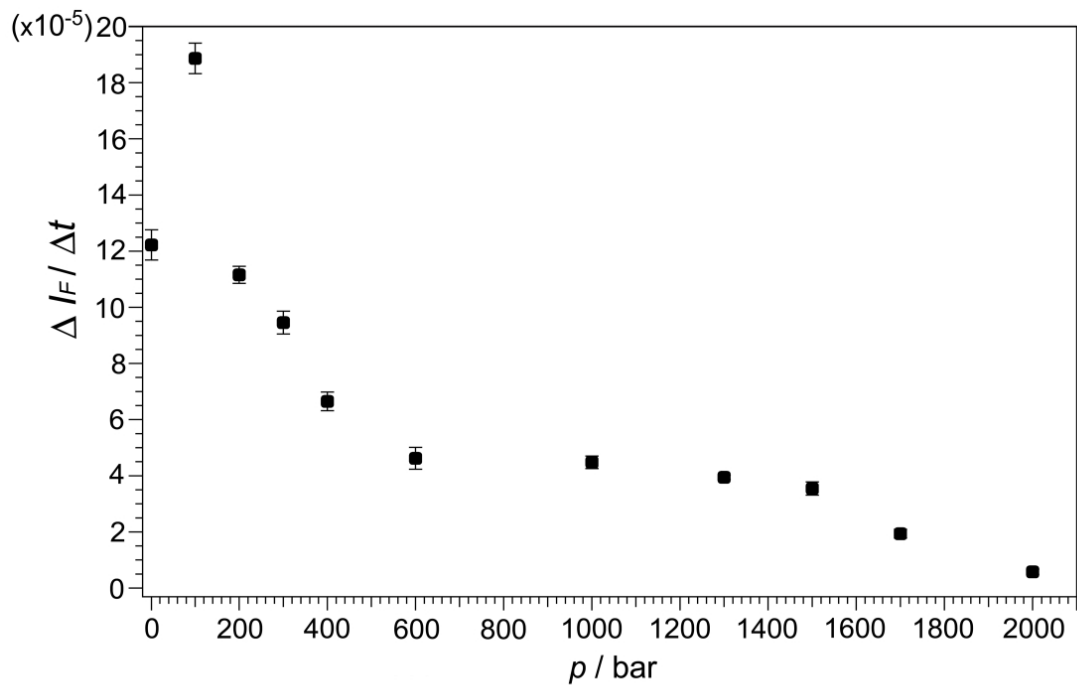
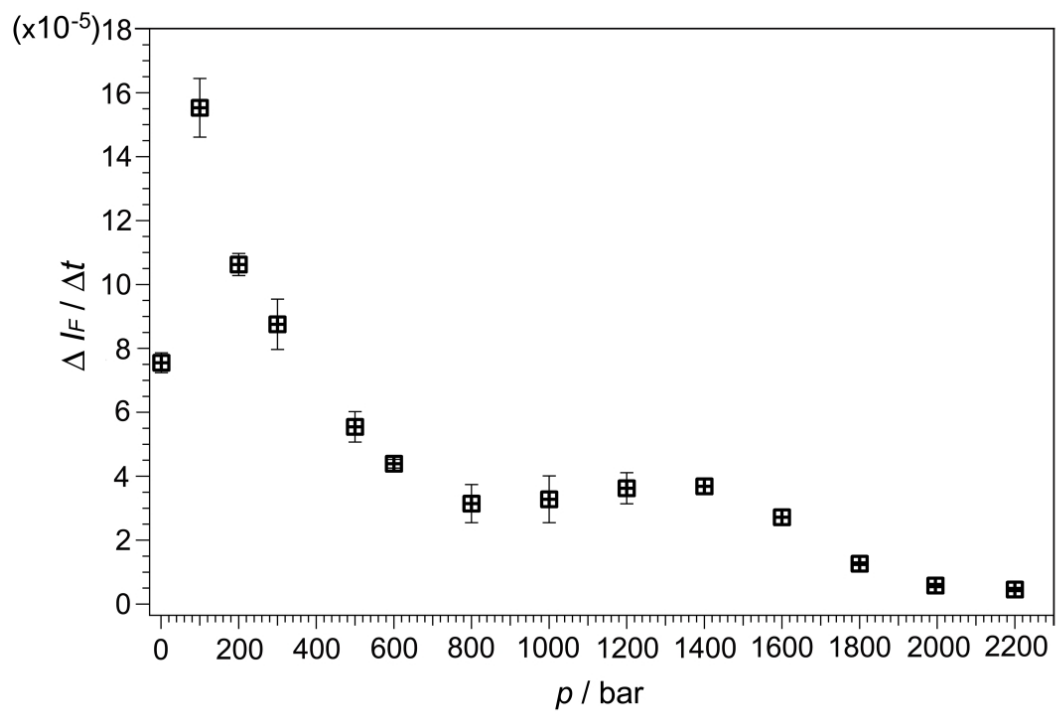


**Figure 5.5:** Decrease of NADH fluorescence intensity (460 nm emission wavelength) at 37 °C for a) the enzyme reconstituted into DMPC and b) the POPC/SM/Chol 1:1:1 model raft mixture for selected pressures in comparison to the plasma membrane-enriched  $\text{Na}^+$ ,  $\text{K}^+$ -ATPase data

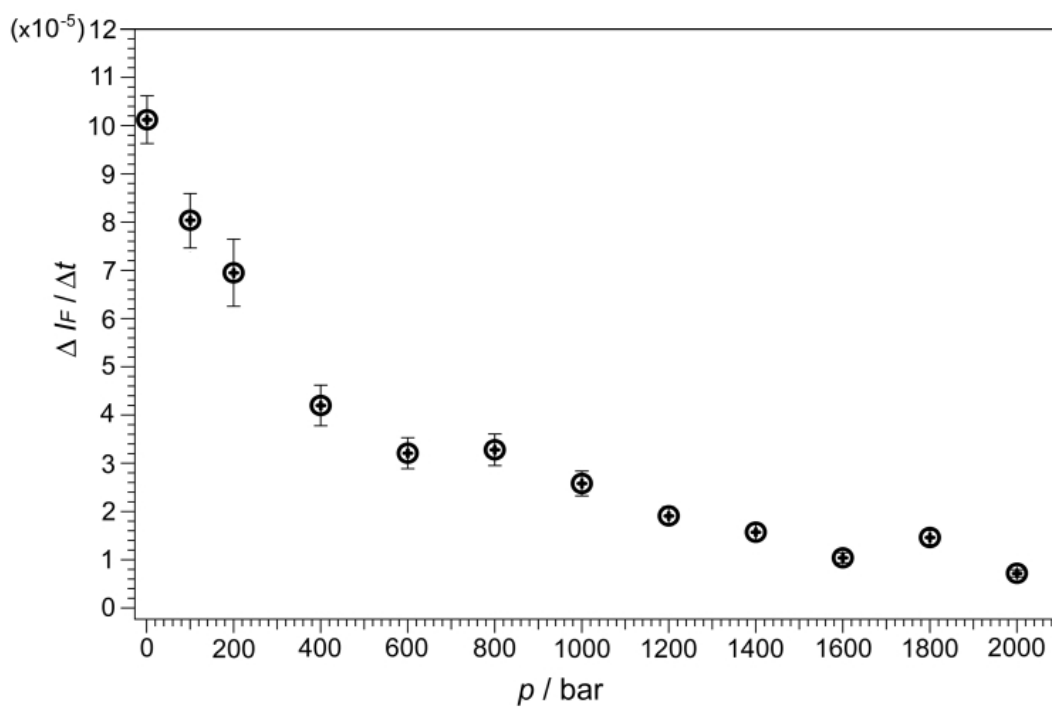
a)



b)



c)



d)

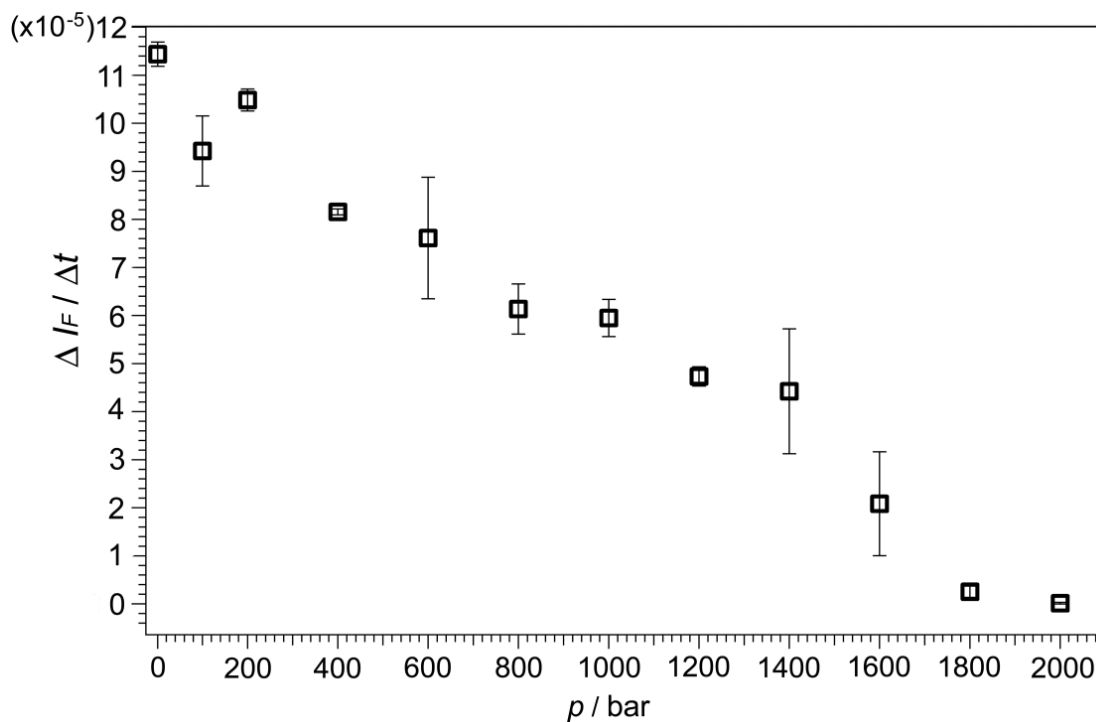


**Figure 5.6:** Rate  $\Delta I_F / \Delta t$  of the NADH fluorescence intensity decrease (as obtained from the long-time tail of the fluorescence intensity data,  $I_F(t)$ ), for selected reconstituted lipid bilayer systems: DMPC (Panel a), DOPC (Panel b), DOPC/DOPE 3:2 (Panel c), and the model raft mixture POPC/SM/Chol 1:1:1 (Panel d) ( $T = 37^\circ \text{C}$ ).

An increase in pressure favours reduction of the volume of a system. Very intriguing is the observation that in the low pressure regime an increase of the enzyme activity is observed (of about 60-100 %) with a maximum activity at about 100 bar for DMPC and DOPC bilayers (Figs. 5.5 a, b). In this range pressure shifts equilibria and accelerates processes for the state that has a smaller volume than the ground state. Above 100-200 bar, this maximum is followed by a steep decrease of the activity up to about 600-800 bar, where a more or less broad plateau value is reached, until the enzyme activity decreases to zero around 2 kbar for all reconstituted systems measured.

The 60-100 % activation observed at low pressures may be related to a decrease in the volume of the ATPase complex induced by compression, which drives the system towards a (negative) activation volume of the ATPase reaction. This effect might also be related to a change in the lipid matrix, which at these low pressures seems to be less likely, however. An increase of 100 bar would lead to a slight increase in lipid acyl-chain length (ca. 0.1 Å [Winter 2002, Eisenblätter 2006]) and packing, only. No pressure-induced fluid-to-gel phase transition occurs at these rather low pressures. The subsequent decrease of the ATPase activity as the pressure is raised above 100-200 bar, may be induced by an increasing hydrophobic mismatch and eventually subunit rearrangement/dissociation at the higher pressures [Kato 2002].

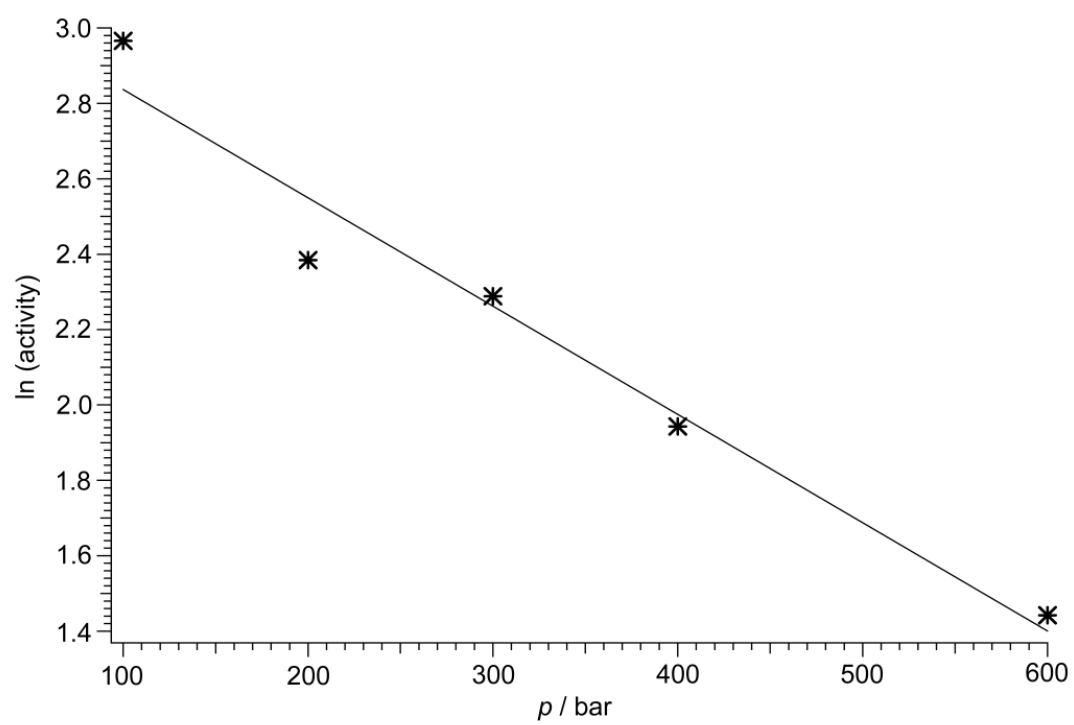
For the DOPC/DOPE 3:2 mixture (Fig. 5.5c), the process of the enzyme inhibition looks similar to DMPC and DOPC systems. There is no acceleration at low pressures, however. We observe a rapid decrease of activity up to 600 bar, only, followed by a less steep decrease of  $\Delta I_F/\Delta t$ . A different scenario is observed for the effect of pressure on the enzyme activity in the model raft mixture (Fig. 7d). In this case, a more or less linear decrease in the activity is observed up to about 2 kbar, where the activity ceases.

It was found that high pressures up to 2 kbar can also lead to a dissociation of the subunits of the Na<sup>+</sup>, K<sup>+</sup>-ATPase [de Almeida 2003]. The pressure dissociation of enzymes and proteins is well-documented in several instances. Chong *et al.* tried to study all the possibilities of inhibition of the Na<sup>+</sup>, K<sup>+</sup>-ATPase [Chong 1985]. Finally they said that the inhibition is due to the stabilization of those intermediate forms of the enzyme that occupy a smaller volume and precede rate-limiting steps of the

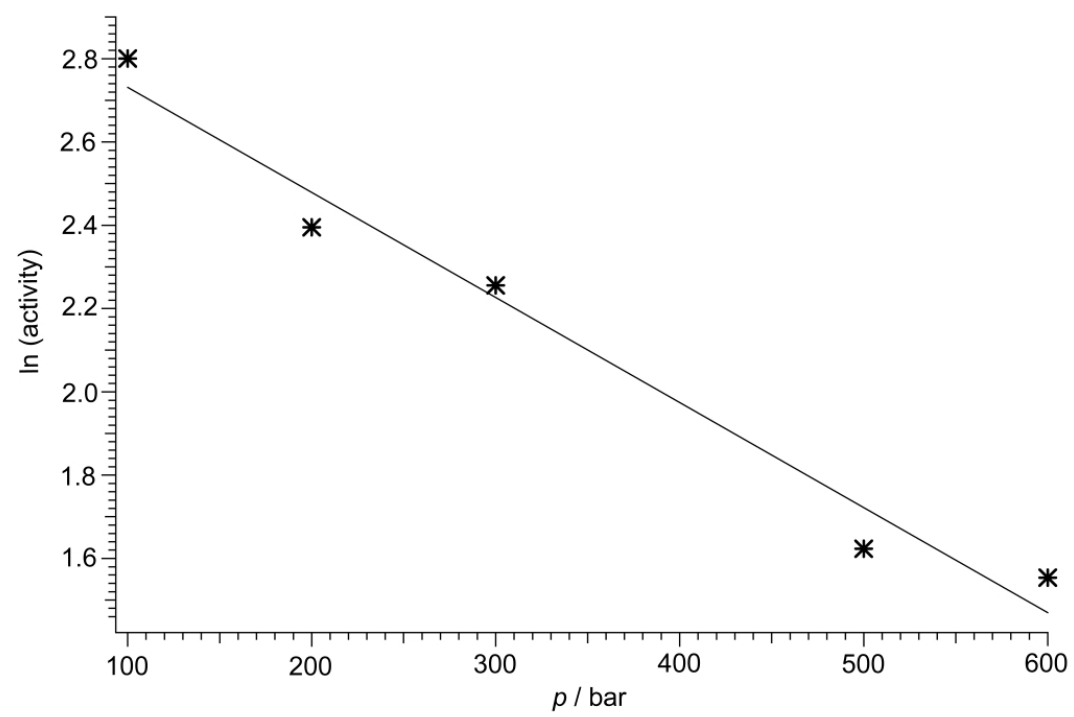
reaction. A decrease in the fluidity of the membrane caused by increased pressure or decreased temperature may hinder the conformational changes that accompany the reaction steps, and thus decrease the rate of the overall reaction. These studies somehow overlap with the most recent studies made by Kato *et al.* [Kato 2002]. They suggest that the activity shows a three step change induced by pressure. From 1 to 1000 bar, than from 1000-2200 bar and higher than 2200 bar. In their opinion at pressure 1000 bar or lower a decrease in the fluidity of lipid bilayer and a reversible conformational change in transmembrane protein is induced, leading to the functional disorder of membrane associated ATPase activity. A pressure of 1000-2000 bar causes a reversible phase transition and the dissociation or conformational changes in the protein subunits. A pressure higher than 2200 bars irreversibly destroys the membrane structure, due to protein unfolding and interface separation, which is amplified by the increasing pressure [Kato 2002].

From the exponentially decaying activity data in the pressure range from about 100 to 600 bar, an apparent activation volume  $\Delta V^\ddagger$  of the reaction may be obtained from the  $\ln(\Delta I_F/\Delta t)$  vs.  $p$  plots for the DMPC, DOPC, DOPC/DOPE mixture, and raft-mixture (Fig. 5.7 a-d). Values for  $\Delta V^\ddagger$  of  $78,54 \pm 10$  mL/mol,  $70,31 \pm 10$  mL/mol,  $49,14 \pm 10$  mL/mol and  $22,23 \pm 10$  mL/mol are obtained for the enzyme incorporated into DMPC, DOPC and DOPC/DOPE 3:2 bilayers, respectively. These values are about a factor of two larger than that of the enzyme in its natural plasma membrane environment (*vide infra*).

a)



b)





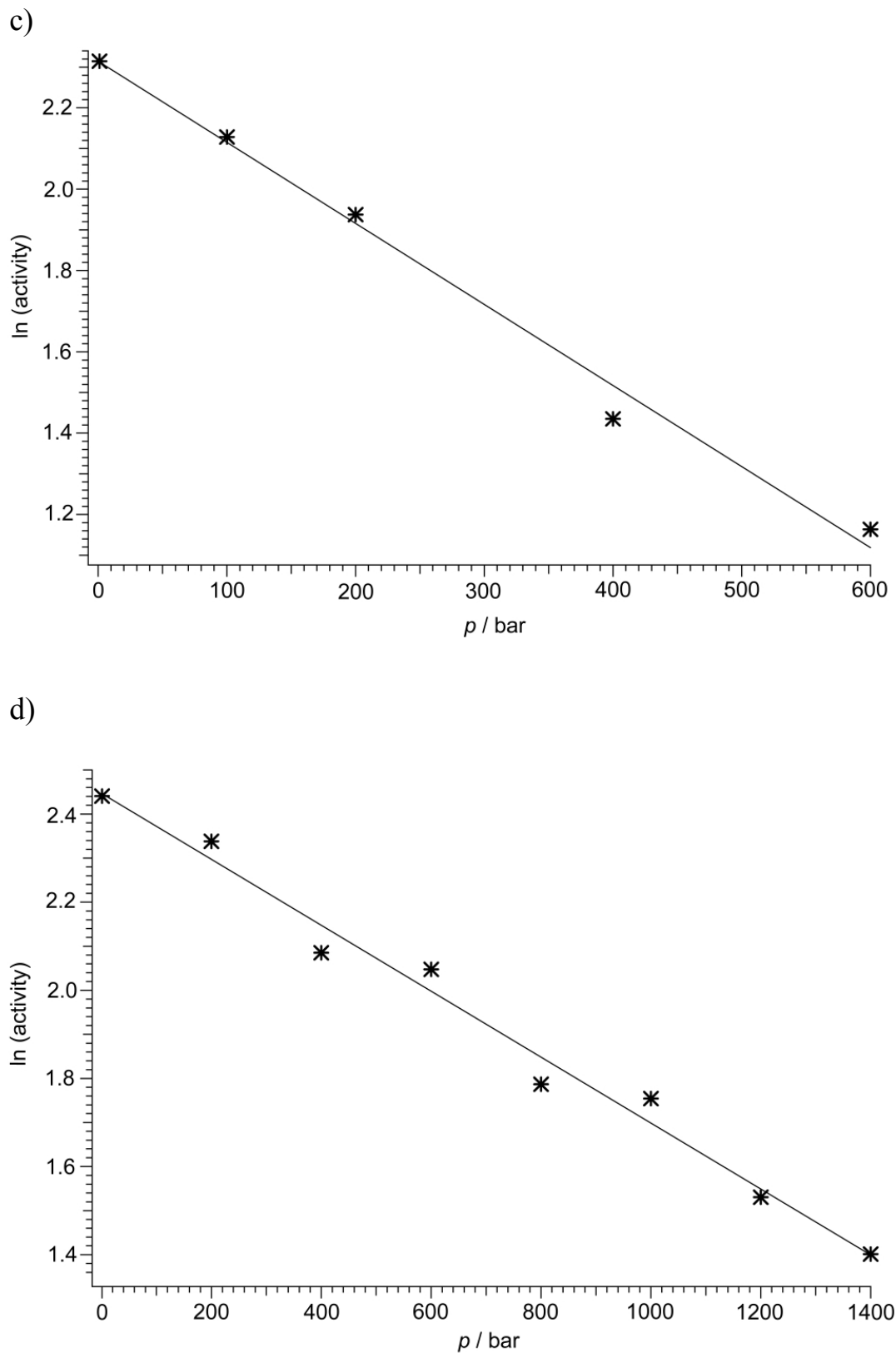


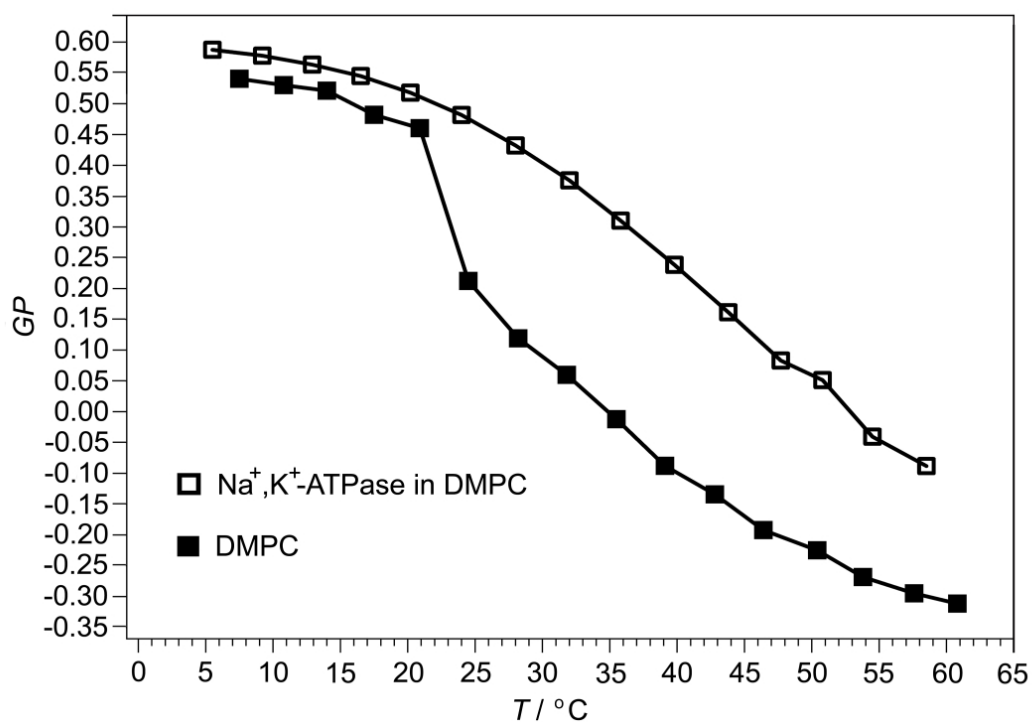
**Figure 5.7:** Logarithmic plots of the activity as a function of pressure (obtained from the almost linear region) in: a) DMPC. b) DOPC. c) DOPC/DOPE 3:2. and d) the raft-mixture.

### 5.3.3 Pressure/Temperature Dependence of GP Values of the Various Lipid Bilayer and Reconstituted Lipid-Enzyme Systems.

To reveal, if the decrease in enzyme activity upon pressurization is related to pressure-induced lipid phase transitions, the temperature and pressure depended Laurdan generalized polarization (*GP*) values of the various lipid and reconstituted proteolipid systems were measured as a function of temperature and pressure as well. As explained above (Experimental Procedures), the *GP* values report on the phase state of the lipid bilayer system. The temperature dependent measurements were carried out in the temperature range 7-70 °C, pressure dependent measurements were done in the range 1-2000 bar at 37 °C.

We first focus on the one-component lipid bilayer systems. For Na<sup>+</sup>, K<sup>+</sup>-ATPase reconstituted in DMPC (Fig 5.8 a,b) we can see that the *GP*(*T*) values first gradually decrease from 5 °C on with increasing temperature. The gel-to-fluid phase transition as observed for pure DMPC bilayers around 23 °C, is not visible any more. Interestingly, the *GP* values of the reconstituted system are larger over the whole temperature range covered, indicating an increased order of the DMPC bilayer containing the enzyme. At 37 °C, the *GP* value of the reconstituted system is about 0.3, which is about 0.35 *GP* units above the *GP* value of the pure DMPC bilayer at that temperature. Figure 8b depicts the pressure dependent data at 37 °C. For pure DMPC bilayers, the pressure-induced fluid-to-gel phase transition around 550 bar is indicated by a significant increase of the *GP* values. For the reconstituted system, the *GP* values are always much higher and increase steadily with increasing pressure, finally reaching *GP* values typical for densely packed gel-like lipids (0.55-0.6) at pressures above about 1200 bar.

a)



b)

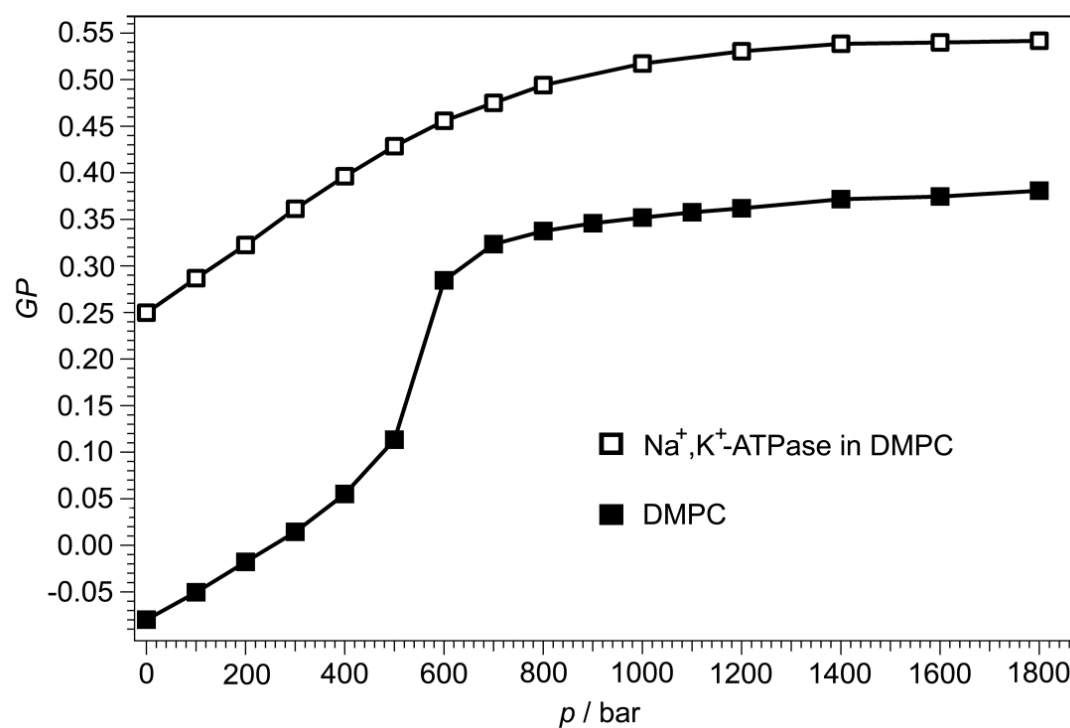
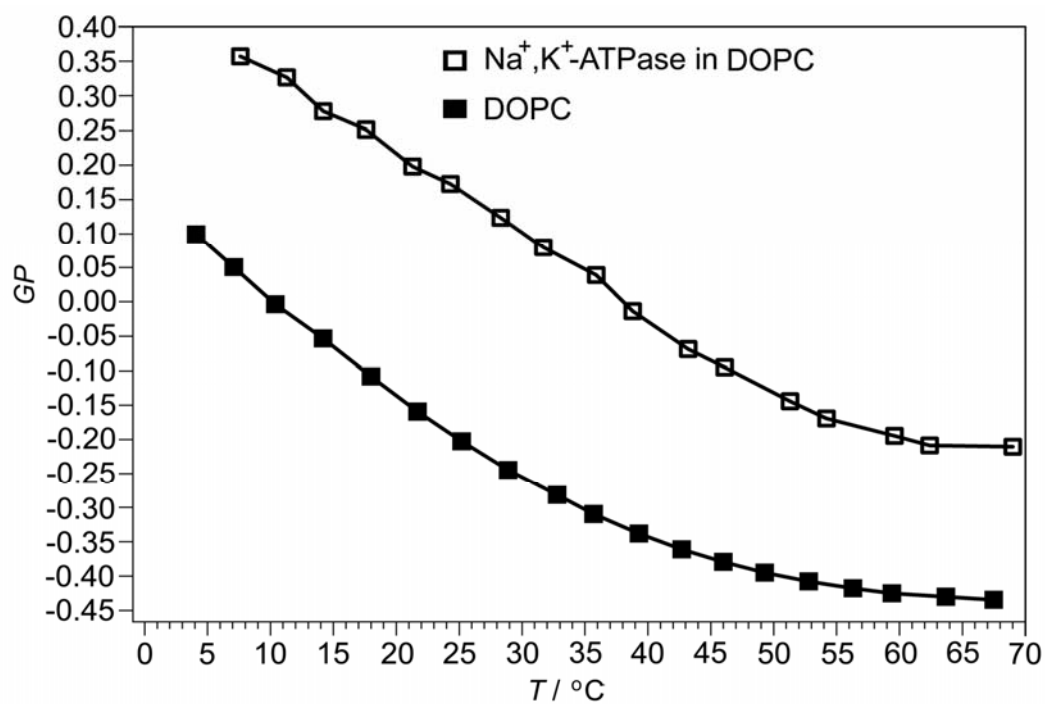


Figure 5.8 a) Temperature dependence of Laurdan  $GP$  values of DMPC vesicles without and with incorporated  $\text{Na}^+, \text{K}^+$ -ATPase. b) Pressure dependence (at  $T = 37^\circ\text{C}$ ) of Laurdan  $GP$  values of DMPC vesicles without and with incorporated  $\text{Na}^+, \text{K}^+$ -ATPase.

The corresponding data for pure DOPC and Na<sup>+</sup>, K<sup>+</sup>-ATPase reconstituted into DOPC bilayers are depicted in Fig. 5.9. At 5 °C, the acyl-chains of fluid DOPC are highly disordered, leading to *GP* values around 0.10. At 37 °C, *GP* values of -0.3 are measured, indicating highly conformational disorder for this system consisting of *cis*-unsaturated lipid chains. As the main transition temperature  $T_m$  of DOPC is ~ -20 °C, no temperature or pressure induced phase transition is observed for this lipid system in the temperature and pressure range covered. Similar to DMPC bilayers, incorporation of Na<sup>+</sup>, K<sup>+</sup>-ATPase into DOPC leads to an increase of *GP* values of about 0.3 units. For both, pure DOPC and the reconstituted DOPC system, the *GP* value increases steadily with increasing pressure. Around 2 kbar, *GP* values of about 0.30 are reached. *GP* values of this order are indicative of a medium high conformational order parameter of the acyl-chains.

a)



b)

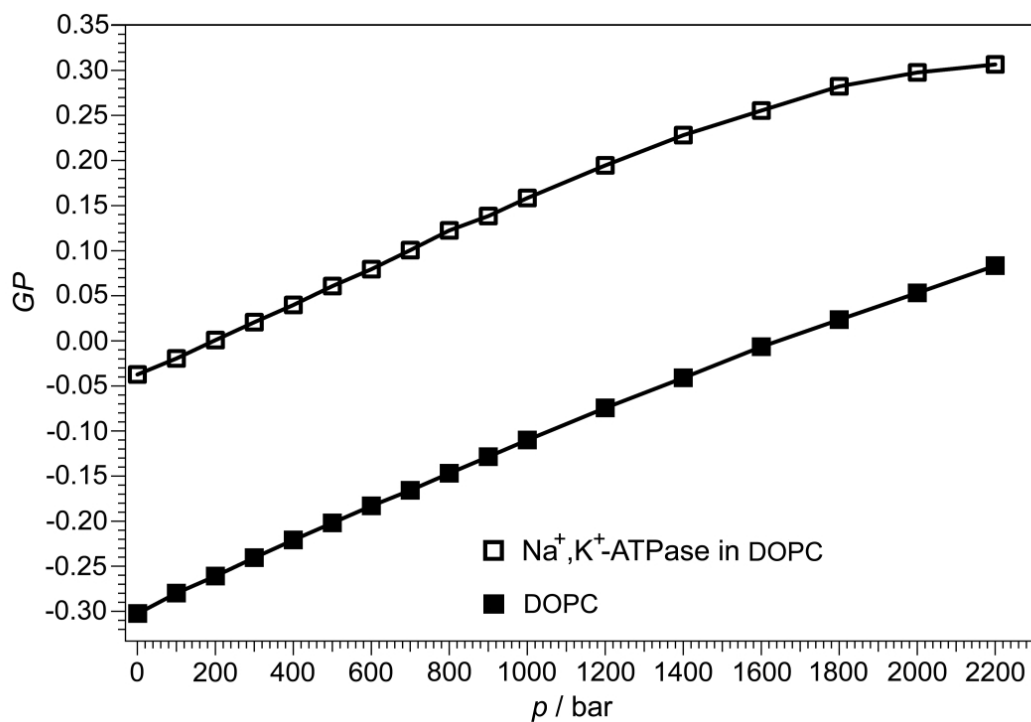


**Figure 5.9:** a) Temperature dependence of Laurdan GP values of DOPC vesicles without and with incorporated  $\text{Na}^+, \text{K}^+$ -ATPase. b) Pressure dependence (at  $T = 37 ^\circ\text{C}$ ) of Laurdan GP values of DOPC vesicles without and with incorporated  $\text{Na}^+, \text{K}^+$ -ATPase.

Next, the DOPE was incorporated into DOPC lipid bilayer in different molar ratio: 1:1; 6:4; 7:3, to create a spontaneous curvature stress condition. The results are presented on Figure 5.10

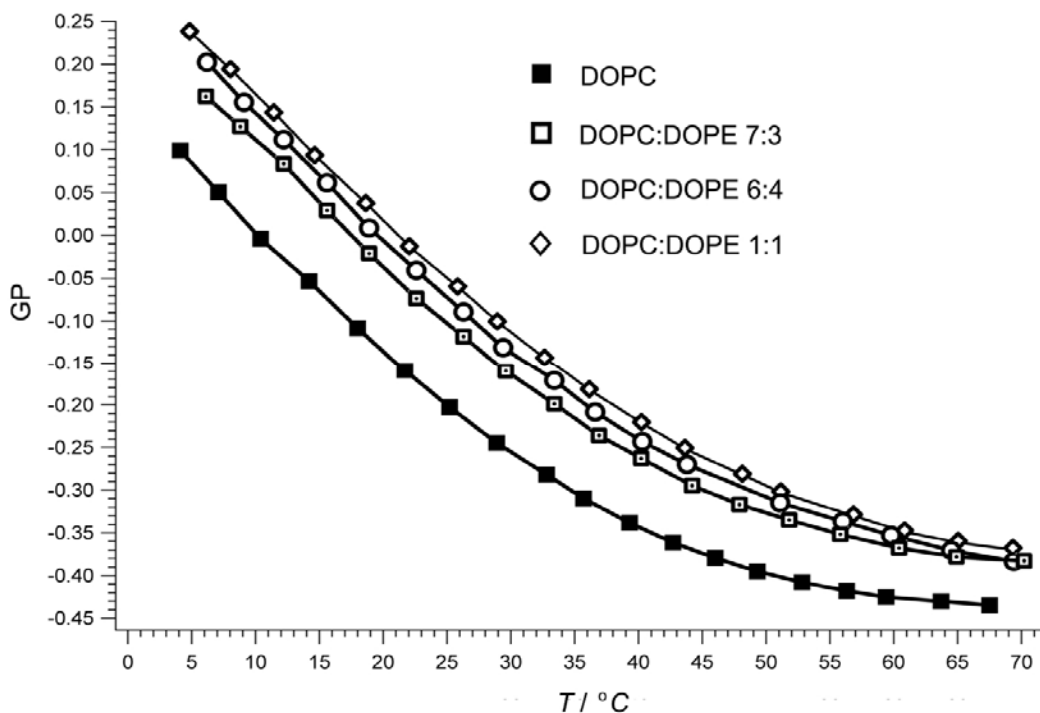


**Figure 5.10:** Temperature dependence of Laurdan GP values of DOPC vesicles and DOPC with addition of DOPE in different molar ratio

In general an increasing amount of incorporated DOPE leads to increasing an order of the lipid bilayer. The amount of DOPE is different in the different tissues, for example in mammalian liver approximately by 28%, and in kidney 17% [Cevc 1993].

For further experiments the molar ratio of DOPC/DOPE 6:4 was chosen. Addition of the DOPE to DOPC increases the lipid order by about 0.1  $GP$  units. Whereas incorporation of the enzyme into DOPC leads to an increase of  $\sim 0.3$   $GP$  units, the incorporation of  $\text{Na}^+$ ,  $\text{K}^+$ -ATPase into the DOPC/DOPE 3:2 mixture leads to an even larger increase ( $\Delta GP \approx 0.4$ ) (Fig. 5.11), indicating that the increased enzymatic activity is accompanied by an increase of the conformational order of the mixed bilayer system. Hence, we may conclude that the enzyme incorporation efficiently releases the stress condition that seems to be favourable for its activity.

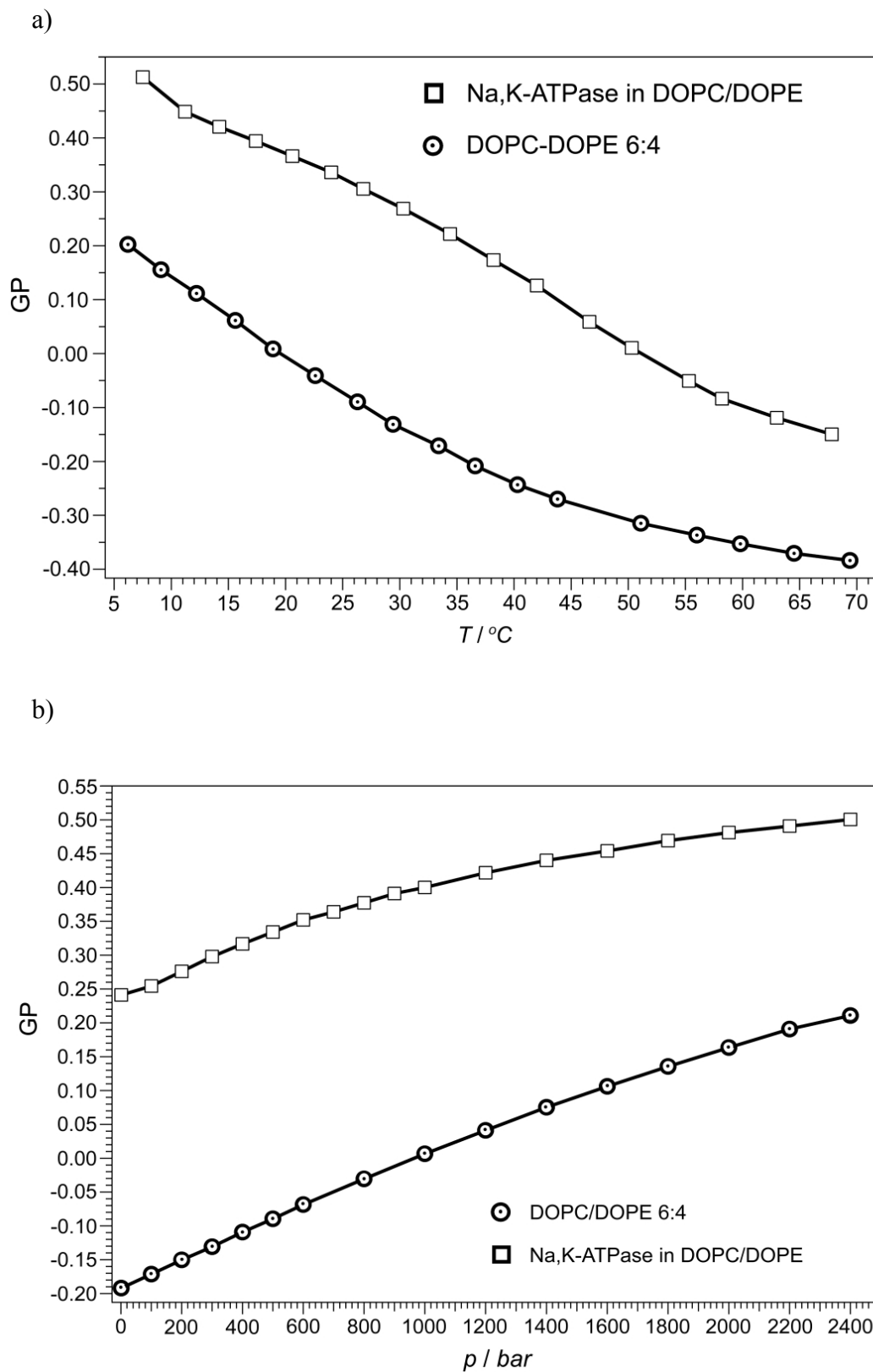
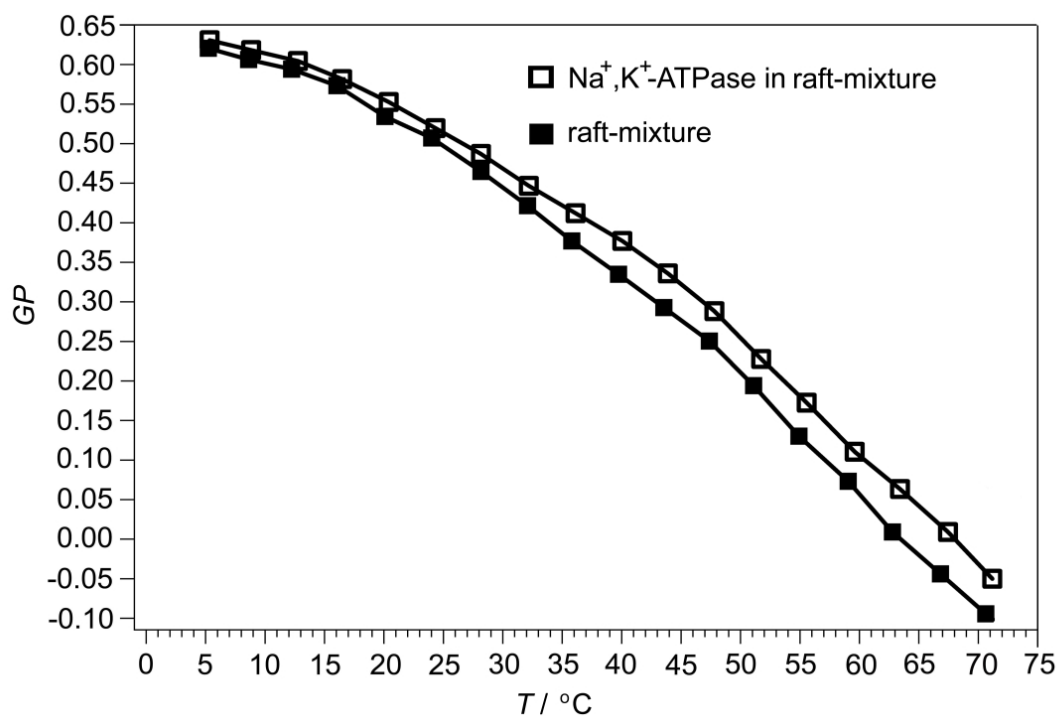


**Figure 5.11:** a) Temperature dependence of Laurdan GP values of DOPC/DOPE 3:2 vesicles without and with incorporated Na<sup>+</sup>, K<sup>+</sup>-ATPase. b) Pressure dependence (at T = 37 °C) of Laurdan GP values of these mixtures.

For the POPC/SM/Chol 1:1:1 model raft mixture (Fig. 5.10 a, b),  $GP$  values are much higher and gradually decrease with increasing temperature, reaching values around zero, typical for an overall fluid state of the lipid membrane, around 65 °C, only. In fact, such a smooth behaviour is expected from Gibbs' phase rule for such three-component lipid mixtures, which is very different from one-component lipid bilayer systems, which generally exhibit sharp gel-to-gel and gel-to-fluid phase transitions in the temperature range covered. Hence, by a more or less continuous increase of liquid-disordered domains, the fluidity and conformational disorder of the membrane gradually increases with increasing temperature, and  $GP$  values typical for pure fluid phases are reached above about 65 °C. Also the effect of pressure on the generalized polarization data of the Laurdan labelled POPC/SM/Chol mixture has been measured. At room temperature (20 °C), the  $GP$  values increase steadily with increasing pressure up to about 800-900 bar, where a plateau value of about 0.6 is reached, indicating that a rather ordered (probably an  $s_o+l_o$ ) state is reached which is not affected upon application of higher pressures (up to 2.5 kbar) any more. At 40 °C, the overall (according to the Gibbs phase rule, probably  $l_o+s_o$ ) ordered lipid state of the POPC/SM/Chol 1:1:1 mixture is reached at ~2 kbar. Hence, a temperature decrease of about 50 °C has a similar effect on membrane ordering as a pressure increase of 1 kbar. At 37 °C, the system is supposed to consist of coexisting  $l_d$  and  $l_o$  domains, leading to an average  $GP$  value of ~0.40. For this model raft mixture, reconstitution leads to a minor increase in  $GP$  values, i.e. phase state of the membrane, only. As the  $GP$  values hardly change, one could also conclude that the enzyme is embedded to a large extent in the  $l_d/l_o$  domain boundary regions. The pressure effect is shown in Fig. 5.10b. The  $GP$  values of the pure lipid mixture as well as of the  $Na^+$ ,  $K^+$ -ATPase – POPC/SM/Chol system gradually increase with increasing pressure, reaching  $GP$  values of ~0.55-0.65 typical of an all-ordered phase state at pressures of ~1500 bar. The effect of incorporation of  $Na^+$ ,  $K^+$ -ATPase leads to a small but readily increase of order parameter value over the whole pressure range. Such an effect was also observed with incorporation of the peptide gramicidin [Periasamy 2006].



a)



b)

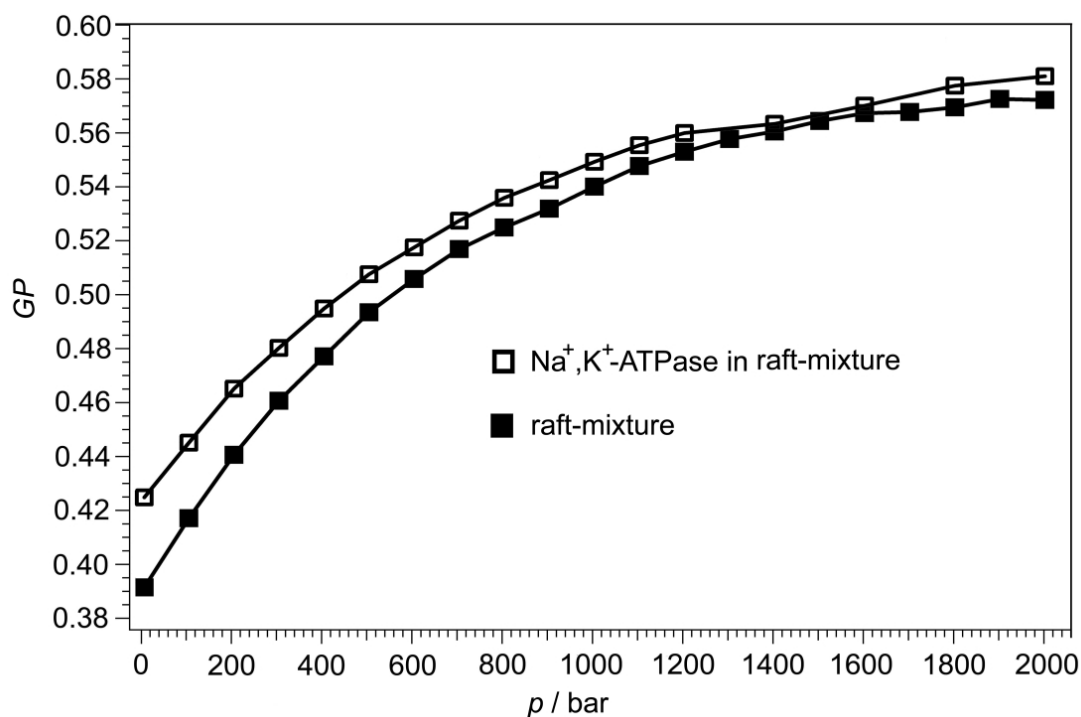
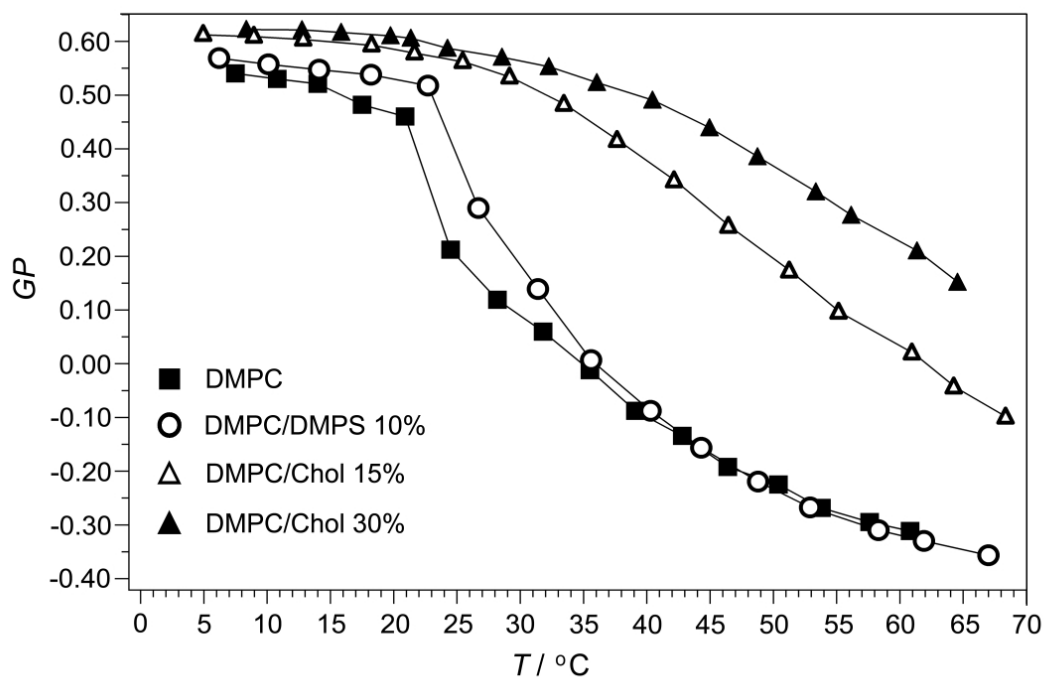


**Figure 5.10:** a) Temperature dependence of Laurdan  $GP$  values of the POPC/SM/Chol 1:1:1 model raft mixture without and with incorporated  $\text{Na}^+$ ,  $\text{K}^+$ -ATPase. b) Pressure dependence (at  $T = 37 ^\circ\text{C}$ ) of Laurdan  $GP$  values of the model raft mixture without and with incorporated  $\text{Na}^+$ ,  $\text{K}^+$ -ATPase.

The effects of incorporation of 10 mol% DMPS and different amounts of cholesterol into DMPC is presented in Figs. 5.11 and 5.12. We observe small but clearly visible changes in  $GP$  values and the phase transition is shifted to a slightly higher temperature in the former case. Above 40 °C, in the fluid-like state, the  $GP$  values are similar for both systems, DMPC and DMPC/ 10 mol% DMPS. The incorporation of cholesterol at levels of 15 and 30 mol% has a significant effect. The order of the lipid bilayer system increases drastically and at 37 °C, the difference in  $GP$  values for DMPC and DMPC/15 mol% cholesterol is  $\sim 0.5$  and for DMPC/30 mol% cholesterol  $\sim 0.6$ , respectively. The same difference is also observed in the pressure dependent  $GP$  measurements (Fig 5.11b). The temperature and pressure dependent  $GP$  data for  $\text{Na}^+$ ,  $\text{K}^+$ -ATPase reconstituted into DMPC/10 mol% DMPS are presented in Fig. 5.12. Similar to the other systems, incorporation of the enzyme leads to a marked increase of  $GP$  values, most pronounced in the fluid-like state ( $\Delta GP \approx 0.3$ ) of the lipid bilayer system.

a)



b)

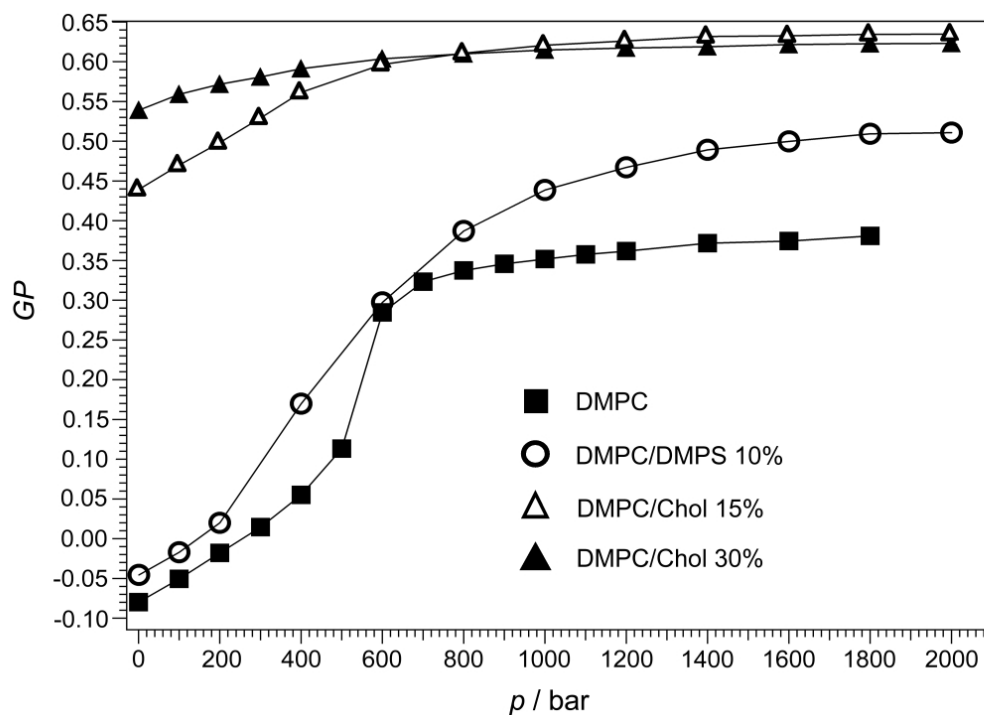
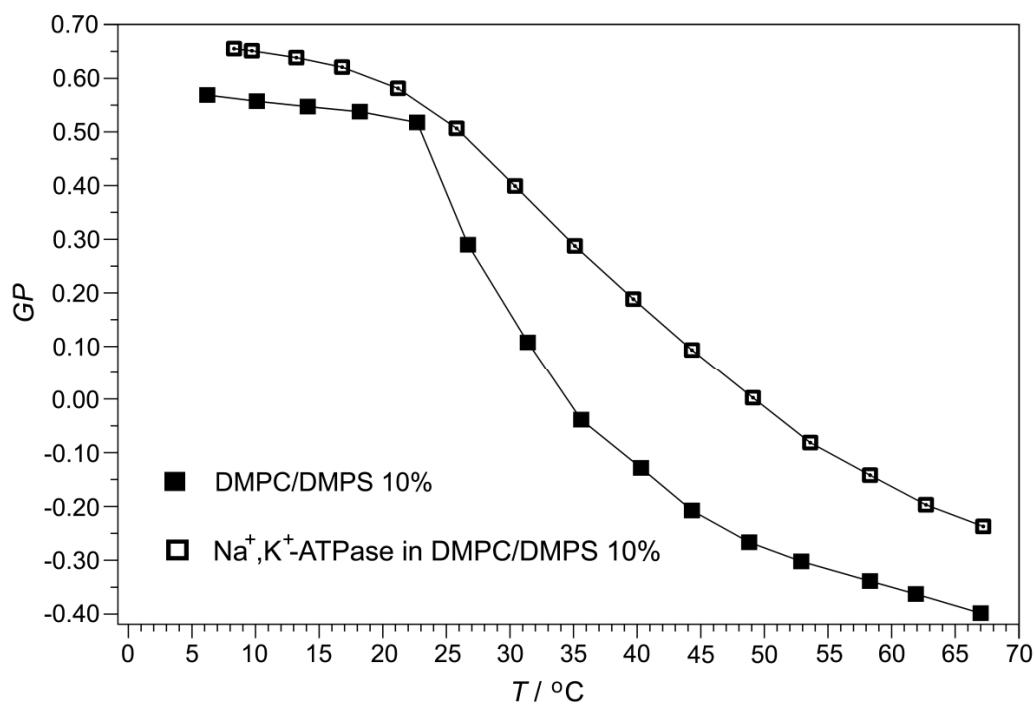


**Figure 5.11:** a) Temperature dependence of Laurdan GP values of DMPC/DMPS (0 and 10 mol%) and DMPC/Chol (15 and 30 mol%) vesicles. b) Pressure dependence (at  $T = 37 ^\circ\text{C}$ ) of Laurdan GP values of these lipid mixtures.

a)



b)

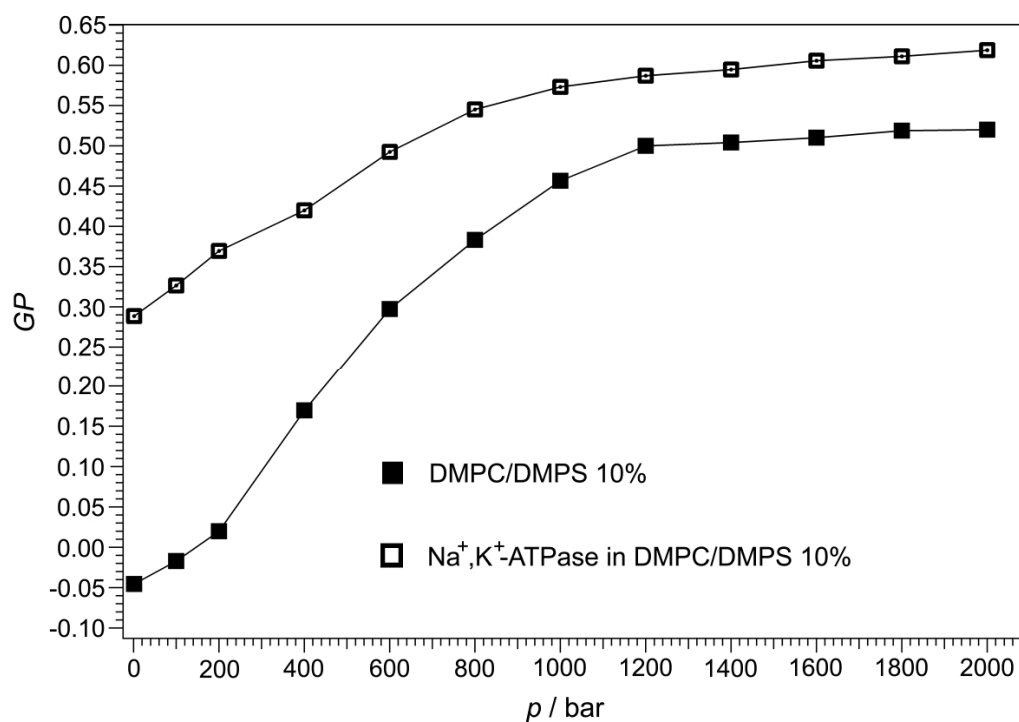
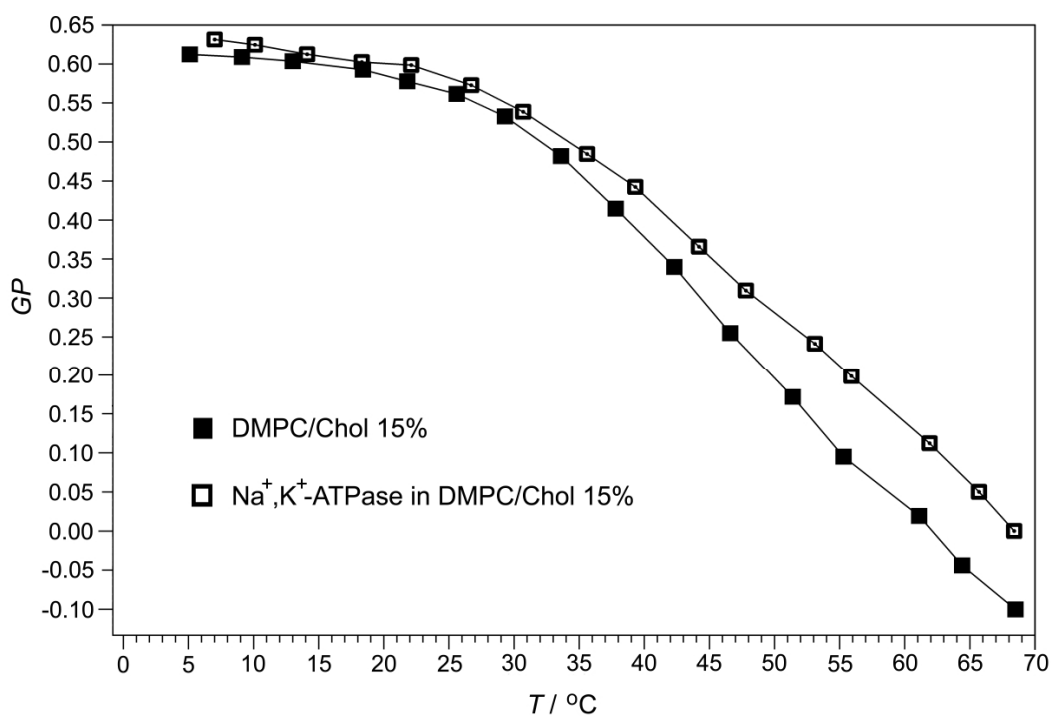


**Figure 5.12:** a) Temperature dependence of Laurdan GP values of DMPC/DMPS (10 mol%) vesicles without and with incorporated  $\text{Na}^+, \text{K}^+$ -ATPase. b) Pressure dependence (at  $T = 37^{\circ}\text{C}$ ) of Laurdan GP values of these mixtures.

For DMPC in the presence of 15 and 30 mol% cholesterol, differences between  $GP$  values between the pure lipid and reconstituted system are small (Figs. 5.13, 5.14). The conformational order of the lipids in the DMPC/Chol systems is already very high so that incorporation of the enzyme does not lead to a marked increase of conformational order of the membrane anymore. The same difference is also observed in the pressure dependent  $GP$  measurements Fig 5.11 b. Incorporation of cholesterol into DOPC in amount of 15 and 30 % also increases significantly the lipid order (Fig 5.15) The changes are similar to the previous example. At 37 °C the difference between DOPC and DOPC/Chol 15% is around 0.35. The activity measurement showed that incorporation of cholesterol into the highly disordered, unsaturated lipid system is more favourable.

a)



b)

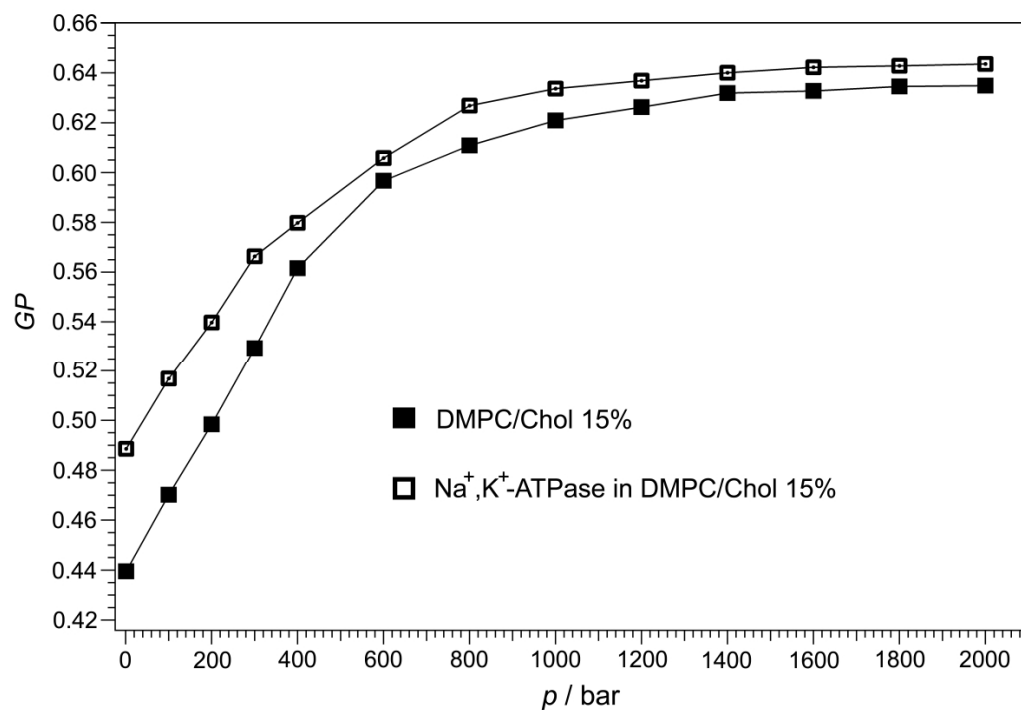


**Figure 5.13:** a) Temperature dependence of Laurdan GP values of DMPC/Chol (15 mol%) vesicles without and with incorporated Na<sup>+</sup>, K<sup>+</sup>-ATPase. b) Pressure dependence (at  $T = 37 ^\circ\text{C}$ ) of Laurdan GP values of these mixtures.

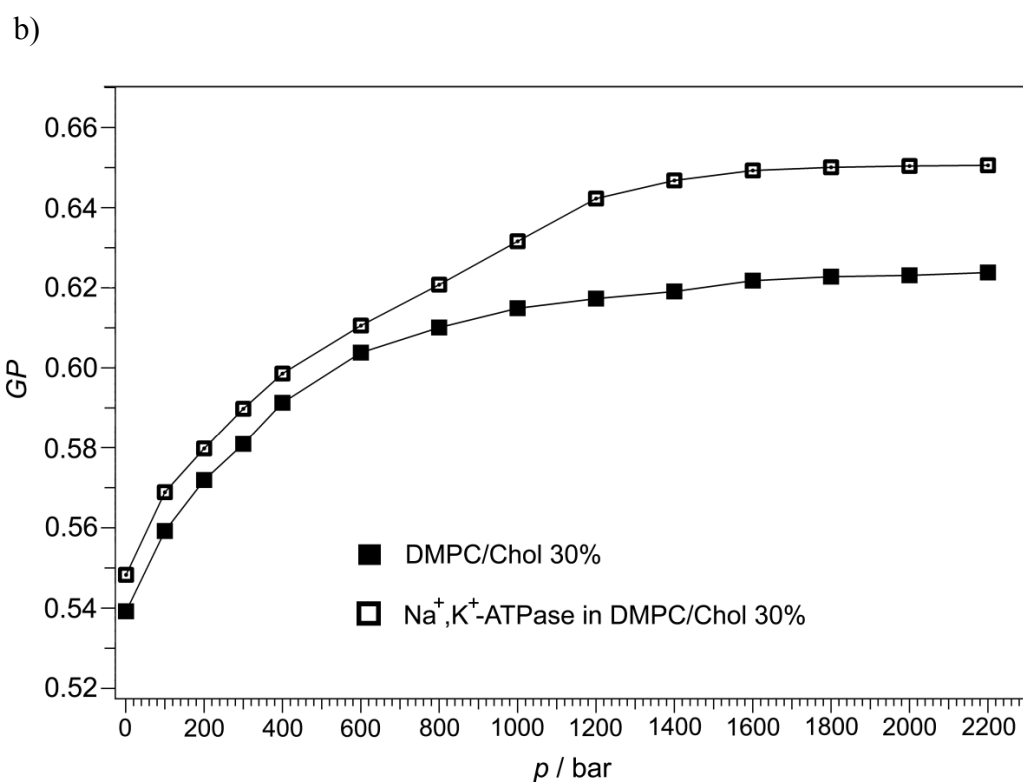
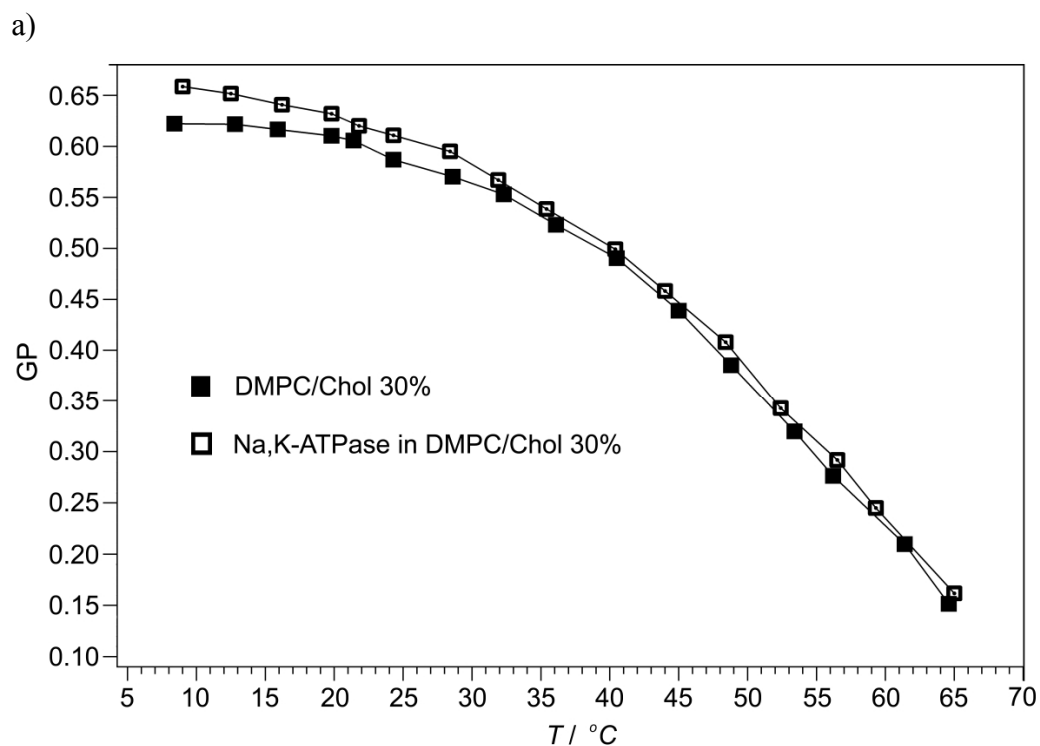


**Figure 5.14:** a) Temperature dependence of Laurdan  $GP$  values of DMPC/Chol (30 mol%) vesicles without and with incorporated  $\text{Na}^+$ ,  $\text{K}^+$ -ATPase. b) Pressure dependence (at  $T = 37^\circ\text{C}$ ) of Laurdan  $GP$  values of these mixtures.

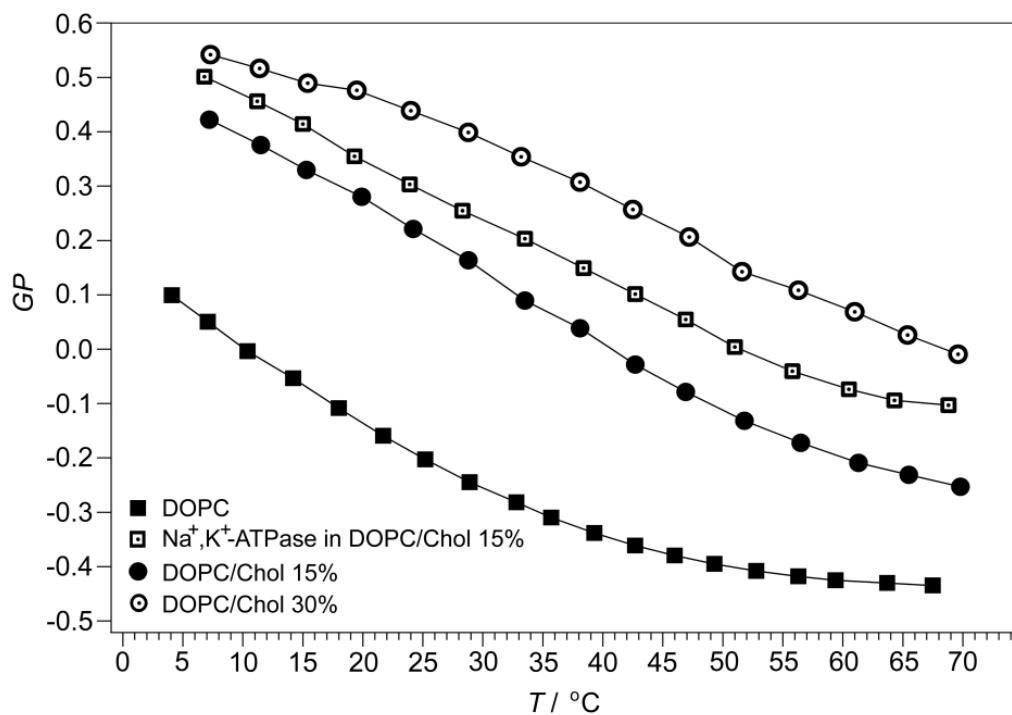


**Figure 5.15:** Temperature dependence of Laurdan  $GP$  values of DOPC, DOPC/Chol (15 and 30 mol%) vesicles, and DOPC/chol 15% with incorporated Na<sup>+</sup>, K<sup>+</sup>-ATPase.



## 6 Summary

Variables used frequently to study properties of biological membranes are temperature and pressure. Changing the temperature of a system results in alterations of the thermal energy as well as the density. In contrast, a pressure change under isothermal conditions introduces only a change in the density of the system. High pressure is also a characteristic feature of certain natural membrane environments [Bernsdorf 1997]. In order to study the pressure-induced changes of biological membranes high hydrostatic pressures from 1-2000 bar were applied to membrane-bound  $\text{Na}^+, \text{K}^+$ -ATPase from pig kidney and then the enzyme was reconstituted in selected lipid-bilayer matrices. In accord with previous studies it was observed that high hydrostatic pressure leads to a retardation of the enzyme activity, enriched in the plasma membrane (Fig. 5.1). Below  $\sim 2000$  bar, the activity is still reversible. Above this pressure, the enzyme is irreversibly destroyed.

In principle, one could think of several general mechanisms of  $\text{Na}^+, \text{K}^+$ -ATPase inhibition by hydrostatic pressure: 1) an increased packing and order of the lipid membrane that hinders (dynamic) conformational changes of the enzyme needed for function, 2) volume changes of the enzyme itself upon pressurization, independent of the lipid phase state, 3) subunit reorientation or dissociation of the enzyme, 4) unfolding and denaturation of the protein, and 5) a pressure-induced decrease of the substrate binding reaction due to a positive activation volume. Certainly, as has been shown by many studies on phospholipid bilayer model systems, by increasing pressure of a few hundred bar only, the acyl-chain conformational order drastically increases and a more or less broad gel-fluid coexistence region as well as gel-phases may be induced at higher pressures [Winter 1998, Winter 2002, Winter 2005, Eisenblätter 2006], which might hinder conformational transitions associated with the ATPase reaction. This would be in accord with the observations of De Smedt *et al.* [de Smedt 1979] who suggested that the inhibition by pressure is due to a shift in the melting temperature of the lipid aliphatic chains. Chong *et al.* [Chong 1985] concluded that the decrease in the fluidity of the membrane caused by increased pressure may hinder the conformational changes that accompany the reaction steps, and thus decrease the rate of the overall reaction. On the other hand, it was also found that high pressures up to 2 kbar may lead to a dissociation of the subunits of the  $\text{Na}^+, \text{K}^+$ -ATPase [Kato 2002]. The pressure dissociation of water-soluble proteins in this

pressure range is well-documented in several instances [Winter 2005, Winter 2003]. In the recent study by Kato *et al.* [Kato 2002] it has been suggested that the activity of the enzyme shows at least three step changes induced by pressure: At pressures below and around 1 kbar a decrease in the fluidity of the lipid bilayer and a reversible conformational change in the transmembrane protein is induced, leading to functional disorder of the membrane associated ATPase activity. Pressures of 1-2 kbar cause a reversible phase transition and the dissociation or conformational changes in the protein subunits, and pressures higher than 2200 bar irreversibly destroy the membrane structure due to protein unfolding and interface separation, which is amplified by the increasing pressure.

Furthermore, it has been shown that the activity of the reconstituted Na<sup>+</sup>,K<sup>+</sup>-ATPase strongly depends on the lipid environment. As seen in Fig. 5.6, the time dependence of the enzymatic reaction, as measured by the fluorescence intensity decay,  $I_F(t)$ , in the NADH assay, exhibits a non-trivial shape with a steeper decay at the late part of the reaction. DMPC and DOPC were chosen as one-component lipid systems which represent saturated and unsaturated lipids, respectively. High activity at 37 °C is obtained for fluid DMPC, which contains fully saturated 14 carbon acyl-chains of hydrophobic length of about 28 Å [Eisenblätter 2006]. Incorporation of the enzyme into the DMPC bilayers also leads to a significant increase of the lipid chain order ( $\Delta GP \approx 0.35$ ). For the longer di-*cis*-unsaturated C<sub>18</sub> phospholipid DOPC, the enzymatic activity is among the lowest ones observed (Fig. 5.3). The enzyme activity increased significantly when mixed DOPC with DOPE at a 3:2 molar ratio to create curvature lipid stress (Fig. 5.3). Addition of the DOPE to DOPC increases the lipid order by about 0.1 *GP* units. Whereas incorporation of the enzyme into DOPC leads to an increase of  $\sim 0.3$  *GP* units, the incorporation of Na<sup>+</sup>, K<sup>+</sup>-ATPase into the DOPC/DOPE 3:2 mixture leads to an even larger increase ( $\Delta GP \approx 0.4$ ), indicating that the increased enzymatic activity is accompanied by an increase of the conformational order of the mixed bilayer system. Hence, we may conclude that the enzyme incorporation efficiently releases the stress condition that seems to be favourable for its activity. Addition of cholesterol to DMPC at levels of 15 and 30 mol%, which leads to an increase in conformational order and acyl-chain length of the fluid bilayer at that temperature, leads to a drastic decrease of the enzymatic activity, probably owing to an increasingly hydrophobic mismatch between the acyl-chain's

and protein's hydrophobic lengths, leading to changes in the conformational mobility of the  $\text{Na}^+$ ,  $\text{K}^+$ -ATPase. In contrast, incorporation of 15 mol% of cholesterol into DOPC has a positive, significant influence on the enzyme activity. Incorporation of the cholesterol into unsaturated lipid accelerates the reaction. As cholesterol is a very important determinant of lipid bilayer thickness, one might conclude that hydrophobic thickness must have obvious importance for the activity of an integral enzyme next to the lipid fluidity. An increase of the anionic lipid content (10% DMPS) of the membrane leads to an additional increase of the activity of the enzyme, accompanied by an increase of conformational order of the membrane, of magnitude similar to that of pure DMPC bilayers ( $\Delta GP \approx 0.3$ ). A significant change in dipole potential of the bilayer in the case of the partially anionic lipid bilayer system produces large differences in the electric field strength within the bilayer in the headgroup region, which seems to modify the electrogenic steps along the reaction path of the enzyme in an accelerating way. Taken together, maximal enzyme activity at ambient pressure - for the systems looked at here - seems to be achieved if the  $\text{Na}^+$ ,  $\text{K}^+$ -ATPase is embedded into fluid-like  $\text{C}_{14}$  lipid bilayers containing a certain amount of anionic lipids, unsaturated lipid with addition of cholesterol in amount of 15 mol%, which is similar to the amount of cholesterol that naturally appears in a pig kidney tissue, and existing curvature elastic stress seems to be favourable as well.

The activity of the enzyme reconstituted into DMPC, DOPC, the model raft and DOPC/DOPE mixtures has also been measured in the pressure range from ambient pressure up to about 2 kbar at 37 °C. Generally, similar to the enzyme activity in the natural plasma membrane, an increase of high hydrostatic pressures leads to a retardation of the activity of the enzyme reconstituted into the various lipid bilayer systems, and in most cases a more-phasic behaviour is observed. Clearly a no two-state transition is observed as for the pressure-induced unfolding reaction of many water soluble proteins [Winter 1998, Winter 2002, Winter 2005, Woenckhaus 2001, Meersman 2006].

Interestingly, in the low pressure regime around 100 bar, a significant increase of the enzyme activity (by 60-100 %) is observed for the enzyme reconstituted into DMPC and DOPC bilayers. Above 100-200 bar, this maximum is followed by a steep decrease of the activity up to about 600-800 bar, where a more or less broad plateau value is reached, until the enzyme activity decreases to zero around 2 kbar for all

reconstituted systems measured (Fig. 5.6). The increased activation at these rather low pressures of about 100 bar may, for example, be related to a drastic decrease in the volume of the ATPase complex induced by compression, which drives the system towards a more negative activation volume of the ATPase reaction. The effect could also be related to a structural change in the lipid matrix, which, at these low pressures, seems to be less likely, however. An increase of 100 bar would lead to a slight (ca. 0.1 Å) increase in average lipid acyl-chain length, only, and no pressure-induced fluid-to-gel phase transition occurs at these rather low pressures [Eisenblätter 2006]. A different scenario is observed for the effect of pressure on the enzyme activity in the model raft mixture. In this case, almost linear decrease in the activity is observed up to about 2 kbar, where the activity ceases. Obviously, the coexistence of  $l_o$  and  $l_d$  domains and the possibility of lipid sorting in this lipid mixture leads to a reduced pressure sensitivity of the enzymatic reaction in the medium pressure range.

The subsequent decrease of the ATPase activity as the pressure is raised above 100-200 bar, may be induced by an increasing hydrophobic mismatch and eventually subunit rearrangement/dissociation. Generally, upon pressurization, a decrease in the fluidity of the lipid bilayer with a concomitant decrease in protein conformational flexibility is expected. Also the thickness of the lipid bilayer increases, which would be expected to alter the environment of the transmembrane protein in the protein/water and protein/lipid contact surface. For example, an increase in the thickness might partially cover the water-soluble region of the enzyme, which could lead to a retardation of the reaction. The physiological  $\text{Na}^+$ ,  $\text{K}^+$ -ATPase reaction involves the two conformational transitions  $E_2 \rightarrow E_1$  and  $E_1P \rightarrow E_2P$ , which might both be pressure sensitive. If a positive volume change would be involved, or induced by these conformational changes, this could be one factor explaining the retardation of the activity upon pressurization. As there is no pressure-induced fluid-to-gel phase transition in DOPC and DOPC/DOPE bilayers in the whole pressure range covered (Figs. 5.9, 5.11), the low plateau value of the enzymatic activity reached around 600-800 bar for DMPC, DOPC and DOPC/DOPE 3:2 speaks for such conformational transitions of the protein rather than a fluid-to-gel transition as major retarding mechanism. Higher pressures above about 2.2 kbar irreversibly destroy the proteoliposome structure, probably due to dissociation and partial unfolding of the subunits.

## 7 Zusammenfassung

Temperatur und Druck sind Parameter, welche zur Untersuchung biologischer Membranen herangezogen werden. Eine Änderung der Temperatur führt zu einer Änderung der thermischen Energie sowie der Dichte des Systems, während eine isotherme Variation des Druckes lediglich zu einer Dichteänderung führt. Desweiteren ist ein hoher Druck eine charakteristische Eigenschaft bestimmter natürlicher Membranumgebungen [Bernsdorf 1997]. Um die druckinduzierten Änderungen in biologischen Membranen zu untersuchen, wurden Drücke von 1 – 2000 bar auf membrangebundene  $\text{Na}^+$ ,  $\text{K}^+$ -ATPase sowie auf das in einer Doppelmembran rekonstituierte Enzym ausgeübt. In Einklang mit älteren Arbeiten wurde beobachtet, dass hohe Drücke zu einer Hemmung der Aktivität des in der Plasmamembran angereicherten Enzyms führen (Abb. 5.1). Unterhalb von  $\sim 2000$  bar ist diese Hemmung reversibel, oberhalb dieses Druckes wird das Enzym irreversibel geschädigt.

Grundsätzlich sind mehrere Mechanismen dieser druckinduzierten Inhibierung der  $\text{Na}^+$ ,  $\text{K}^+$ -ATPase denkbar: Erstens könnte eine dichtere und geordnetere Packung der Lipidmembran die Dynamik und konformativen Änderungen des Enzyms, welche für die volle Funktionalität notwendig sind, behindern. Zweitens könnten durch den erhöhten Druck – unabhängig von der Lipidphase - Volumenänderungen innerhalb des Proteins verursacht werden. Desweiteren könnte drittens der Hochdruck eine Umorientierung oder Dissoziation der Untereinheiten induzieren oder viertens gar zu einer Denaturierung des Proteins führen. Fünftens könnte es bei erhöhtem Druck aufgrund eines positiven Aktivierungsvolumens zu einer Abnahme der Substratbindung kommen. Sicher ist, wie viele Studien an Modellsystemen aus Phospholipiden belegen, dass ein Druck von nur mehreren hundert bar die konformative Ordnung der Acyl-Ketten drastisch erhöht, und dass unter erhöhten Drücken ein mehr oder weniger breiter gel-fluider Koexistenzbereich sowie mehrere Gelphasen induziert werden können [Winter 1998, Winter 2002, Winter 2005, Eisenblätter 2006], so dass konformative Übergänge, die mit der ATPase-Reaktion verknüpft sind, behindert werden können. Dies stünde in Einklang mit Beobachtungen von De Smedt *et al.* [de Smedt 1979], welche vorschlagen, dass die druckinduzierte Hemmung Resultat der Verschiebung der Schmelztemperatur der aliphatischen

Lipidketten ist. Chong *et al.* [Chong 1985] schlussfolgerten, dass die Fluiditätsabnahme der Membran mit ansteigendem Druck die Änderungen in der Konformation, welche mit der Reaktion einhergehen, behindert und so die Reaktionsrate herabsetzen kann. Andererseits konnte allerdings auch festgestellt werden, dass Drücke bis zu 2 kbar zu einer Dissoziation der Untereinheiten der  $\text{Na}^+, \text{K}^+$ -ATPase führen können [Kato 2002]. Die Dissoziation wasserlöslicher Proteine unter entsprechenden Drücken ist anhand einiger Beispiele gut dokumentiert [Winter 2005, Winter 2003]. In einer neueren Arbeit von Kato *et al.* [Kato 2002] wird vorgeschlagen, dass die Aktivität des Enzyms mindestens drei Änderungen mit Druckänderung erfährt: Bei Drücken unter oder um 1 kbar wird eine Fluiditätsabnahme und eine konformative Änderung des Transmembranproteins induziert, die zu einer Störung der membranassoziierten ATPase-Aktivität führt. Drücke zwischen 1-2 kbar führen zu einer reversiblen Phasenumwandlung und zu einer Dissoziation bzw. Konformationsänderung der Proteinuntereinheiten. Drücke oberhalb von 2200 bar zerstören irreversibel die Membranstruktur durch Proteinfaltung und Grenzflächentrennung.

Darüberhinaus konnte gezeigt werden, dass die Aktivität rekonstituierter  $\text{Na}^+, \text{K}^+$ -ATPasen stark von der Lipidumgebung abhängt. Wie Abb. 5.6 zu entnehmen ist, weist die Zeitabhängigkeit der Enzymreaktion, wie sie durch zeitabhängige Fluoreszenzmessungen  $I_F(t)$  von NADH bestimmt werden kann, einen komplexen Verlauf mit einem steileren Abfall in der späteren Phase der Reaktion auf. DMPC und DOPC wurden als Ein-Komponenten-Lipidsystem gewählt, welche als Modelle für gesättigte bzw. ungesättigte Lipide dienen sollen. Eine hohe Aktivität wird bei 37 °C in der fluiden Phase von DMPC festgestellt, das vollständig gesättigte Acylketten aus 14 Kohlenstoffatomen mit einer Länge von etwa 28 Å enthält [Eisenblätter 2006]. Der Einbau des Enzyms in die DMPC-Doppelschicht führt darüber hinaus zu einer erhöhten Ordnung der Lipidketten ( $\Delta GP \approx 0,35$ ). Für das längere, di-cis-ungesättigte  $\text{C}_{18}$ -Phospholipid DOPC befindet ist Enzymaktivität die niedrigste, die beobachtet wurde (siehe Abb. 5.3). Die Enzymaktivität erhöhte sich signifikant, wenn DOPC mit DOPE in einem Verhältnis von 3:2 gemischt wurde, um Krümmungsspannung in den Lipidmembranen zu erzeugen (Abb. 5.3). Die Zugabe von DOPE zu DOPC erhöhte den Ordnungsgrad der Lipide um 0,1 *GP*-Einheiten. Dagegen führte der Einbau des Enzyms in DOPC zu einer Erhöhung von  $\sim 0,3$  *GP*-Einheiten, der Einbau der  $\text{Na}^+, \text{K}^+$ -

ATPase in eine 3:2-DOPC/DOPE-Mischung sogar zu einem noch höheren Anstieg ( $\Delta GP \approx 0,4$ ), was anzeigt, dass die erhöhte Enzymaktivität mit einem Anstieg der konformativen Ordnung des gemischten Doppelmembran-Systems einhergeht. Daraus kann man schließen, dass der Einbau des Enzyms die Stressbedingung effizient herabsetzt, welche die Enzymaktivität zu begünstigen scheint. Die Zugabe von Cholesterin zu 15 bzw. 30 mol %, was bei dieser Temperatur zu einem Anstieg der konformativen Ordnung sowie einer Streckung der Acylketten in der Doppelmembran der fluiden Phase führt, geht mit einer drastischen Abnahme der Enzymaktivität einher. Dieses beruht wahrscheinlich auf einem ansteigenden hydrophoben *mismatch* zwischen den Acylketten und den hydrophoben Bereichen des Proteins, was zu einer Änderung der konformativen Beweglichkeit der  $\text{Na}^+$ ,  $\text{K}^+$ -ATPase führt. Dahingegen hat die Zugabe von 15 mol % Cholesterin zu DOPC eine aktivitätsfördernde Wirkung auf das Enzym. Der Einbau von Cholesterin in ungesättigte Lipide beschleunigt die Reaktion. Da Cholesterin ein bestimmender Faktor der Dicke der Membrandoppelschicht ist, könnte man daraus schließen, dass die hydrophobe Dicke neben der Fluidität der Lipide eine Rolle für die Aktivität des integralen Proteins spielt. Eine Erhöhung des Anteils anionischer Lipide in der Membran (10 % DMPS) führt zu einer weiteren Erhöhung der Enzymaktivität, welche von einem Anstieg der konformativen Ordnung innerhalb der Membran begleitet wird. Der Anstieg liegt in einer vergleichbaren Größenordnung wie der von reinen DMPC-Doppelschichten ( $\Delta GP \approx 0,3$ ). Eine signifikante Änderung des Dipol-Potentials der Doppelschicht erzeugt im Falle des partiell-anionischen Lipid-Doppelschicht-Systems starke Unterschiede in der Stärke des elektrischen Feldes innerhalb der Kopfgruppen-Region, was anscheinend die elektrogenen Schritte entlang des Reaktionspfades des Enzyms beschleunigt. Insgesamt scheint bei Normaldruck eine maximale Enzymaktivität für die hier untersuchten Systeme erreicht zu werden, wenn die  $\text{Na}^+$ ,  $\text{K}^+$ -ATPase in einer  $\text{C}_{14}$ -Lipid-Doppelschicht eingebaut wird, die der fluiden Phase analog ist und die eine bestimmte Menge an anionischer Lipide enthält. Ungesättigter Lipide, die ca. 15 mol % Cholesterin beinhalten, diese Cholesterinkonzentration ist vergleichbar zu der Menge, die auch unter natürlichen Bedingungen im Schweinenierengewebe gefunden wird, und das Vorhandensein von Krümmungsspannungen scheint auch günstig zu sein.

Die Aktivität der in DMPC-, DOPC-, *model raft*- und DOPC/DOPE-Mischungen rekonstituierten Enzyme wurde ebenfalls bei 37 °C in einem Druckbereich von Normaldruck bis ca. 2 kbar untersucht. Im Allgemeinen, analog zur Enzymaktivität in der Plasmamembran, führt ein hoher Druck zu einer Verminderung der Enzymaktivität der in den verschiedenen Modellmembranen rekonstituierten Enzyme. In den meisten Fällen wird ein Mehrphasensystem gefunden. Es wird kein Zwei-Zustands-Übergang gefunden, wie es auch für die Druckdenaturierung vieler wasserlöslicher Proteine beobachtet wird [Winter 1998, Winter 2002, Winter 2005, Woenckhaus 2001, Meersman 2006].

Interessanterweise wird im niedrigen Druckbereich um 100 bar ein signifikanter Anstieg der Enzymaktivität (ca. 60-100 %) für die in DMPC- und DOPC-Doppelmembranen rekonstituierten Proteine gefunden. Über 100-200 bar folgt diesem Aktivitätsmaximum ein steiler Abfall der Aktivität bis ca. 600-800 bar, wo ein mehr oder minder breiter Plateauwert erreicht wird, bis die Enzymaktivität einen Wert um Null bei etwa 2 kbar für alle untersuchten Systeme erreicht (Abb. 5.6). Die erhöhte Aktivität bei diesen relativ niedrigen Drücken um 100 bar könnte, z.B., durch eine drastische Volumenverminderung des ATPase-Komplexes durch Kompression verursacht sein, welches das System in Richtung eines niedrigeren Aktivierungsvolumens der ATPase-Reaktion verschiebt. Der Effekt könnte aber auch mit einer strukturellen Änderung der Lipid-Matrix zusammenhängen, was allerdings bei niedrigen Drücken eher unwahrscheinlich ist. Der Anstieg um 100 bar würde nur zu einer leichten Änderung der mittleren Länge der Acylketten führen (ca. 0,1 Å), und ein druckinduzierter Übergang von fluider zur Gelphase findet bei derlei niedrigen Drücken nicht statt [Eisenblätter 2006]. Ein anderes Szenario wird beim Einfluss des Druckes auf die Enzymaktivität im Falle der *model raft*-Mischungen gefunden. In diesem Fall wird ein mehr oder minder linearer Abfall der Aktivität bis zu ca. 2 kbar beobachtet, wo die Aktivität auf fast Null abgefallen ist. Offensichtlich führt hier die Koexistenz der  $l_o$ - und  $l_d$ -Domänen sowie die Möglichkeit des *lipid sorting* in dieser Lipid-Mischung zu einer verminderten Druckempfindlichkeit der enzymatischen Reaktion im mittleren Druckbereich.

Die folgende Abnahme an ATPase-Aktivität mit ansteigendem Druck über 100-200 bar könnte durch einen zunehmenden hydrophoben *mismatch* und vielleicht durch eine Umorientierung bzw. Dissoziation der Untereinheiten erklärt werden. Im Allgemeinen erwartet man mit zunehmenden Druck eine Abnahme der



Doppelmembranfluidität sowie eine einhergehende Abnahme an konformativer Flexibilität für das Protein. Die Dicke der Lipid-Doppelmembran steigt ebenfalls, was zu einer Änderung der Umgebung für das Transmembranprotein an den Grenzflächen zwischen Protein und Wasser sowie Protein und Lipid führt. Zum Beispiel könnte bei Zunahme der Membrandicke der wasserlösliche Bereich des Proteins teilweise bedeckt werden, was zu einer Verminderung der Reaktionsrate führt. Die physiologische  $\text{Na}^+$ ,  $\text{K}^+$ -ATPase-Reaktion beinhaltet zwei konformative Änderungen ( $\text{E}_2 \rightarrow \text{E}_1$  und  $\text{E}_1\text{P} \rightarrow \text{E}_2\text{P}$ ), welche beide drucksensitiv sein könnten. Wenn diese konformativen Änderungen eine positive Volumenänderung beinhalten oder induzieren, könnte dies ein Faktor sein, der die Aktivitätsverminderung bei erhöhtem Druck erklärt. Da kein druckinduzierter Übergang von fluiden Phase zu Gelphase in DOPC- und DOPC/DOPE-Doppelmembranen im untersuchten Druckbereich vorkommt (Abb. 5.9, 5.11), spricht der niedrige Plateau-Wert der Enzymaktivität, welcher zwischen 600 und 800 bar für DMPC, DOPC und DOPC/DOPE (3:2) gefunden wird, eher für solche konformativen Übergänge des Proteins anstelle eines Phasenübergangs von fluiden zur Gelphase als Hauptgrund der Aktivitätsminderung. Höhere Drücke jenseits von 2,2 kbar zerstören, wahrscheinlich aufgrund von Dissoziation und partieller Entfaltung der Untereinheiten, irreversibel die Proteoliposomstruktur.

## 8 References

- Ahmed, S. N., Brown, D. A., London, E. (1997) *Biochemistry* 36, 10944-10953.
- Alberts, B., Bray, D., Lewis, J., Raff, M., Keith, R., Watson, J. (1983) *Molecular Biology of The Cell*, Garland Publishing, Inc., NY.
- Alberts, B., Johnson, A., Lewis, J., Raff, M., Keith, R., Walter, P. (2002) *Molecular Biology of The Cell, 4<sup>th</sup> ed*, Garland Science, Taylor & Francis group, NY.
- Bagatolli, L. A., Gratton, E. (2000) *Biophys. J.* 79, 434-47.
- Baird, B., Sheets, E. D., Holowka D. (1999) *Biophys. Chem.* 82, 109-19.
- Balny, C. (2004) *J. Phys. Condens. Matter* 16, 1245-1253.
- Bernsdorff, C., Wolf, A., Winter, R., Gratton, E. (1997) *Biophys. J.* 72, 1264-1277.
- Bhairi S.M. (2001) *Detergents-A guide to the properties and uses of detergents in biological systems*, Calbiochem – Novabiochem, San-Diego, USA.
- Brotherus, J. R., Moller, J. V., Jorgensen, P. L. (1981) *Biochem. Biophys. Res. Commun.* 100, 146-54.
- Brown, B. S. (1996) *Biological Membranes*, University of Arizona.
- Brown, R. E. (1998) *J. Cell Sci.* 111, 1-9.
- Brown, D. A., London, E. (2000) *J. Biol. Chem.* 275, 17221-4.
- Brown, D. A., Rose, J. K. (1992) *Cell* 68, 533-544.
- Cerneus, D. P., Ueffing, E., Posthuma, G., Strous, G. J., van der Ende, A. (1993) *J. Biol. Chem.* 268, 3150-5.
- Cevc, G. (Ed), (1993) *Phospholipids Handbook*, Marcel Dekker, Inc, New York.
- Chong, P. L., Fortes, P. A. G., Jameson, D. M. (1985) *J. Biol. Chem.* 260, 14484-14490.
- Cornelius, F. (1991) *Biochim. Biophys. Acta* 1071, 19-66.
- Cornelius, F. (2001) *Biochemistry* 40, 8842-8851.
- Cornelius, F., Turner, N., Christensen, H. (2003) *Biochemistry* 42, 8541-8549.
- Crowe, J. H., Tablin, F. (2002) *J. Cell. Physiol.* 190, 117-28.

- Cullis, P., Fenske, D., Hope, M., Vance, D. E., Vance, J. E. (1996) *Biochemistry of Lipids, Lipoproteins and Membranes*, chapter 1.
- Dan, N., Safran, S. A. (1998) *Biophys. J.* 75, 1410-1414.
- De Almeida, R.F., Fedorov, A., and Prieto, M. (2003) *Biophys J.* 85, 2406-2416.
- de Lima Santos, H., Lopes, M. L., Maggio, B., Ciancaglini, P. (2005) *Colloids Surf.* 41, 239-248.
- De Pont, J. J. H. H. M., van Prooijen-van Eeden, A., and Bonting, S. L. (1978) *Biochim. Biophys. Acta* 508, 464-477.
- De Smedt, H., Borghgraef, R., Ceuterick, F., and Heremans, K. (1979) *Biochim. Biophys. Acta* 556, 479-489.
- Dietrich, C., Bagatolli, L. A., Volovyk, Z. N., Thompson, N. L., Levi, M., Jacobson, K., Gratton, E. (2001) *Biophys. J.* 80, 1417-28.
- Edidin, M. (2003) *Annu. Rev. Biophys. Biomol. Struct.* 32, 257-283.
- Eisenblätter, J., and Winter, R. (2006) *Biophys. J.* 90, 956-966.
- Fedsova, N. U., Cornelius, F., Klodos, I. (1998) *Biochemistry* 37, 13634-13642.
- Fiske, C. H., and Subbarow, Y. (1925) *J. Biol. Chem.*, 66, 375-388.
- Fleming, K. (2005) *Techniques in Biophysics* 250.690, handout 8.
- Fridriksson, E. K., Shipkova, P. A., Sheets, E. D., Holowka, D., Baird, B., McLafferty, F. W. (1999) *Biochemistry* 38, 8056-63.
- Garcia, J. J., Martinez-Ballarín, E., Millan-Plano, S., Allue, J. L., Albendea, C., Fuentes, J. F., Escanero, J. F. (2005) *J. Trace Elem. Med. Biol.* 19, 19-22.
- Gorodinsky, A., Harris, D. A. (1995) *J. Cell. Biol.* 129, 619-27.
- Gousset, K., Wolkers, W. F., Tsvetkova, N. M., Oliver, A. E., Field, C.L., Walker, N. J., Hanada, K., Nishijima, M., Akamatsu, Y., Pagano, R. E. (1995) *J. Biol. Chem.* 270, 6254-60.
- Gravito, M. R., Ferguson-Miller S. (2001) *J. Biol. Chem.* 276, 32403-32406.
- Grell, E., Schick, E., and Lewitzki, E. (2001) *Thermochim. Acta* 380, 245-254.
- Grinberg, A. V., Gevondyan, N. M., Grinberg, N. V., and Grinberg, V. Y. (2001) *Eur. J. Biochem.* 268, 5027-5036.

Hayashi, Y., Kameyama, K., Kobayashi, T., Hagiwara, E., Shinji, N., Takagi, T. (1997) *Ann NY Acad Sci.* 834, 19-29.

Houslay, M. D., Stanley, K. K. (1982) *Dynamics of Biological Membranes*, John Wiley & Sons Ltd.

Heerklotz, H. (2002) *Biophys. J.* 83, 2693-701.

Heremans, K. (1978) Pressure effects on biochemical systems, in *High Pressure Chemistry* (Kelm, H., Ed.) pp 467-487, Reidel Publishing Company, Dordrecht.

Heremans, K., Smeller, L. (1998) *Biochim. Biophys. Acta* 1386, 353-370.

Huang, J., Buboltz, J. T., Feigenson, G. W. (1999) *Biochim. Biophys. Acta* 1417, 89-100.

Humphrey, P. A., Lupfert, Ch., Apell, H. J., Cornelius, F., Clarke, R. J. (2002) *Biochemistry* 41, 9496-9507.

Jensen, M., Mouristen, O. G. (2004) *Biochim. Biophys. Acta* 1666, 205-226.

Jorgensen, P. L. (1982) *Biochim. Biophys. Acta* 694, 27-68.

Jorgensen, P. L., Nielsen, J. M., Rasmussen, J. H., Pedersen, P. A. (1998) *Acta Physiol. Scand. Suppl.* 643, 79-87.

Kahya, N., Scherfeld, D., Bacia, K., Poolman, B., Schwille, P. (2003) *J. Biol. Chem.* 278, 28109-15.

Kasturi, R., Yuan, J., McLean, L. R., Margolies, M. N., Ball, W. J. Jr (1998) *Biochemistry* 37, 6658-66.

Kato, M., Hayashi, R., Tsuda, T., Tanaguchi, K. (2002) *Eur. J. Biochem.* 269, 110-118.

Kenworthy, A. K., Petranova, N., Edidin, M. (2000) *Mol. Biol. Cell.* 11, 1645-55.

Kinne, R., Kinne-Saffran, E., Schölermann, B. and Schütz, H. (1986) *Pflügers Arch.* 407, S168 - S173.

Le Maire, M., Champeil, P., Moller, J. V. (2000) *Biochim. Biophys. Acta* 1508, 86-111.

Lodish, H. (2005) *Molecular Cell Biology 5<sup>th</sup> ed.*, Freeman, N.Y.

Linnertz, H., Urbanova, P., Obsil, T., Herman, P., Amler, E., Schoner, W. (1998) *J. Biol. Chem.* 273, 28813-21.

MacGregor, S. E., Walker, J. M. (1993) *Comp. Biochem. Physiol.* 105C, 1-9.

- Meersman, F., Smeller, L., and Heremans, K. (2006) *Biochim. Biophys. Acta* 1764, 346-354.
- Mohraz, M. (1999) *J. Struct. Biol.* 125, 76-85.
- Mouritsen, O. G. (2003) *Life as a matter of fat*, Springer-Verlag Berlin Heidelberg.
- Nicolini, C., Kraineva, J., Khurana, M., Periasamy, N., Funari, S., and Winter, R. (2006) *Biochim. Biophys. Acta* 1758, 248-258.
- Parasassi, T., De Stasio, G., d'Ubaldo, A., Gratton, E. (1990) *Biophys. J.* 57, 1179-1186.
- Parasassi, T., De Stasio, G., Ravagnan, G., Rusch, R. M., Gratton, E. (1991) *Biophys. J.* 60, 179-189.
- Parasassi, T., Krasnowska, E. K., Bagatolli, L., Gratton E. (1998) *J. Fluoresc.* 8, 365-373.
- Parkson, L., Chong, G., Fortes, P. A.G., Jameson, D.A. (1985) *J. Biol. Chem.*, 260 (27): 14484-14490.
- Periasamy, N., Winter, R. (2006) *Biochim. Biophys. Acta* 1764, 398-404.
- Pike, L. (2004) *Biochem. J.* 378, 281-292.
- Pressley, T. A. (1996) *Miner. Electrolyte Metab.* 22, 264-71.
- Parkson, L., Chong, G., Fortes, P. A.G., Jameson, D.A. (1985) *J. Biol. Chem.* 260, 14484-14490.
- Raffy, S., Teissie, J. (1999) *Biophys. J.* 76, 2072-2080.
- Reithmeier R. A. F., Vance, D. E., Vance, J. E. (1996) *Biochemistry of Lipids, Lipoproteins and Membranes*, chapter 16.
- Royer, C. A. (1995) *Biophys. J.* 68, 1191-1195.
- Santos, H. L., Lamas, R. P., Ciancaglini, P. (2002) *Braz. J. Med. Biol. Res.* 35, 277-288.
- Schutz, G. J., Kada, G., Pastushenko, V. P., Schindler, H. (2000) *EMBO J.* 19, 892-901.
- Seddon, A. M., Curnow, P., Booth, P. J. (2004) *Biochim. Biophys. Acta* 1666, 105-117.
- Silvius, J. R. (1992) *Annu. Rev. Biophys. Biomol. Struct.* 21, 323-48.

- Simons, K., Ikonen, E. (1997) *Nature*, 5, 569-72.
- Simons, K., Toomre, D. (2000) *Nat. Rev. Mol. Cell. Biol.* Oct 1, 31-9.
- Singer, S. J., Nicolson, G. L. (1972) *Science* 175, 720-731.
- Skou, J. C., Esmann, M. (1992) *J. Bioenerg. Biomemb.* 24, 249-261.
- Sotomayor, C. P., Aguilar, L. F., Cuevas, F. J., Helms, M. K., and Jameson, D. M. (2000) *Biochemistry* 39, 10928-10935.
- Szymanska, G., Kim, H. W., Kranias, E. G. (1991) *Biochim. Biophys. Acta* 1091, 127-134.
- Taheri-Araghi, S. (2006) *Interactions of Cationic Peptides and Ions with Negatively Charged Lipid Bilayer*. A thesis presented to the University of Waterloo, Ontario, Canada.
- Ulmer, H. M., Herberhold, H., Fahsel, S., Gänzle, M. G., Winter, R., and Vogel, R. F. (2002) *Appl. Environm. Microbiol.* 68, 1088-1095.
- Varma, R., Mayor, S. (1998) *Nature* 394 (6695).
- Weber, G., Farris, F. J. (1979) *Biochemistry* 18, 3075-3078.
- Wilson, B. S., Pfeiffer, J. R., Oliver, J. M. (2000) *J. Cell. Biol.* 149, 1131-42.
- Winter, R. (2002) *Biochim. Biophys. Acta* 1595, 160-184.
- Winter, R. (2005) High pressure effects in molecular bioscience, in *Chemistry at Extreme Conditions*, (Manaa, M. R., Ed.), pp. 29-82, Elsevier B.V.
- Winter, R., Erbes, J., Czeslik, C., Gabke, A. (1998) *J. Phys. Condens. Matter.*, 10, 11499-11518.
- Winter, R., (Ed.), (2003) *High Pressure Bioscience and Biotechnology II*, Springer-Verlag, Heidelberg.
- Woenckhaus, J., Köhling, R., Thiyagarajan, P., Littrell, K., Seifert, S., Royer, C. A., and Winter, R. (2001) *Biophys. J.* 80, 1518-1523.
- Wu, B. J., Else, P. L., Storlien, L. H., and Hulbert, A. J. (2001) *J. Exp. Biol.* 204, 4271-4280.
- Yeagle, P. (Ed), (1992) *The Structure of Biological Membranes*, CRC Press, Boca Raton.
- Yeagle, P. L., Joung, J., and Rice, D. (1988) *Biochemistry* 27, 6449-6452.
- Yuan, C., Furlong, J., Burgos, P., Johnston, L. J. (2002) *Biophys. J.* 82, 2526-35.

Zeng, J., Chong, P. L. G. (1995) *Biophys. J.* 68, 567-573.





## Personal Information

Name: Powalska Ewa  
Date of birth: 24.12.1979  
City of birth: Elblag  
Nationality: Polish

### Education:

1994-1998 1<sup>st</sup>- High-School, Bio-Chem. Class, Elblag.  
1998-2003 Adam Mickiewicz University of Poznan, Poland  
Faculty of Chemistry  
Degree: M.Sc. in Chemistry obtain in:  
Institute of Bioorganic Chemistry, Polish Academy of Science.  
2003-2006 Dortmund University, Department of Biophysical Chemistry.